


12-2016

CONCOMITANT TARGETING OF THE MTOR/MAPK PATHWAYS: NOVEL THERAPEUTIC STRATEGY IN SUBSETS OF NON-SMALL CELL LUNG CANCER

Dennis Ruder

Follow this and additional works at: http://digitalcommons.library.tmc.edu/utgsbs_dissertations

 Part of the [Cancer Biology Commons](#), [Genetics Commons](#), [Genomics Commons](#), and the [Medicine and Health Sciences Commons](#)

Recommended Citation

Ruder, Dennis, "CONCOMITANT TARGETING OF THE MTOR/MAPK PATHWAYS: NOVEL THERAPEUTIC STRATEGY IN SUBSETS OF NON-SMALL CELL LUNG CANCER" (2016). *UT GSBS Dissertations and Theses (Open Access)*. 725.
http://digitalcommons.library.tmc.edu/utgsbs_dissertations/725

This Dissertation (PhD) is brought to you for free and open access by the Graduate School of Biomedical Sciences at DigitalCommons@TMC. It has been accepted for inclusion in UT GSBS Dissertations and Theses (Open Access) by an authorized administrator of DigitalCommons@TMC. For more information, please contact laurel.sanders@library.tmc.edu.

**CONCOMITANT TARGETING OF THE MTOR/MAPK PATHWAYS: NOVEL
THERAPEUTIC STRATEGY IN SUBSETS OF NON-SMALL CELL LUNG CANCER**

by

Dennis Ruder, B.S.

APPROVED:

Ignacio I. Wistuba, M.D.
Chair, Advisory Professor

Veera Baladandayuthapani, Ph.D.

Juan Fueyo, M.D.

Faye M. Johnson, M.D., Ph.D.

Jonathan M. Kurie, M.D.

Jeffrey N. Myers, M.D., Ph.D.

APPROVED:

Dean, Graduate School of Biomedical Sciences
The University of Texas Health Science Center at Houston

**CONCOMITANT TARGETING OF THE MTOR/MAPK PATHWAYS: NOVEL
THERAPEUTIC STRATEGY IN SUBSETS OF NON-SMALL CELL LUNG CANCER**

A

DISSERTATION

Presented to the Faculty of

The University of Texas

Health Science Center at Houston

and

The University of Texas

MD Anderson Cancer Center

Graduate School of Biomedical Sciences

in Partial Fulfillment

of the Requirements

for the Degree of

DOCTOR OF PHILOSOPHY

by

Dennis Ruder, B.S.

Houston, Texas

December, 2016

Dedication

To my family: thank you for your unconditional love, support, and encouragement throughout the years. Words cannot express how thankful I am. I am forever grateful and I love you!

To my friends, former and new: to many more life-long memories as we continue to grow personally and professionally. I would not have made it this far without all of our discussions, memories, and good times.

Importantly, this accomplishment is dedicated to all those affected by cancer. May we, the research community, never lose sight of the true meaning behind our work and what it means to the patients, and the contributions made to science and medicine.

Acknowledgements

This has been an incredible journey and it wouldn't have been possible without the acknowledgement of numerous people that have made an impact on me in indescribable ways.

First and foremost, I would like to thank Dr. Ignacio Wistuba and Dr. Julie Izzo for giving me the opportunity to join this lab and serving as inspiring mentors over the last couple of years. Thank you for providing me the flexibility to be curious, the continuous support and encouragement, the scientific discussions, and the optimistic outlook when experimental results were frustrating. Also, I am grateful for the opportunities to present my work at local and national conferences, allowing me to grow professionally and network with other brilliant minds in the field. With your help, this journey shaped me into a more patient, curious, independent, and knowledgeable person and scientist than I ever imagined to be, and for that I am truly thankful.

An enormous gratitude goes to my advisory committee members: Dr. Veera Baladandayuthapani, Dr. Juan Fueyo, Dr. Faye Johnson, Dr. Jonathan Kurie, and Dr. Jeffrey Myers. Thank you for devoting the time out of your busy schedules to attend my committee meetings and personal meetings. Your endless support, constructive feedback, and overall guidance to my project and career is greatly appreciated.

I would also like to acknowledge the current and former members of the Translational Molecular Pathology (TMP) lab. I would like to personally thank Milind Suraokar, Erick Riquelme, Kazuhiko Shien, Jody Vykoukal, Cathy Dumbrava, Barbara Mino, Edwin Parra, and Jaime Rodriguez for helping me along the way, whether it be scientifically, around the lab, or friendly conversation. I would also like to recognize

other members in the TMP department: Helene Pelicano and Saradhi Mallampati for your generous help and advice scientifically; Barbara Sadeghi, Bert Shaw, and Gabriela Mendoza for your continued administrative support, words of encouragement, and friendship.

Thank you to Dr. Ann Killary, Dr. Subrata Sen, Dr. Eduardo Vilar-Sanchez, and Dr. Gilbert Cote for your continuous encouragement and support of my work, the HMG program, and dedicating your time to mentor and train us, students, outside of your primary professional duties.

A big thank you to all my friends, both inside and outside of graduate school. I could not have done this without you all. You should know who you are! Also, thank you to the amazing Outreach Program coordinators, staff, and active volunteers. It's been an honor and a wonderful experience to be a part of this charitable organization.

I would also like to acknowledge the GSBS administrative staff for serving as a true role model of what GSBS stands for. Your compassion, enthusiasm, and dedication to the mission of the graduate school resonates and makes us proud to be students at such an amazing institution, backed by all of you. A big thank you for making our lives easier and always being so accommodating to our needs. I would like to especially thank Lily D'Agostino, Bunny Perez, Joy Lademora, Tracey Barnett, Cheryl Spitzenberger, Karen Weinberg, Marendra Wilson-Pham, Brenda Gaughan, Michael Valladolid, and Michael Orlando. You all have been instrumental to my success, so thank you for all the smiles, laughter, encouragement, and assistance throughout the years!

To my parents, thank you for making my dream a reality and setting the sky as the limit. The sacrifices you made to ensure a better future for my brother and me resemble the selfless, loving, devoted parents that you are. You have always believed that I have the talent to reach my goals, and that I should never settle for less than what I deserve. Without you, none of these opportunities would have been possible. To my brother, thanks for setting the bar so high for me and being such an inspiring role model in all aspects of life. You have paved the path for me countless times, and I am truly grateful to have you as my best friend despite being away. Thank you to my beloved better half, Tara Molina. You have been a true inspiration to me from the beginning and continue to amaze me. I am so proud of all your accomplishments, a true reflection of your persistence, dedication, and hard work ethic—all traits that you helped me to achieve to successfully complete this phase of my education. Thanks for always supporting me through thick and thin, the ups and downs, and for giving me the best support and unconditional love I could ever ask for. I am truly blessed to have you by my side as we continue our life's journey together. Without each of you, I would not be near becoming the person I am today, or the person I'm striving to be. Words can't express my appreciation and love.

CONCOMITANT TARGETING OF THE MTOR/MAPK PATHWAYS: NOVEL THERAPEUTIC STRATEGY IN SUBSETS OF NON-SMALL CELL LUNG CANCER

Dennis Ruder, B.S.

Advisory Professor: Ignacio I. Wistuba, M.D.

Over the last decade, a paradigm-shift in lung cancer therapy has evolved into targeted-driven medicinal approaches. However, patients frequently relapse and develop resistance to available therapies. Herein, we utilized genomic mutation data from advanced chemorefractory non-small cell lung cancer (NSCLC) patients enrolled in the Biomarker-Integrated Approaches of Targeted Therapy for Lung Cancer Elimination (BATTLE-2) clinical trial to characterize novel actionable genomic alterations potentially of clinical relevance. We identified *RICTOR* alterations (mutations, amplifications) in 17% of lung adenocarcinomas and found *RICTOR* expression correlates to worse overall survival. There was enrichment of MAPK pathway genetic aberrations in key oncogenes (e.g. *KRAS*, *BRAF*, *NF1*) associated with *RICTOR* altered cases, underscoring that RICTOR could serve as an important co-oncogenic driver in specific molecular settings. Moreover, we utilized a panel of *RICTOR* amplified NSCLC cell lines and found that *RICTOR* genetic blockade impaired malignant properties seen by reduced effects on cell survival and tumorigenicity potential. We uncovered a compensatory activation of the MAPK signaling pathway following *RICTOR* knockdown specifically in *KRAS* co-mutational settings, exposing a unique therapeutic vulnerability. Our *in vitro* and *in vivo* data

testing concomitant pharmacologic inhibition of both pathways (PI3K/AKT/mTOR and MAPK) via AZD2014 (mTORC1/2 inhibitor) and selumetinib (MEK1/2) resulted in synergistic responses of antitumor effects. Given the large population of patients affected by NSCLC, our study provides a treatment rationale for a specific subset of patients who may benefit from genomic stratification based on *RICTOR/KRAS* alterations, further underscoring the need for proper patient selection to gain optimal therapeutic response.

Table of Contents

Approval signatures	i
Title page	ii
Dedication	iii
Acknowledgements	iv
Abstract	vii
Table of contents	ix
List of figures	xii
List of tables	xv
List of abbreviations	xvi
Chapter 1: Introduction	1
1.1 Lung cancer overview	1
1.2 Paradigm shift in therapy and molecular characterization of NSCLC	1
1.3 The PI3K/AKT/mTOR signaling pathway	6
1.4 The RAS/RAF/MEK/ERK (MAPK) signaling pathway	11
1.5 Cross-talk between PI3K/mTOR and MAPK Pathways	14
1.6 Therapeutic implications of targeting the PI3K/AKT/mTOR pathway	18
1.7 Therapeutic implications of targeting the RAS/RAF/MEK (MAPK) pathway	21
1.8 RICTOR's mTORC2-dependent and independent tumorigenic functions	24
1.9 Hypothesis and specific aims	26
Chapter 2: Materials and Methods	28

Chapter 3: Results	37
3.1 Identification of <i>RICTOR</i> alterations in advanced NSCLC	37
3.2 <i>RICTOR</i> mRNA expression is higher in <i>RICTOR</i> amplified than non-amplified NSCLC.	43
3.3 Associating <i>RICTOR</i> mRNA expression to clinical outcome	44
3.4 Surveying the co-mutational landscape of <i>RICTOR</i> alterations	44
Chapter 4: Results	49
4.1 Selection and mutational background of <i>RICTOR</i> cell line panel	49
4.2 <i>RICTOR</i> signaling in <i>RICTOR</i> amplified versus non-amplified cell lines	52
4.3 <i>RICTOR</i> knockdown decreases colony formation and anchorage-independent growth in amplified cells	54
4.4 <i>RICTOR</i> knockdown decreases cell proliferation in part through G ₀ /G ₁ cell cycle arrest	54
4.5 <i>RICTOR</i> knockdown reduces the migration and invasion capacity of <i>RICTOR</i> amplified NSCLC cells	58
4.6 <i>RICTOR</i> knockdown results in reduced tumorigenicity <i>in vivo</i>	62
Chapter 5: Results	64
5.1 Compensatory MAPK signaling activation following <i>RICTOR</i> inhibition in <i>KRAS</i> mutant settings	64
5.2 Compensatory MEK1/2 activation following <i>RICTOR</i> knockdown may be mediated through de-repression of inhibitory CRAF phosphorylation.....	67

5.3 Human p-MAPK array reveals <i>RICTOR</i> knockdown affects the activity of several mediators of cellular stress and survival pathways.	71
Chapter 6: Results	73
6.1 <i>RICTOR</i> knockdown enhances the pharmacologic efficacy of MAPK pathway inhibition in <i>RICTOR/KRAS-altered</i> NSCLC cell lines	73
6.2 Combined mTORC1/2 and MEK inhibition is an effective therapeutic approach in <i>RICTOR/KRAS-altered</i> settings and results in synergistic anti-tumor effects <i>in vitro</i>	76
6.3 Comparative effects of mTORC1/2 and MEK1/2 pathway inhibition <i>in vivo</i>	82
Chapter 7: Discussion, Conclusions, and Future Directions	86
Chapter 8: Appendix	104
Bibliography	105
Vitae	138

List of Figures

Figure 1. Non-small cell lung cancer (NSCLC) frequency based on histology	2
Figure 2. Frequency of molecular aberrations in various driver oncogenes in lung adenocarcinomas and current available drugs against these oncogenic proteins.....	4
Figure 3. The mTOR signaling pathway.....	9
Figure 4. The RAS-RAF-MEK-ERK signaling pathway.....	12
Figure 5. Pathway crosstalk.....	17
Figure 6. Identifying novel actionable targets in refractory NSCLC using the BATTLE-2 clinical trial.....	38
Figure 7. Frequency of potentially actionable genes that carry mutations and/or amplifications from the NGS FoundationOne targeted panel.....	39
Figure 8. <i>RICTOR</i> alterations are present in early and advanced stage lung adenocarcinoma at similar frequencies.....	40
Figure 9. Cross-cancer mutational frequency of <i>RICTOR</i> in the TCGA database	42
Figure 10. Correlation of <i>RICTOR</i> amplification to mRNA gene expression in lung adenocarcinoma cases.....	43
Figure 11. Surveying the co-mutational landscape of <i>RICTOR</i> -altered cases ...	46
Figure 12. Selection of <i>RICTOR</i> cell line panel used for <i>in vitro</i> studies	50
Figure 13. Establishment of inducible sh <i>RICTOR</i> cell line models	50

Figure 14. Comparison of signaling and RICTOR expression in amplified versus non-amplified cell lines	52
Figure 15. <i>RICTOR</i> knockdown decreases colony formation and anchorage-independent growth in amplified cells	55
Figure 16. <i>RICTOR</i> knockdown decreases the cell proliferative capacity	57
Figure 17. <i>RICTOR</i> knockdown reduces migration potential in <i>RICTOR</i> amplified cell lines.....	60
Figure 18. <i>RICTOR</i> knockdown reduces invasion potential in <i>RICTOR</i> amplified cell lines.....	61
Figure 19. <i>RICTOR</i> knockdown using <i>RICTOR</i> shRNA results in reduced tumorigenicity <i>in vivo</i>	63
Figure 20. Compensatory MAPK signaling activation following <i>RICTOR</i> knockdown in <i>KRAS</i> mutant settings	66
Figure 21. Compensatory MEK1/2 activation following <i>RICTOR</i> knockdown may be mediated through de-repression of inhibitory CRAF phosphorylation	70
Figure 22. Human p-MAPK array reveals <i>RICTOR</i> is linked to several mediators of cellular stress and survival.....	72
Figure 23. <i>RICTOR</i> knockdown enhances the pharmacologic efficacy of MAPK pathway inhibition in <i>RICTOR/KRAS-altered</i> NSCLC cell lines	74

Figure 24. Combined mTORC1/2 and MEK1/2 inhibition is an effective therapeutic approach in *RICTOR/KRAS*-altered *in vitro* settings 78

Figure 25. AZD2014 and selumetinib act synergistically to block mTOR and MAPK pathway signaling *in vitro* 80

Figure 26. Selumetinib in combination with sh*RICTOR* or AZD2014 results in the strongest anti-tumor activity *in vivo* 84

List of Tables

Table 1. Univariate overall survival analysis of <i>RICTOR</i> mRNA expression in lung adenocarcinoma patients by Cox proportional hazards model	44
Table 2. List of co-mutant genes and their frequency of alterations (TCGA Lung Adenocarcinoma dataset)	47
Table 3. Mutational profile of RICTOR NSCLC cell line panel	51

Abbreviations

4EBP1: Eukaryotic Translation Initiation Factor 4E Binding Protein 1

AKT: V-Akt Murine Thymoma Viral Oncogene Homolog 1

ALK: Anaplastic Lymphoma Receptor Tyrosine Kinase

AMPK: AMP-activated protein kinase

ARAF/BRAF/CRAF: A/B/C-Raf Proto-Oncogene, Serine/Threonine Kinase

ARFRP1: ADP Ribosylation Factor Related Protein 1

ATCC: American Type Culture Collection

ATM: Ataxia Telangiectasia Mutated

ATR: Ataxia Telangiectasia And Rad3-Related Protein

AZD2014: Vistusertib

AZD6244: Selumetinib

BATTLE-2: The Biomarker-integrated Approaches of Targeted Therapy for Lung Cancer Elimination trial

BCL2L2: BCL2 Like 2

BCL6: B-Cell CLL/Lymphoma 6

CAV1: Caveolin 1

CCLC: Characterized Cell Line Core

CCLE: Cancer cell line encyclopedia

CCND1: Cyclin D1

CCNE1: Cyclin E1

CDC42: Cell Division Cycle 42

CDK4: Cyclin Dependent Kinase 4

CEBPA: CCAAT/Enhancer Binding Protein Alpha

CI: Confidence interval

CNV: Copy number variation

CREB: CAMP Responsive Element Binding Protein 1

CRISPR/Cas9: Clustered regularly interspaced short palindromic repeats/CRISPR associated protein-9

CRKL: CRK Like Proto-Oncogene, Adaptor Protein

CUL1: Cullin-1

CUL3: Cullin-3

DEPTOR: DEP Domain Containing MTOR-Interacting Protein

DMSO: Dimethyl sulfoxide

DNA-PK: Protein Kinase, DNA-Activated, Catalytic Polypeptide

Doxy: Doxycycline

EGFR: Epidermal Growth Factor Receptor

eIF: Eukaryotic translation initiation factors

EMT: Epithelial-to-mesenchymal transition

ER positive: Estrogen receptor positive

ERBB2: Erb-B2 Receptor Tyrosine Kinase 2

ERK1/2: Mitogen-Activated Protein Kinase 1/3

EZH2: Enhancer Of Zeste 2 Polycomb Repressive Complex 2 Subunit

FGF-19, 3, 10, 4, 12: Fibroblast Growth Factor 19, 3, 10, 4, or 12

FGFR1: Fibroblast Growth Factor Receptor 1

FKBP12: FK506 binding protein 12

FOXO: Forkhead box O family of proteins

GAPs: GTPase-activating protein

GEFs: Guanine nucleotide exchange factors

GPR124: G-Protein Coupled Receptor 124

GRB2: Growth Factor Receptor Bound Protein 2

GSK3: Glycogen Synthase Kinase 3 Beta

GSK3a/b: Glycogen Synthase Kinase 3 Alpha/Beta

HBEC: Immortalized human bronchial epithelial cells

HGF: Hepatocyte Growth Factor

HR: Hazard ratio

HRAS: Harvey Rat Sarcoma Viral Oncogene Homolog

HSP27: Heat Shock 27kDa Protein 1

IKZF1: IKAROS Family Zinc Finger 1

IL7R: Interleukin 7 Receptor

ILK: Integrin linked kinase

IRS: Insulin receptor substrate

JNK: c-Jun N-terminal kinases

KDR: Kinase Insert Domain Receptor

KEAP1: Kelch Like ECH Associated Protein 1

KIT: KIT Proto-Oncogene Receptor Tyrosine Kinase

KLHL6: Kelch Like Family Member 6

KRAS: Kirsten Rat Sarcoma Viral Oncogene Homolog

MAP3K13: Mitogen-Activated Protein Kinase Kinase Kinase 13

MAPK: Mitogen-Activated Protein Kinase

MBN: Proteinase 3

MDM2: MDM2 Proto-Oncogene, E3 Ubiquitin Protein Ligase

MEK1/2: Mitogen-Activated Protein Kinase Kinase 1/2

MET: MET Proto-Oncogene, Receptor Tyrosine Kinase

mLST8: MTOR Associated Protein, LST8 Homolog

MMP9: Matrix Metalloproteinase 9

mSIN1: Mitogen-Activated Protein Kinase Associated Protein 1

mTOR: Mechanistic Target Of Rapamycin

mTORC1/2: Mechanistic Target Of Rapamycin Complex 1/2

MTS: (3-4, 5-dimethyl-thiazol-2-yl)-5-(3-carboxymethoxyphenyl-2-(4-solfophenyl)-2H-tetrazolium)

MTT: Methylthiazolyldiphenyl-tetrazolium bromide

MYC: V-Myc Avian Myelocytomatosis Viral Oncogene Homolog

NDRG1: N-Myc Downstream Regulated 1

NF1: Neurofibromin 1

NFE2L2: Nuclear Factor, Erythroid 2 Like 2

NFkB1A: Nuclear Factor Kappa B Subunit 1

NGS: Next-generation sequencing

NKX2-1: NK2 Homeobox 1

NRAS: Neuroblastoma RAS Viral Oncogene Homolog

NSCLC: Non-small cell lung cancer

NTC: Non-targeting control (shRNA or siRNA)

OS: Overall survival

P38: Mitogen-Activated Protein Kinase 14

P53: Tumor Protein P53

P70S6K: Ribosomal Protein S6 Kinase B1

PDK1: Pyruvate Dehydrogenase Kinase 1

PET: Polyethylene terephthalate filters

PH domain: Pleckstrin homology domain

PI3K: Phosphoinositide 3-kinase

PIK3CA: Phosphatidylinositol-4,5-Bisphosphate 3-Kinase Catalytic Subunit Alpha

PIK3R1: Phosphoinositide-3-Kinase Regulatory Subunit 1

PIKK family: Phosphatidylinositol 3-kinase-related kinases

PIP2: Phosphatidylinositol-4,5-bisphosphate

PIP3: Phosphatidylinositol-3,4,5-trisphosphate

PKB: Protein kinase B

PKC: Protein kinase C

PMS2: PMS1 Homolog 2, Mismatch Repair System Component

PRAS40: Proline-rich AKT1 substrate 1

PROSPECT: Profiling of Resistance Patterns and Oncogenic Signaling Pathways in
Evaluation of the Thorax dataset

PROTOR-1: Protein observed with Rictor-1

PTB domains: Phosphotyrosine-binding domains

PTEN: Phosphatase And Tensin Homolog

RAC1: Ras-Related C3 Botulinum Toxin Substrate 1 (Rho Family, Small GTP Binding Protein Rac1

Ra1A: RAS Like Proto-Oncogene A

RAPTOR: Regulatory Associated Protein Of MTOR Complex 1

RBX1: Ring-Box 1

RET: RET proto-oncogene

RHEB: Ras Homolog Enriched In Brain

RhoA: Ras Homolog Family Member A

RhoGAP5: Rho GTPase Activating Protein 5

RhoGDI: Rho GDP-dissociation inhibitor

RICTOR: RPTOR Independent Companion Of MTOR Complex 2

RIT1: Ras-Like Without CAAX 1

ROS1: ROS Proto-Oncogene 1, Receptor Tyrosine Kinase

RSK: Ribosomal S6 kinase

RTKs: Receptor tyrosine kinases

RUNX1T1: RUNX1 Translocation Partner 1

S6RP: S6 ribosomal protein

SCLC: Small cell lung cancer

SGK: Serum/Glucocorticoid Regulated Kinase

SH2 domains: Src Homology 2 domain

SNP array: Single nucleotide polymorphism array

SOS: Son of sevenless

SOX2: SRY-Box 2

STK11: Serine/Threonine Kinase 11; LKB1

TCGA: The Cancer Genome Atlas

TGF β : Transforming Growth Factor Beta 1

TIPARP: TCDD Inducible Poly(ADP-Ribose) Polymerase

TKIs: Tyrosine kinase inhibitors

TSC1/2: Tuberous Sclerosis 1/2

VEGFR: Vascular Endothelial Growth Factor Receptor 1

WD40 domain: WD or beta-transducin repeats

ZNF703: Zinc Finger Protein 703

Chapter 1

Introduction

1.1 Lung Cancer Overview

Lung cancer continues to affect the lives of more than 1.6 million new patients annually and remains a major global health problem. It is estimated to affect more than 224,000 people and lead to over 159,000 new deaths in the US each year (1). Despite advancements in detection methods and standard of care, over a third of patients that are diagnosed with lung cancer present at late stage with metastatic disease, resulting in a dismal 5-year survival rate of less than 5% which has remained stagnant over the past few decades (2). What was once considered a single disease entity, lung tumors exist as diverse subtypes with unique pathologies. The two major forms of lung cancer are non-small cell lung cancer (NSCLC) (accounts for approximately 85% of all lung tumors) and small-cell lung cancer (SCLC) (about 15%). Specifically, NSCLC can be further subdivided into three major histotypes: lung adenocarcinoma (50%), squamous-cell carcinoma (30%), and large-cell lung cancer (15%) (Figure 1) (3).

1.2 Paradigm Shift in Therapy and Molecular Characterization of NSCLC

It is well recognized that heterogeneity amongst the molecular architecture of tumors is responsible for diverse clinical outcomes and responses even in patients with similar clinical staging and histologic characteristics. This is due to our increased understanding that NSCLC is a disease comprised of diverse clinical, histological, and genetically distinct subtypes.

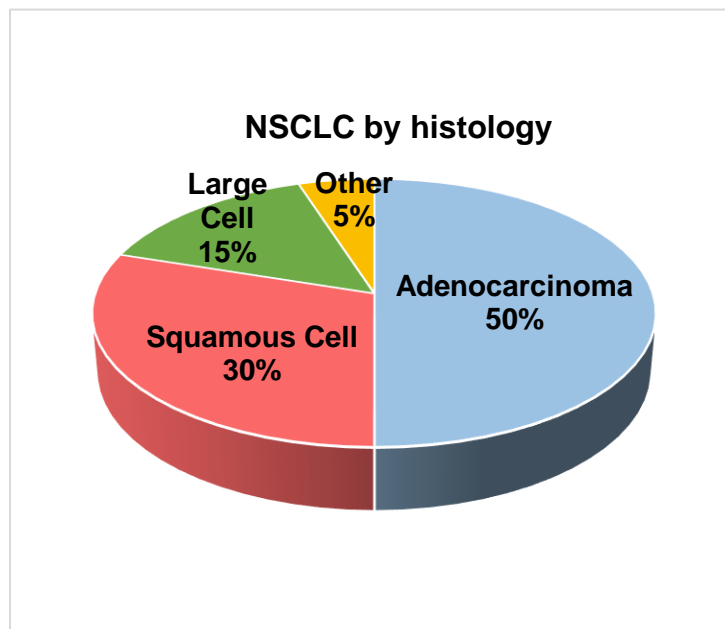


Figure 1. Non-small cell lung cancer (NSCLC) frequency based on histology.

With significant advancements in genomic sequencing technologies, treatment strategies and management of NSCLC, particularly in lung adenocarcinomas, are heavily based on screening tumors for an array of biomarkers that are of predictive and/or prognostic value to help oncologists assign patients that would be most sensitive to specific targeted therapies (4). A multitude of oncogenic driver mutations that feed into key signaling pathways have now been elucidated that lead to tumorigenesis and tumor progression (Figure 2) (5). Specifically, significant effort in the last decade had centered upon developing targeted agents against mutations of the epidermal growth factor receptor (*EGFR*, ~17% mutations) and in anaplastic lymphoma kinase (*ALK*) fusions/rearrangements (~7%), with much success attributed to examples such as EGFR tyrosine kinase inhibitors (TKIs) and crizotinib, respectively. In both subgroups, the response rates in patients properly stratified to

these targeting agents were as high as 70% in crucial phase 3 clinical trials (6, 7). Identification of such driver mutations and the responses seen in patients appropriately stratified serve as classic examples for the impetus of rational design of new and improved targeted agents that hit other key oncogenes in NSCLC. Such alterations are often found in receptors or protein kinases and can activate a complex cascade of oncogenic signaling paths such as the mitogen-activated protein kinase (MAPK) cascade and the phosphoinositide 3-kinase (PI3K)-PKB (AKT) pathway. The frequency of other genomic alterations that occur in lung adenocarcinomas include *KRAS* (25%), *NF1* (8.3%), *MET* (3%), *ROS1* (2%), *BRAF* (2%), *RET* (2%), and others (Figure 2) (5, 8). Ultimately, these mutant onco-drivers stimulate such pathways that lead to uncontrolled cancer cell growth, proliferation and pro-survival transcriptional reprogramming (9-12). However, approximately 25-30% of lung adenocarcinomas do not have known, targetable mutations, and therefore these patients are treated with standard cytotoxic chemotherapies with limited success. Moreover, although targeted therapies against discovered alterations lead to remarkable initial responses, the inevitable emergence of drug resistance still occurs and patients ultimately relapse. Mechanisms of resistance can occur either through the acquisition of secondary mutations in the targeted kinase that can potentially negate the drug binding affinity, or by compensating via alternate bypass signaling mechanisms, though other resistance mechanisms are possible (13, 14). Therefore, it is imperative to take into account the molecular underpinnings of each patient's tumor and utilize a personalized medicine approach to identify novel actionable targets and therapeutic strategies tailored to that individual.

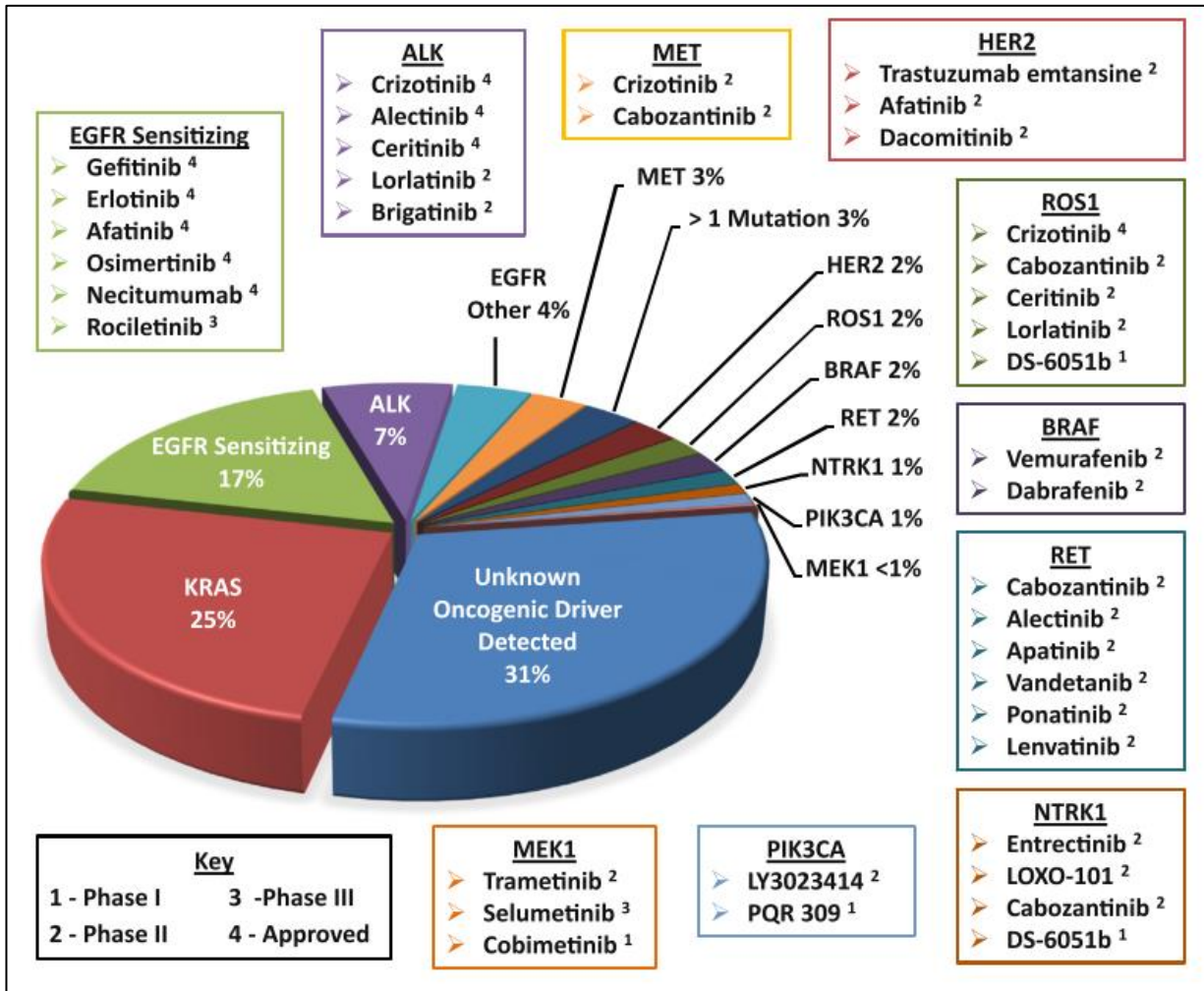


Figure 2. Frequency of molecular aberrations in various driver oncogenes in lung adenocarcinomas and current available drugs against these oncogenic proteins. These frequencies are a combination of data from the Lung Cancer Mutation Consortium and frequencies listed in Shea et al. (15). Shown in the boxes are the available drugs in addition to their developmental phase. EGFR, epidermal growth factor receptor; ALK, anaplastic lymphoma receptor tyrosine kinase; MET, mesenchymal-to-epithelial transition factor; HER2, erb-b2 receptor tyrosine kinase 2; ROS1, ROS proto-oncogene 1, receptor tyrosine kinase; BRAF, B-Raf proto-oncogene, serine/threonine kinase; RET, ret proto-oncogene; NTRK1, neurotrophic

tyrosine kinase receptor type 1; PIK3A, phosphatidylinositol-4,5-bisphosphate 3-kinase catalytic subunit alpha; MEK1, mitogen-activate protein kinase kinase 1; KRAS, Kirsten rat sarcoma viral oncogene homolog.

Reprinted with permission from: Tsao AS et al. Scientific Advances in Lung Cancer 2015. J Thorac Oncol. 2016;11(5):613-38. (5) License # 3957960028670

1.3 The PI3K/AKT/mTOR signaling pathway

The phosphatidylinositol 3-kinase (PI3K)-protein kinase B (PKB/AKT)-mammalian target of rapamycin (mTOR) (PI3K/AKT/mTOR) pathway is one of the most frequently deregulated signaling pathways in cancer and heavily enhances tumorigenic potential with its regulatory processes involving cellular growth, proliferation, survival, migration/invasion, and angiogenesis (16-18) (Figure 3). Under physiological condition, this intricate pathway is stimulated via ligand activation of receptor tyrosine kinases (RTKs) such as EGFR, ErbB3 IGF1-R, resulting in phosphorylation of tyrosine residues on the intracellular portion of the receptors (16, 19). This results in the direct recruitment of PI3K to the membrane of the cell where conversion of the second messenger phosphatidylinositol-4,5-bisphosphate (PIP₂) to phosphatidylinositol-3,4,5-trisphosphate (PIP₃) can occur (20). PIP₃ is then able to recruit 3-phosphoinositide dependent protein kinase-1 (PDK1) and the serine/threonine kinase AKT, via their pleckstrin homology (PH) domains, to the plasma membrane. PDK1 then phosphorylates AKT on Thr308 in the catalytic domain and the mammalian target of rapamycin complex 2 (mTORC2) serves to fully activate AKT on Ser473 in the hydrophobic motif (21). Active AKT mediates numerous cellular processes including survival, proliferation, apoptosis, migration and invasion via regulation of downstream effectors spanning multiple pathways (22-27). Typically, AKT can then lead to phosphorylation and inactivation of the GTPase-activating proteins (GAPs) tuberous sclerosis 1 and 2 (TSC1/TSC2), resulting in the accumulation of GTP-bound Ras homologue enriched in brain (RHEB) ultimately leading to activation of mammalian target of rapamycin complex 1 (mTORC1). Once activated, mTORC1 can directly regulate cellular processes involved in metabolism

and biosynthesis. Specifically, mTORC1 phosphorylates p70 S6 kinase and the translation repressor 4E-binding protein 1 (4EBP1). Phosphorylation of 4EBP1 inhibits the binding ability to eIF4E and initiates cap-dependent translation (28, 29). Similarly, S6K activation aids in the cap-dependent translation mechanism and also promotes S6 ribosomal protein (S6RP) phosphorylation. Collectively, this pathway converges on important cellular mechanisms resulting in increased protein translation, ribosome biogenesis and inhibition of autophagy (30-32).

Moreover, key components of the mTOR pathway are the two structurally and functionally distinct mTOR complexes. The essential mTORC1 subunits are the Ser/Thr kinase mTOR, the regulatory-associated protein of mTOR (RAPTOR) which serves as a scaffolding unit, mammalian lethal with Sec13 protein 8 (mLST8), proline-rich AKT substrate 40 kDa (PRAS40), and DEP-domain-containing mTOR-interacting protein (DEPTOR) (33, 34). The functional and regulatory mechanisms of mTORC1 have been characterized extensively since the discovery of rapamycin, an antifungal metabolite produced from the bacterium *Streptomyces hygroscopicus*, which inhibits mTOR and was later discovered to exhibit anti-proliferative and immunosuppressive effects (35). mTORC1 activity can be modulated by amino acid availability, nutrient levels, cellular energy status, and growth factors and ultimately coordinates regulatory signaling for translation and ribosome biogenesis (as described above). Moreover, mTORC1 is directly linked to the regulation of autophagy, and this link has been extensively studied due to important implications to cancer biology and treatment (36, 37). The process of autophagy can be either pro-oncogenic, acting as a survival mechanism to aid in growth advantage during stressful cellular conditions, or tumor

suppressive in function by preventing the buildup of damaged molecules such as organelles and proteins (37-40).

mTOR can function as part of a second complex, mTORC2, which contains some overlapping and distinct protein subunits, namely rapamycin-insensitive companion of mTOR (RICTOR), mammalian stress-activated protein kinase interacting protein (mSIN1), protein observed with Rictor-1 (PROTOR-1), DEPTOR, and mLST8 (36). Relative to mTORC1, the biology of regulation and functionality of mTORC2 is still in its infancy, although there is increased appreciation of the importance of this complex. Further, although it is established that activation of mTORC2 can be mediated by growth factors and PI3K signaling, the precise mechanism is poorly understood. One of the major roles elucidated for mTORC2 is the phosphorylation and full activation of AKT on Ser473 (21, 41). It can also phosphorylate and activate several other protein A/G/C (AGC) kinase family members such as serum glucocorticoid-induced kinase (SGK) and protein kinase C (PKC) isoforms, regulating cytoskeletal reorganization, cell survival, and lipid metabolism (41-43).

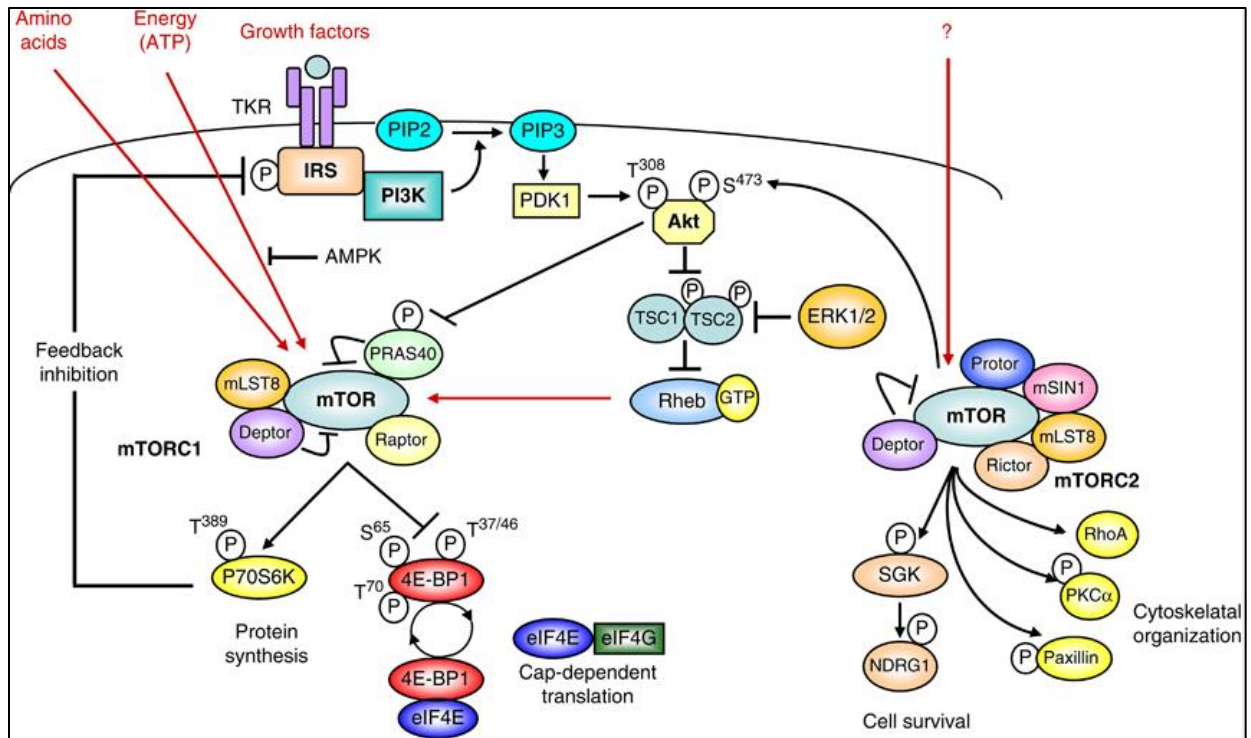


Figure 3. The mTOR signaling pathway. Red lines indicate the different mechanisms of mTOR activation. Abbreviations: AMPK, AMP-activated kinase; deptor, DEP-domain-containing mTOR interacting protein; 4E-BP1, eIF4E-binding protein 1; eIF, eukaryotic initiation factors; ERK1/2, extra-cellular regulated kinase 1/2; FKBP12, FK506 binding protein 12; IRS, Insulin receptor substrates; mLST8, mammalian lethal with Sec13 protein 8; mTORC, mammalian target of rapamycin complex; NDRG1, N-Myc downstream regulated gene-1; PDK1, phosphoinositide-dependent kinase 1; PI3K, phosphatidylinositol 3-kinase; PIP2, phosphatidylinositol bisphosphate; PIP3, phosphatidylinositol triphosphate; PRAS40, proline-rich Akt1 substrate 1; protor, protein observed with Rictor-1/Proline rich Akt substrate of 40kDa; P70S6K1, p70 S6 kinase 1; Rheb, Ras homolog enriched in brain; mSin1, stress

activated protein kinase interaction protein 1; SGK, serum and glucocorticoid protein kinase; TSC, tuberous sclerosis complex; TKR, tyrosine kinase receptor.

Reprinted with permission from: Chapuis N. et al. Perspectives on inhibiting mTOR as a future treatment strategy for hematological malignancies. Leukemia. 2010;24(10):1686-99 (44). License # 3960460046414

1.4 The RAS/RAF/MEK/ERK (MAPK) signaling pathway

The mitogen-activated protein kinase (MAPK) signaling pathway is a highly conserved family of kinases and is deregulated in about one-third of all human cancers (45). An overview of this signaling pathway is illustrated in Figure 4 (46). This pathway is primarily induced by cell surface receptors such as RTKs. Dimerization of these receptors following ligand binding activates the receptors and autophosphorylation of tyrosine residues occurs in the intracellular domain. Phosphorylation of these residues acts as docking sites for various proteins containing Src homology 2 (SH2) or phosphotyrosine-binding (PTB) domains (e.g. Grb2, growth factor receptor-bound protein 2). Grb2, serving as an adaptor molecule, can then recruit son of sevenless (SOS), a GTPase exchange factor (RasGEF), to localize to the cell membrane. Inactive Ras-GDP is largely associated with the plasma membrane, but following activation and catalytic transformation to Ras-GTP by SOS, RAS is able to recruit the RAF family of kinases (A-RAF, B-RAF, C-RAF) to the membrane and activate them. Subsequent activation loop phosphorylations occur in which RAF activates downstream MEK1/2, and MEK1/2 ultimately activates ERK1/2 at threonine and tyrosine residues, leading to a cascade of reactions regulating cell survival, proliferation, and motility. The main downstream targets elucidated of MEK1/2 are ERK1/2, while ERK1/2 has numerous downstream effectors (47).

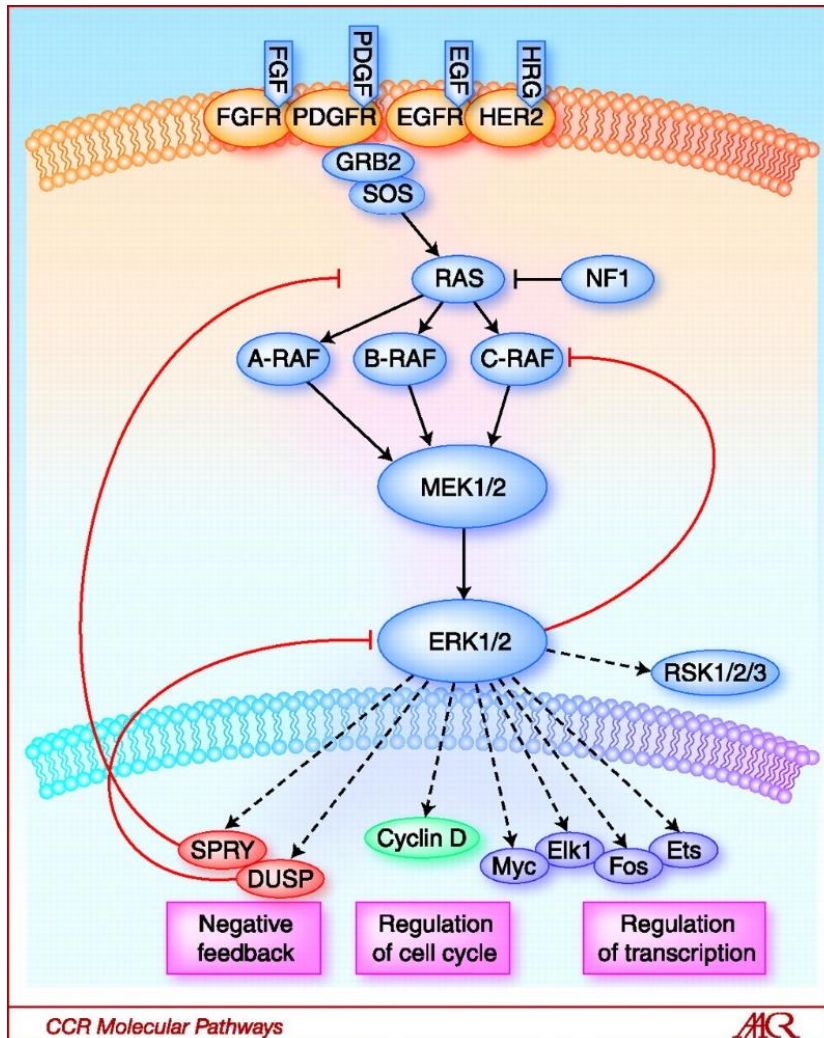


Figure 4. The RAS-RAF-MEK-ERK signaling pathway. The classical MAPK pathway is activated in human tumors by several mechanisms including the binding of ligand to receptor tyrosine kinases (RTK), mutational activation of an RTK, by loss of the tumor suppressor NF1, or by mutations in RAS, BRAF, and MEK1. Phosphorylation and thus activation of ERK regulates transcription of target genes that promote cell cycle progression and tumor survival. The ERK pathway contains a classical feedback loop in which the expression of feedback elements such as SPRY and DUSP family proteins are regulated by the level of ERK activity. Loss of expression of SPRY and DUSP family members due to promoter methylation or

deletion is thus permissive for persistently elevated pathway output. In the case of tumors with V600EBRAF expression, pathway output is enhanced by impaired upstream feedback regulation.

Reprinted with permission from: Pratilas CA, Solit DB. Targeting the mitogen-activated protein kinase pathway: physiological feedback and drug response. Clinical cancer research: an official journal of the American Association for Cancer Research. 2010;16(13):3329-34. (46) License # 3960600731382

1.5 Cross-talk between PI3K/mTOR and MAPK Pathways

Traditional views of major signaling networks such as the PI3K/AKT/mTOR and RAS/RAF/MEK/ERK (MAPK) pathways arrange these mechanisms as linear and independent pathways that determine cellular fate. However, numerous reports to date have described that these parallel pathways are very intricate and in fact there are multiple nodes of cross-talk, resulting in cross-activation, inhibition, and convergence of pathways on effector targets (48, 49). This is evidenced by reports suggesting that approximately 802 active proteins exist that are involved in PI3K-mediated signaling and over 2,000 connections exist that relate to the MAPK pathway family kinases (50, 51). Thus, the opportunity for cross-regulatory mechanisms amongst these interactomes to occur is not surprising and both of these major oncogenic pathways affect each other at various phases of signal transduction, depending on the cellular context and need. A summary of major cross-talk mechanisms that have been reported are highlighted in Figure 5 (49).

In both pathways, there are various kinases that have limited specificity of known substrates (e.g. mTORC1, RAF, MEK) and others that activate various members of their respective pathways on top of a multitude of other effector targets (e.g. S6K, ERK, AKT, RSK) (49). The integration of the PI3K/mTOR and MAPK pathways therefore mostly occurs through the latter kinases noted. Cross-inhibition of these pathways has been elucidated following studies utilizing chemical methods of blockade, wherein one pathway is blocked inducing a release mechanism of the basal cross-inhibitory effects leading to activation of the alternate pathway. For instance, inhibitors of MEK have been shown to increase epidermal growth factor (EGF)-

mediated activation of AKT through the recruitment of PI3K to the EGFR receptor (52, 53).

Moreover, a cross-inhibitory mechanism between RAF and AKT has been proposed that is induced by levels of IGF1 stimulation (54). Studies reported that the negative regulations of downstream ERK signaling by AKT occur through AKT's inhibition on phosphorylation sites in the upstream RAF N-terminus domain, specifically on the Ser364/259 residues (55-57). These conserved sites are recognized by 14-3-3 dimers which can immobilize the auto-inhibited RAF in the cytosolic region away from its upstream and downstream effectors RAS and MEK, respectively (58).

Cross-activation can also occur between both pathways. The MAPK pathway can activate the PI3K/mTOR pathway through direct regulation of PI3K, mTORC1, and TSC2. Activated RAS, when bound to GTP, can allosterically activate PI3K through direct binding (59-61). Moreover, constitutive activation from a mutant RAS, EGF stimulation, or phorbol esters can lead to hyperactive MAPK signaling, resulting in ERK and its effector ribosomal s6 kinase (RSK) to stimulate mTORC1 activity by inhibiting the GTPase-activating protein (GAP) function of the TSC1/2 complex (62). Additionally, pathway convergence can occur via multiple mechanisms signaled by S6K, AKT, ERK, and RSK since these key proteins share similar substrates and sometimes activate the same target simultaneously to fulfill specific processes such as cell survival, proliferation, motility and metabolism. Prime examples include the regulation of the forkhead box O (FOXO) and glycogen synthase kinase 3 (GSK3) (49). The FOXO family of proteins control expression of molecules involved in the apoptotic cascade and key cell cycle regulators, with the primary role of inhibiting cell

survival and proliferation. ERK, AKT, and SGK can all phosphorylate various members of the FOXO proteins on specific residues that lead to their ultimate degradation and sequestration, therefore restricting their nuclear translocation and preventing apoptotic transcriptional machinery (63-66). Moreover, GSK3 can be directly regulated by ERK, AKT, PKC, and S6K. GSK3 functions to inhibit survival, proliferation, and motility targets including beta-catenin and various adhesion proteins. It can also phosphorylate and activate TSC2 and lead to inactivation of mTORC1 signaling (67).

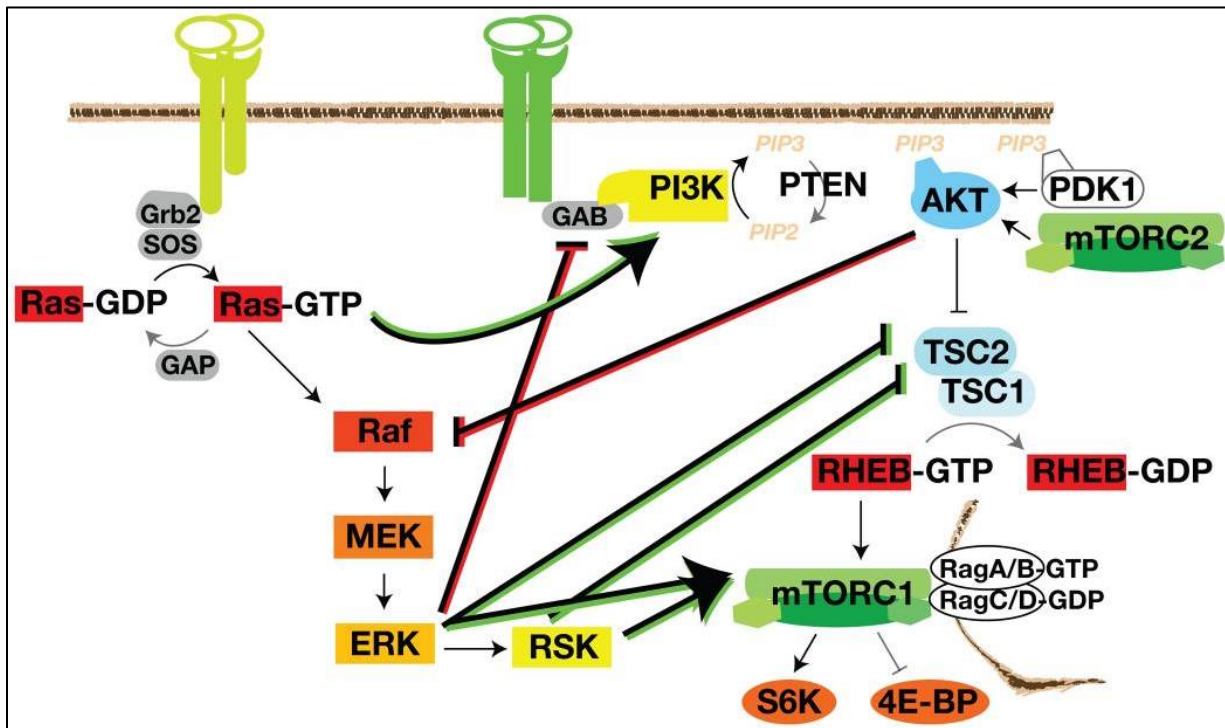


Figure 5. Pathway Crosstalk. The Ras-MAPK and PI3K-mTORC1 pathways regulate each other via cross-inhibition (red) and cross-activation (green). Each pathway has a mechanism to negatively feed onto the other: ERK phosphorylation of GAB and AKT phosphorylation of Raf. Components of the Ras-ERK pathway (Ras, Raf, ERK, and RSK) also positively regulate the PI3K-mTORC1 pathway. TSC2 and mTORC1 are key integration points that receive many inputs from both the Ras-ERK and PI3K signaling. Positive regulation of the substrate protein is shown as an arrow. Negative regulation of the substrate protein is depicted as a blunt-ended line.

Reprinted with permission from: Mendoza MC, Er EE, Blenis J. The Ras-ERK and PI3K-mTOR pathways: cross-talk and compensation. Trends in biochemical sciences. 2011;36(6):320-8. doi: 10.1016/j.tibs.2011.03.006. (49) License # 3961020803450

1.6 Therapeutic implications of targeting the PI3K/AKT/mTOR pathway

NSCLC harbors molecular alterations involving the PI3K/AKT/mTOR and MAPK pathways, and thus, pharmacologic inhibitors of both pathways are given extensive priority for development to further test in the clinic. Deregulations of the PI3K/AKT/mTOR pathway occur at variable frequencies in lung tumorigenesis and have been correlated with more advanced stage disease as well as tumor grade (68). Aberrant mechanisms of activation can occur through a variety of ways, including upregulation of RTK activity upstream of PI3K, amplification and/or mutations in *PIK3CA*, *KRAS*, *STK11*, *AKT*, or inactivating mutations in the negative regulator phosphatase and tensin homolog (*PTEN*) (69). Collectively, targeting these pathways remains both an opportunity and a challenge for cancer treatment.

The earliest mTOR inhibitor discovered was rapamycin and was initially developed for use as an active anti-fungal and immunosuppressive agent. The anti-proliferative effects first seen in studies involving cancer cell lines led to the active interest in the mTOR pathway as a potential anti-cancer target of interest. The mechanism by which rapamycin exerts its effects is by allosteric inhibition of the mTORC1 complex with high affinity to the FKBP-12/rapamycin binding (FRB) domain of mTOR (70). Additionally, rapamycin has been shown to selectively inhibit mTORC1 activity and have minimal effects against mTORC2; although extended treatments have shown to increase sensitivity of this complex to the drug in some cellular contexts (71). The general effects seen in the clinic with rapamycin have been modest and mainly result in stability of disease. Analogs of rapamycin have since been developed, which have similar molecular structures but differing physiochemical properties. Examples of these rapalogs include everolimus, temsirolimus, and

deforolimus, and have undergone numerous clinical trials in a wide range of cancers. Thus far, everolimus and temsirolimus have been approved for advanced renal cell carcinoma (72, 73). To increase the anti-tumor response, numerous strategies have been proposed including the combinations of rapalogs with chemotherapeutic drugs to induce cell death or combining targeted therapies specific for the PI3K/AKT/mTOR pathway or parallel pathways.

Moreover, one of the major limitations in the effectiveness of rapalogs has been the discovery of de-repression of negative feedback loops mediated by mTORC1. Studies have elucidated that mTORC1 inhibition releases a negative feedback loop on the insulin receptor substrate (IRS-1) and growth-factor-receptor-bound protein 10 (GRB10), resulting in increased RTK signaling to PI3K, AKT, and/or to other pathways through ERK1/2. Also, rapalogs have been shown to shut down downstream S6K signaling completely, but only inhibit the translational repressor 4EBP1 transiently, therefore protein synthesis, cell proliferation and survival mechanisms can still continue to occur (69, 74, 75). The increased understanding of the drawbacks of first generation mTOR inhibitors resulted in the advent of new catalytic ATP-competitive inhibitors being developed targeting the mTOR kinase domain, with the expectation to inhibit both of the critical mTORC1 and mTORC2 complexes and prevent feedback activation of AKT (76, 77). Early clinical trials identified mTORC1/2 inhibitors having superior single agent activity compared with previous rapalogs. Partial responses have been reported in NSCLC, estrogen receptor (ER) positive breast cancer, and hepatocellular carcinoma using either of two mTORC1/2 inhibitors (AZD2014 and CC-223); however, optimized patient selection is

still further warranted and these drugs have not yet reached the initial expectations as single agents (78, 79).

The critical role of PI3K in cancer led to significant efforts in developing drugs targeting it, many of which are still undergoing clinical evaluation in various phases of trials. There are three distinct PI3K classes which are further subdivided into varying isoforms. Class IA PI3Ks are the most studied and are made up of a p110 catalytic subunit (encoded by three homologous isoforms: p110 α , p110 β and p110 δ) and a p85 regulatory subunit (16). Compared to other targeted drugs aimed at oncogenic kinases (e.g. EGFR, RAF, ALK), inhibitors against PI3K have had limited efficacy as single arm treatments in early phase clinical trials in tumors that harbored PI3K pathway hyperactivation (18). First generation pan-PI3K inhibitors were initially developed, such as wortmannin and LY294002, but were hindered in early phases of human trials due to their toxicities and lack of specificity. Most of these inhibitors in early clinical trials are catalytic ATP-competitive inhibitors and target all class I PI3K isoforms with similar effectiveness. This could be problematic in that these drugs target all the class I PI3K isoforms regardless of their actual oncogenic role, and moreover, have been shown to display off-target effects on other effectors of the phosphatidylinositol 3-kinase-related kinases (PIKK) family, including ATM Serine/Threonine Kinase (ATM), Ataxia Telangiectasia And Rad3-Related Protein (ATR), and DNA-dependent Protein Kinase (DNA-PK) (80, 81). Therefore, isoform-specific inhibitors are now being developed for clinical testing with the expectation for achieving better safety and efficacy profiles and reduce toxicity. Determining the specific disease settings by which the different PI3K isoforms contribute to the tumorigenic phenotype will be crucial to increase the effectiveness of these inhibitors.

Furthermore, AKT inhibitors have also been developed, particularly since this master regulator integrates the central node of the PI3K/mTOR pathway. Several ATP mimetics and inhibitors of non-catalytic sites of AKT have been pushed into the clinic for evaluation. Although AKT1 activating mutations occur infrequently in NSCLC, overexpression of AKT1 and AKT2 occurs at higher rates, exposing possible therapeutic vulnerability to these AKT inhibitory agents (69, 82). However, early phase trials have shown, at best, stability in disease as the most encouraging overall response with anti-proliferative, rather than anti-tumorigenic, effects mediated by single agent therapy (83, 84). Furthermore, experimental models and early clinical trials have suggested that AKT-specific inhibitors may be most efficacious in specific molecular settings, particularly in tumors harboring *PTEN* loss or *PIK3CA* mutations, leading to the hyperactivity of the AKT mediated pathway. Importantly, resistance mechanisms such as the relief of mTORC1 feedback inhibition on IRS-1 signaling (mentioned above), and de-repression of FOXO leading to increased activation of RTKs, PI3K, PDK1, and other targets downstream of AKT, have been also elucidated (85). In all, AKT inhibitors are being approached with caution as their disturbance to the AKT pathway can lead to metabolic dysregulations and hyperglycemia (86).

1.7 Therapeutic implications of targeting the RAS/RAF/MEK (MAPK) pathway

Three RAS genes (*HRAS*, *NRAS*, *KRAS*) have been identified and aberrant mutations in these isoforms have been discovered to have major oncogenic implications. Specifically, *KRAS* mutations are the most prevalent and have been found in 1/3 of all cancers, including colon, pancreatic, and lung. The most frequent codons of *KRAS* that are mutated in lung cancers occur at codons 12, 13 and 61 (87). Mutations in this oncogene result in a constitutively active *KRAS* leading to

hyperactivity of the MAPK and mTOR pathways. For over two decades, numerous strategies were attempted to target oncogenic *KRAS* signaling, including direct inhibitors of the protein, RNA interference, inhibitors that prevent localization of RAS to the membrane, and targeting drugs of downstream effectors (88). One of the earliest efforts to block RAS was through abrogation of its localization via farnesylation to the plasma membrane via farnesyl transferase inhibitors. However, this drug class failed when pursued for evaluation in pre-defined mutant *KRAS* cancers, since eventual recognition that *KRAS* could be alternatively modified via other mechanisms to relieve the translocation repression, ultimately allowed *KRAS* back to the plasma membrane even in the absence of farnesylation (89).

Refocused therapeutic strategies have gained momentum over the years by developing targeted therapies against effectors downstream of *KRAS*. Notably, the identification of *BRAF* mutations in melanomas have sparked clinical testing of multiple RAF kinase inhibitors. *BRAF* mutations have been reported in about 2-3% of lung adenocarcinomas. Based on previous marked anti-tumor activity in *BRAF*^{V600E} mutant melanoma, mutant *BRAF* inhibitors (e.g. dabrafenib, vemurafenib) have made it into clinical evaluation for advanced stage *BRAF* positive NSCLC (90). However, the efficacy of these inhibitors in the *KRAS* mutant setting still remains to be resolved as responses with single agent RAF inhibitors have been poor, specifically in *KRAS* mutant settings. Studies have elucidated paradoxical reactivation of downstream ERK1/2 following *BRAF* inhibition. Specifically, *BRAF* inhibitors resulted in either relief of RAF-inhibitory autophosphorylation mechanisms or RAF inhibitor-induced transactivation of RAF dimerization, leading to increased ERK signaling (91-94).

Thus, combination regimens to combat such bypass mechanisms of resistance are still being established and evaluated in the clinical setting.

Resistance mechanisms of RAF inhibition prompted avid development of downstream MEK targeted therapies with the hopes of more durable pathway inhibition. Selumetinib and trametinib are two allosteric MEK1/2 inhibitors that have been evaluated as either single agents or in combination with cytotoxic agents to target mutant *KRAS* NSCLC. Early stage clinical trials showed that selumetinib as a single agent led to tumor responses in advanced cancer patients; however, phase II trials in selected patient populations with previously treated NSCLC (including some patients with *KRAS* mutations) showed little clinical activity (95, 96). Further, based on pre-clinical *in vivo* evidence, studies showed that cytotoxic agents such as docetaxel in combination with selumetinib resulted in synergistic anti-tumor effects, and thus sparked clinical trials of this dual combination. Results from a phase II trial evaluating this combination in advanced stage (III-IV) chemo-refractory *KRAS* mutant NSCLC patients found a trend in better overall survival (OS), but the study failed to meet the primary endpoint, and only a fraction of the patients were partial responders (97). In addition, trametinib has also been examined in the clinic. A phase II trial evaluating trametinib as monotherapy versus docetaxel in *KRAS* mutant NSCLC resulted in no statistically significant or clinically meaningful endpoints (98). Current studies are evaluating the combination of trametinib with chemotherapy drugs such as docetaxel or pemetrexed. Collectively, it can be concluded that although MEK inhibitors can have the potential for significant anti-tumor effects, better patient selection, optimization of dosing regimens, and rational combinatorial therapeutic strategies are necessary to find significant clinical utility of these agents.

1.8 RICTOR's mTORC2-dependent and independent tumorigenic functions

The mTORC2 complex is comprised of mTOR and the essential components RICTOR, mSIN1, and mLST8. This complex regulates a variety of important cellular functions including proliferation, survival, and metabolism through phosphorylation of various AGC kinase family members such as AKT, PKC α , and SGK (99). RICTOR and mSIN1 function as adaptor molecules serving as critical regulators of mTORC2 substrate specificity and binding. Specifically, RICTOR's Gly-934 residue is critical in the formation of the RICTOR/mSIN1 heterodimer interaction required for the structural integrity, stability, and functionality of the complex (100).

Increasing reports have elucidated the contribution of RICTOR toward tumorigenic phenotypes functioning through mTORC2-dependent and independent manners. Initially, RICTOR's ortholog studied in *Dictyostelium* was found to be a mediator of cell migration and chemotaxis (101). Moreover, multiple *in vitro* studies have indicated RICTOR's role, in conjunction with mTORC2, in cell migration and cytoskeletal regulation via the phosphorylation of PKC α , paxillin, RhoA, and Rac1 (41, 102). Moreover, mTORC2 activity is elevated in gliomas, as evidenced by overexpression of RICTOR in cell lines and primary tumor cells, resulting in enhanced growth and cellular motility (103). Although most of the functional roles of RICTOR have been characterized as part of mTORC2, RICTOR carries exclusive independent roles. For example, RICTOR was shown to form a separate complex with Myo1c, independent of mTORC2, and participates in cortical actin remodeling events (104). Recently, insight into the mechanism underlying RICTOR's regulation of cell migration and potential contribution to metastasis was elucidated by finding that RICTOR suppresses RhoGDI2, independently of the mTORC1/2 complexes, promoting the

activity of the Rho proteins RAC1 and CDC42 (105, 106). Importantly, RhoGDI2 has been previously implicated as an invasion and metastasis suppressor gene and thus, its loss has been associated with metastatic cancers (107).

Additionally, RICTOR can interact with integrin-linked kinase (ILK) to increase AKT phosphorylation and regulate cancer cell survival, and this RICTOR/ILK complex is also a critical component and mediator of TGF β -1-induced epithelial-to-mesenchymal transition (EMT) in mammary epithelial cells (108, 109). Further, a kinase-independent function for RICTOR has been proposed through its specific association with CULLIN-1 and RBX1, forming a functional E3 ubiquitin ligase complex that promotes SGK1 ubiquitination and degradation, providing a mechanistic explanation for the high SGK1 expression in various cancers (110, 111). Micro-RNA (miRNA) regulation of RICTOR has also been reported by linking the overexpression of RICTOR as a target of *miR-218*, suggesting that the epigenetic silencing of this miRNA and subsequent activation of the AKT signaling pathway significantly contributes to oral carcinogenesis (112). Lastly, RICTOR has been shown to be required for the development of prostate cancer in the context of *PTEN* loss, and the targeting of RICTOR can induce G1 cell cycle arrest and reduction in cyclin D1 expression levels in colon, breast, and prostate cancer cells (113-115). In summary, RICTOR's oncogenic role is increasingly becoming evident, as this scaffold molecule can regulate a multitude of tumorigenic events such as cellular motility, morphology, cell proliferation, survival, and protein degradation.

1.9 Hypothesis and specific aims

In summary, the paradigm shift of treatment and diagnosis of lung cancer has emerged from a single disease entity with limited therapeutic opportunity to one that is comprised of multiple histotypes, each with its own genomic profile, sparking a personalized medicinal approach to therapy. Although there are specific examples of targeted therapies making drastic impact on overall survival of patients with tumors that are driven by specific oncogenes (e.g. *EGFR*, *ALK*, *B-RAF*), over 30% of lung adenocarcinomas are still yet to uncover the genetic underpinnings driving these tumors (Figure 2). In an effort to identify novel potentially actionable targets that contribute to mechanisms of resistance to targeted therapies, we utilized molecular profiling data associated with the BATTLE-2 clinical trial, which enrolled advanced stage chemorefractory NSCLC patients with the goal of evaluating the effects of targeted therapies based on *KRAS*-mutated lung tumors (116). Since the majority of enrolled cases were lung adenocarcinomas, we focused our studies on this lung cancer subtype and identified a subgroup (17%) of advanced stage patients with *RICTOR* genomic alterations (mutations or amplifications). *RICTOR*'s precise role in the context of NSCLC has not been extensively evaluated. A recent study classified *RICTOR* amplifications as a novel subset of patients with lung cancer that may respond to dual mTORC1/2 inhibitors (117). To expand on this finding, we were interested to further define settings where *RICTOR* or *RICTOR*-associated signaling blockade in combination with targeted therapy may enhance response in metastatic disease and improve outcome.

Therefore, the proposed hypothesis is that *RICTOR* alterations promote oncogenic properties and RICTOR-associated signaling blockade could serve as an effective therapeutic strategy in *KRAS* mutant NSCLC.

To pursue this hypothesis, the following specific aims were developed:

- **Specific Aim 1:** To assess the prevalence of *RICTOR* alterations in early and advanced stage NSCLC and determine if these alterations correlate with clinical outcome.
- **Specific Aim 2:** To determine the phenotypic consequences of *RICTOR* knockdown in *in vitro* and *in vivo* NSCLC models.
- **Specific Aim 3:** To evaluate the potential therapeutic benefit of RICTOR-associated signaling blockade in pre-clinical NSCLC models.

Chapter 2

Materials and Methods

Cell lines and reagents

NSCLC cell lines (H23, H2009, H1792, H1650, H3122, H2172, H2126, A549, HCC44, CALU6, HCC193, and H1819) were either obtained from American Type Tissue Collection (ATCC, Manassas, VA) or were obtained from collaborators and authenticated via STR DNA fingerprinting at the University of Texas MD Anderson Characterized Cell Line Core (CCLC). All cell lines were grown in RPMI 1640 supplemented with 10% FBS (Cellgro, Mediatech, Manassas, VA) with no antibiotics. Whole genome single nucleotide polymorphism (SNP) array profiling (previously described (118)) was obtained for the cell line panel to determine *RICTOR* amplified (copy number variation (CNV ≥ 3.5) and non-amplified cell lines (CNV = 2). Immortalized human bronchial epithelial cells (HBEC) expressing wild-type *KRAS* (HBEC3-KT) or *KRAS*-mutant with stable *p53* knockdown (HBEC3-KT53KC12) cell lines were provided by Drs. Adi Gazdar and John Minna (University of Texas Southwestern Medical Center, Dallas, TX) and maintained in keratinocyte-SFM medium with bovine pituitary extract and human recombinant epidermal growth factor (Invitrogen). Generation of stable *RICTOR* knockdown cell lines were developed using pTRIPZ inducible lentiviral shRNA-encoding plasmids (*RICTOR* shRNA #RHS4696, Non-silencing shRNAmir Control (NTC) #RHS4743) (GE Dharmacon, Lafayette, Colorado) for the inducible knockdown of *RICTOR* in the presence of 2 μ g/mL doxycycline hyclate (SIGMA) and were selected with 2 μ g/mL puromycin (SIGMA). RFP expression was also utilized for monitoring transduction and

knockdown efficiency. Targeted inhibitors AZD2014 (vistusertib), AZD6244 (selumetinib), and GSK1120212 (trametinib) were obtained from Selleck Chemicals (Houston, TX) and dissolved in DMSO to create stock solutions. All additional dilutions were performed using the respective cell culture medium for working concentrations.

Immunoblotting and antibodies

Western blotting analyses were performed on total protein lysates extracted from NSCLC cell lines. In brief, cell cultures were washed with ice-cold phosphate buffered saline (1X PBS) containing protease and phosphatase inhibitor tablets (Roche, Basel, Switzerland) and homogenized in 1X RIPA buffer (SIGMA-Aldrich, St. Louis, MO). The cells were scraped and samples were centrifuged at 14,000 rpm for 25 minutes at 4C and protein concentrations of supernatants were quantified by DC Protein Assay per manufacturer's instructions (Bio-Rad, Hercules, CA). Equal amounts of protein were separated by pre-cast 4-15% gradient gels (Bio-Rad) via SDS-PAGE and transferred onto nitrocellulose membranes using the Trans-Blot Turbo Transfer System (Bio-Rad). Membranes were blocked with 5% milk for 1 hour, and all washes were in TBS-T. The membranes were incubated with the following commercial antibodies: RICTOR, p-RICTOR (Thr1135), p-AKT (Ser473), AKT, p-MEK1/2 (Ser217/221), MEK1/2, p-p44/42 MAPK (Thr202/Tyr204) (p-ERK1/2), ERK1/2, c-PARP, PARP, p-mTOR (S2481), mTOR, p-NDRG1 (Thr346), NDRG1, mSIN1 are from Cell Signaling Technologies (Danvers, MA); β -actin-HRP (used as equal loading control) and p-PKC α (Ser657) are from Santa Cruz Biotechnology (Santa Cruz, CA). Secondary antibodies included horseradish peroxidase-conjugated anti-rabbit or anti-mouse antibodies obtained from Cell Signaling Technologies.

Immunoreactivity was visualized by use of Western Lightning Plus-ECL (Perkin-Elmer, Waltham, MA) and exposure to x-ray film according to manufacturer instructions. Densitometric quantification of bands was performed using Image Studio Lite 5.0 software (Lincoln, Nebraska).

siRNA knockdown studies

Knockdown studies were performed using ON-TARGETplus SMARTpool siRNAs targeting the gene of interest at a final concentration of 30 nmol/L using DharmaFECT I transfection reagent (GE Dharmacon, RNAi Technologies, Thermo). ON-TARGETplus Non-targeting siRNA pools served as negative controls. siRNAs were prepared using Opti-MEM I serum free media (ThermoFisher), and added to culture dishes for 24 hours. Fresh complete media was replaced after 24 hours and incubation continued for a total of 72-96 hours before downstream analysis.

Cell viability assays

For MTS assay testing cell viability, NSCLC cells were seeded in octuplicate at a density of 2,000 cells per well in 96-well plates. An endpoint viability assay was performed using MTS assay (3-(4, 5-dimethyl-thiazol-2-yl)-5-(3-carboxymethoxyphenyl)-2-(4-sulfophenyl)-2H-tetrazolium, inner salt) at the indicated time points according to the manufacturer's protocol (Promega, Madison, WI). For experiments evaluating the effect of *RICTOR* knockdown with mTORC1/2 and/or MEK1/2 inhibitors, the crystal violet staining and MTT dye reduction method was used. Stable inducible sh*RICTOR* cell lines were seeded at 2×10^4 cells per well in 6-well plates in the presence of 2 μ g/mL doxycycline. The next day, each well was treated with either selumetinib, trametinib, AZD2014, or DMSO (control) at the

indicated concentrations and incubation was continued for a further 7 to 10 days, with drug/media changed every 3 days. MTT solution (Methylthiazolyldiphenyl-tetrazolium bromide, 1 mL per well, 2mg/mL; SIGMA-Aldrich) was added to each well, followed by incubation for 2-3 hours at 37°C. The media was then removed and the dark blue crystals in each well were dissolved in 400µL of DMSO and transferred to 96-well plates. Absorbance was measured at test and reference wavelengths of 550 and 630 nm, respectively, using a FLUOstar Omega microplate reader (BMG LABTECH, Ortenberg, Germany). The percentage of cell viability is shown relative to untreated controls.

Cell proliferation assay

Cell proliferation was performed using stably transduced sh*RICTOR* cell lines (H23, H2009, H1792) by seeding 4×10^5 cells in 10cm dishes in +/- doxycycline containing media. Time points were analyzed at 4, 8, 12, and 16 days of continuous sh*RICTOR* (+doxycycline) treatment to evaluate the effects of *RICTOR* knockdown. Total cell number was counted and recorded using the Cellometer K2 Image Cytometer (Nexcelom, Lawrence, MA). A fixed ratio of cells was subsequently split into new dishes and sub-cultured for the indicated time points of the experiment.

Cell cycle analysis

For cell cycle analysis, cells were harvested via trypsinization, washed with ice-cold 1X PBS, and fixed with 70% ice-cold ethanol. Fixed cells were then re-washed, treated and stained with propidium iodide/RNase using the Propidium Iodide Flow Cytometry Kit (Abcam, Cambridge, UK) per manufacturer's protocol. Stained cells

were immediately analyzed using the BCI Gallios Analyzer flow cytometer (Beckman Coulter, Brea, CA).

Human p-MAPK Array

A Proteome Profiler Array (Human Phospho-MAPK Array Kit) (R&D Systems, Inc., Minneapolis, MN) was used to assess the relative level of phosphorylation of 26 kinases involved in the three major families of MAPK pathways. Array was performed according to manufacturer's instructions. H23 cells were treated with either NTC or *siRICTOR* for 72 hours, and the cells were subjected to lysis using the buffer provided in the kit. The arrays were then blocked with blocking buffer and incubated with the cell lysates (300 µg/sample) overnight at 4C. The next day, arrays were washed and incubated with a biotinylated antibody for 2 hours, washed, and incubated with a streptavidin-horseradish-peroxidase-conjugated detection antibody, treated with Western Lightning Plus-ECL, and exposed to x-ray film.

Clonogenic survival assay

NSCLC cells were seeded in 6-well plates (250-500 cells per well) in the presence or absence of 2µg/mL doxycycline for inducible *shRICTOR* cell lines or non-targeting control (or siRNA against RICTOR) for 2-3 weeks, with change of media every 2-3 days. After the endpoint, wells were washed with PBS and fixed with 4% paraformaldehyde for 10 minutes, followed by staining with 0.05% crystal violet for 30 minutes. Stained wells were then washed thoroughly with water to clear any unbound crystal violet. Colony area was calculated using Image J software (NIH, Bethesda, Maryland) to determine percentage area stained relative to control. Soft agar assay testing anchorage independent growth was performed using Millipore's Cell

Transformation Detection Assay per manufacturer's recommendations (Merck KGaA, Darmstadt, Germany). In brief, 6-well plates were prepared with 0.8% base agar layer and allowed to solidify. 2,500 cells/well were resuspended in 0.4% top agar solution and aliquoted appropriately on top of the base agar layer (pre-warmed to 37°C).

Doxycycline containing media was used to induce continuous sh*RICTOR* knockdown compared to NTC. Cells were incubated for 21-28 days at 37°C until colonies were formed, with frequent media change every 3 days. Colonies were then visualized with the accompanied cell stain solution and quantified with the cell quantification solution by measuring absorbance at 490nm. A well containing only base and top agar layers without cells served as background control for quantification.

Migration and Invasion assays

The cell migration assay was performed using a 24-well transwell plate with 8µm polyethylene terephthalate (PET) membrane filters (Corning Inc., Corning, NY) that separate the top and bottom culture chambers. In brief, respective NSCLC cell lines were transfected with siRNA targeting *RICTOR* for 72 hours, harvested, and plated in the upper chamber at a density of 20,000 cells per well in 500µL of 0.5% reduced serum RPMI 1640 media. The bottom chambers contained 750µL of either 5% serum (serves as chemoattractant) or 0.5% reduced serum conditions. Cells were allowed to migrate for 24 hours, and filters were then removed and non-migrant cells on the upper side were wiped away with use of a cotton swab. Filters were fixed and stained using the Diff-Quik Stain Set Kit (Siemens Healthcare Diagnostics, Newark, DE) per manufacturer's protocol and mounted onto microscope slides. Five random fields were quantified at 10X objective lens in a light microscope, and results are displayed as the average number of cells migrated. The cell invasion assay was

similar to the described protocol above, except that the transwell chambers used were Corning BioCoat Growth Factor Reduced Matrigel invasion chambers and cells were fixed and stained after 48 hours of incubation.

Xenograft tumor models

All animal procedures and care were approved by the MD Anderson Cancer Center Institutional Animal Care and Usage Committee. Animals received humane care as per the Animal Welfare Act and the NIH "Guide for the Care and Use of Laboratory Animals". For tumorigenicity studies evaluating the effects of *RICTOR* knockdown, H1792 and H23 stable sh*RICTOR* inducible cell lines were expanded and harvested, washed, and pre-cooled in serum-free RPMI 1640 medium mixed 1:1 with Corning growth factor reduced Matrigel Matrix (Corning, NY). Female athymic nude mice, between 6-8 weeks old, were injected subcutaneously in the flank with H1792 (2×10^6) or H23 (5×10^6) sh*RICTOR* cells. Mice were divided into two groups with 6 mice per arm: doxycycline feed (600mg/kg; BioServ, Flemington, NJ) immediately after inoculation of cells, or control group (regular feed). Tumors were measured twice weekly with a digital caliper, and size was calculated as $(\text{length} \times \text{width}^2/2)$. The mice were euthanized and the tumors were collected for protein lysate analysis. Protein lysates were prepared by homogenization using the Precellys24 tissue homogenizer (Bertin Instruments, France).

For studying the effects of drug treatments on xenograft growth, H1792 sh*RICTOR* cells (4×10^6) were prepared as described above and injected subcutaneously in the flanks of 6-8 week old female athymic nude mice. After the average tumor volumes reached 100mm^3 , mice were randomized into 1 of 5

treatment arms (6 mice/arm), and the indicated treatment regimens were performed by oral gavage for 22 days. The treatment arms consisted of: vehicle (1% tween-80, *bid*), selumetinib (25mg/kg, *bid*), selumetinib (25mg/kg, *bid*) + doxycycline feed (600mg/kg), AZD2014 (15mg/kg, *qd*), and selumetinib + AZD2014 (equivalent dosages used as per individual inhibitor treatments). Selumetinib was obtained from Selleck Chemicals and AZD2014 was obtained from MedChem Express (Monmouth Junction, NJ). Tumor volumes and body weights were recorded twice weekly. Tumors were extracted on the final day 3 hours following the last treatment, and protein lysates were prepared as described above.

Clinical datasets and patient sample characteristics

A total of 3 datasets were analyzed independently in our study: the Biomarker Integrated Approaches of Targeted Therapy for Lung Cancer Elimination (BATTLE-2, n=92 lung adeno cases with mutation data; n=107 lung adeno cases with mRNA expression data), The Cancer Genome Atlas (TCGA Lung Adenocarcinoma, n=230 with mutation cases, n=496 with mRNA expression data), and Profiling of Resistance Patterns and Oncogenic Signaling Pathways in Evaluation of the Thorax (PROSPECT, n=151). The BATTLE-2 trial is a randomized phase II, multi-center biopsy-mandated and biomarker-based clinical trial of targeted therapy in advanced stage chemorefractory NSCLC (116). Clinical and genomic data for 230 mostly early-stage, surgically resected lung adenocarcinomas that were analyzed in the TCGA dataset was obtained from the cBio Cancer Genomics Portal and GDC data portal (<https://gdc.nci.nih.gov/>) (119, 120). The PROSPECT dataset includes surgically resected tumor tissue collected from patients with lung adenocarcinoma at MD Anderson Cancer Center. Bioinformatics analyses and support was provided by Dr.

Jing Wang and Li Shen (Department of Bioinformatics and Computational Biology, MD Anderson Cancer Center).

Statistical analyses

The results presented are the average of at least two experiments each performed at least in triplicate. Data obtained from cell culture assays were summarized using descriptive and inferential statistical analyses accompanied by graphs and conducted by using GraphPad Prism 6 (GraphPad Software, La Jolla, CA). Differences between groups were calculated by the *t*-test unless otherwise noted. A *P*-value < 0.05 was considered significant. Cox hazard proportional models were applied for association between mRNA expression and overall survival.

Chapter 3

Results

3.1 Identification of *RICTOR* alterations in advanced NSCLC

NSCLC is biologically and genomically diverse and has differing responses to standard chemotherapy and targeted therapy developed to inhibit key molecular aberrations that drive cancer progression. However, over 30% of lung adenocarcinomas that are diagnosed have alterations that do not have a therapeutic target. In an effort to identify novel potentially actionable targets in advanced stage NSCLC, we utilized genomic profiling from an ongoing clinical trial termed the **B**iomarker-Integrated **A**pproaches of **T**argeted **T**herapy for **L**ung Cancer **E**limination (BATTLE-2) as a platform for our studies. The BATTLE-2 was a phase II trial that specifically targeted advanced stage, chemorefractory NSCLC patients who have failed at least one prior chemotherapeutic regimen (116). Patients were adaptively randomized by *KRAS* status to one of four treatment arms: erlotinib (EGFRi), erlotinib plus MK2206 (AKTi), MK2206 plus selumetinib (AZD6244; MEKi), or sorafenib (RAFi/VEGFRi) (Figure 6). Prospective biopsies based on specified tumor markers were utilized for adaptive randomization to assign patients to the treatment arm with the most potential benefit on the basis of cumulative data at the time. Molecular profiling was performed on all acquired biopsies via the FoundationOne hybridization capture-based next-generation sequencing (NGS) test which evaluated over 182 cancer-related genes (Foundation Medicine, Inc.).

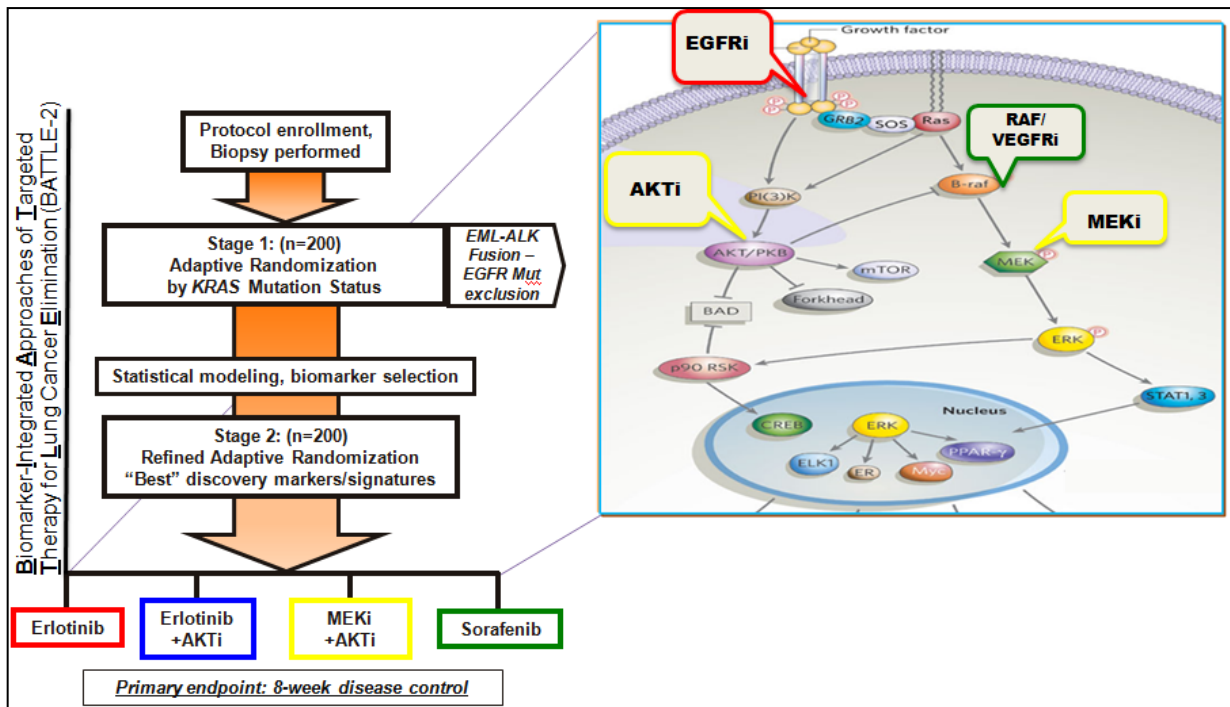


Figure 6. Identifying novel actionable targets in refractory NSCLC using the BATTLE-2 clinical trial. The **B**iomarker-Integrated **A**pproaches of **T**argeted **T**herapy for **L**ung **C**ancer **E**limination (BATTLE-2) is a phase II trial that specifically targets advanced stage, chemorefractory *KRAS* mutated NSCLC patients that have failed at least one prior chemotherapeutic regimen. Exclusion criteria included tumors with sensitizing *EGFR* mutations or *ALK* gene fusions if they had not been previously treated with erlotinib or crizotinib. Patients agree to a baseline tumor biopsy (for biomarker analysis) and were adaptively randomized by *KRAS* status to one of four treatment arms: erlotinib (EGFRi), erlotinib plus MK2206 (AKTi), MK2206 plus selumetinib (AZD6244, MEKi), or sorafenib (RAFi, VEGFRi). The primary endpoint was 8-week disease control rate based on Response Evaluation Criteria in Solid Tumors (RECIST). The specific nodes of the pathways targeted are illustrated.

The detailed protocol and analysis of the NGS assay has been previously reported (121). The frequency of selected genes identified from the NGS targeted panel that carry mutations and/or amplifications are shown in Figure 7, which includes the entire NSCLC BATTLE-2 cases sequenced. The criteria used to identify potentially actionable targets were to first identify genes that were amplified or mutated, followed by if they were targetable. We focused our attention on *RICTOR* alterations as they have not been extensively studied in the context of NSCLC and are present at a relatively high frequency, suggesting possible actionability.

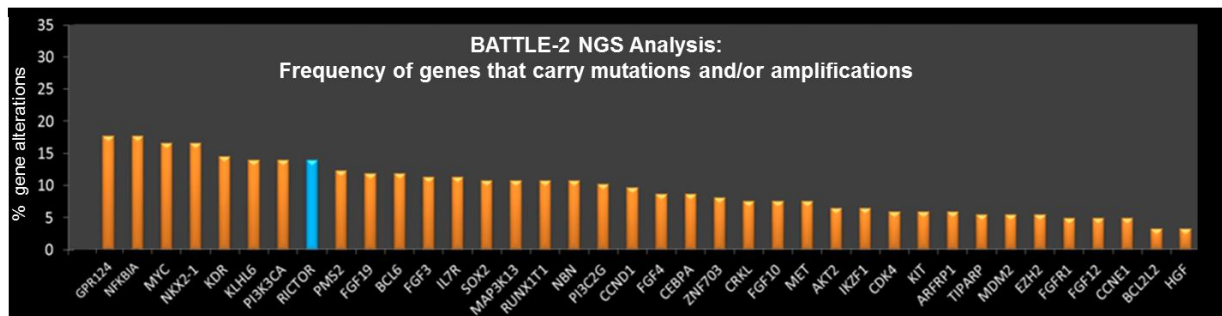


Figure 7. Frequency of potentially actionable genes that carry mutations and/or amplifications from the NGS FoundationOne targeted panel. The percentage shown is out of 159 NSCLC cases that have mutation/copy number alteration data. Frequently altered genes, such as *KRAS* and *EGFR*, were excluded from this graph since these were not novel targets. Genes are listed in Abbreviations section. The frequency of *RICTOR* gene alterations (~13.2%, 21/159) is highlighted in blue.

Moreover, we filtered our studies to lung adenocarcinoma cases since the majority of the enrolled patient population in the BATTLE-2 trial were of this NSCLC subtype. A total of 92 chemorefractory lung adenocarcinoma tumor biopsies have undergone NGS profiling. We identified *RICTOR* gene alterations in a total of 17.4%

(16/92) of cases, including 11.9% amplifications (11/92) and 5.4% mutations (5/92), which were mutually exclusive (Figure 8A, left).

A)

<i>RICTOR</i> Gene Alterations (BATTLE-2; Lung Adenocarcinoma)			<i>RICTOR</i> Gene Alterations (TCGA; Lung Adenocarcinoma)		
<i>RICTOR</i> alterations	# of Cases (out of 92)	Percentage (%)	<i>RICTOR</i> alterations	# of Cases (out of 230)	Percentage (%)
Amplifications	11	11.9	Amplifications	23	10.0
Mutations	5	5.4	Mutations	12	5.2
Total	16	17.4	Total	31	13.4

B)

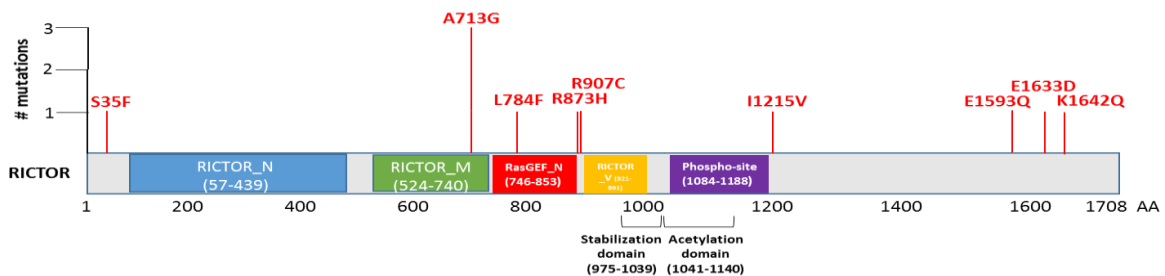


Figure 8. *RICTOR* alterations are present in early and advanced stage lung adenocarcinomas at similar frequencies. (A) Summary of frequency of *RICTOR* gene alterations (mutations or amplifications) in chemorefractory advanced lung adenocarcinoma samples (BATTLE-2, n=92) and in early stage lung adenocarcinoma samples (TCGA, n=230) (8). (B) Schematic of novel *RICTOR* gene mutations from the BATTLE-2 NSCLC cohort and number of mutant cases.

Mutations in the *RICTOR* gene have not been previously identified, particularly the functional roles of these mutations. Figure 8B illustrates the location along the *RICTOR* gene in which these novel mutations occur. The significance of these *RICTOR* mutations are yet to be determined, as the crystal structure of RICTOR has not been elucidated and current bioinformatics tools have failed to identify functional domains of this scaffold protein. However, a recent study attempted to shed light into RICTOR's poorly understood domain architecture by searching for conserved regions to assign structural and functional domains (122). The study identified that similar to its counterpart RAPTOR, RICTOR also has HEAT, WD40, and PH domains that might be utilized for common motif binding to mTORC, mediating cellular localization and transmission of signaling to downstream effectors. Although this is the first such report analyzing RICTOR's domain structure, experimental confirmation is still needed to validate these findings.

Furthermore, to determine whether *RICTOR* alterations are an early event in lung cancer progression, we surveyed the frequency of alterations in early stage lung adenocarcinoma cases utilizing The Cancer Genome Atlas (TCGA) database (120, 123). We identified a similar frequency of a total 13.4% (31/230) of *RICTOR*-altered cases, which included 10% amplifications (25/230) and 5.2% mutations (12/230). Interestingly, in contrast to the BATTLE-2 advanced stage tumors, some early stage tumors from the TCGA incurred concomitant amplifications and mutations (Fig. 8A, right). In addition, in surveying the frequency of *RICTOR* alterations across various cancer types, we found the highest prevalence of alterations in NSCLC, particularly lung adenocarcinoma, compared to other reported tumor types (Figure 9).

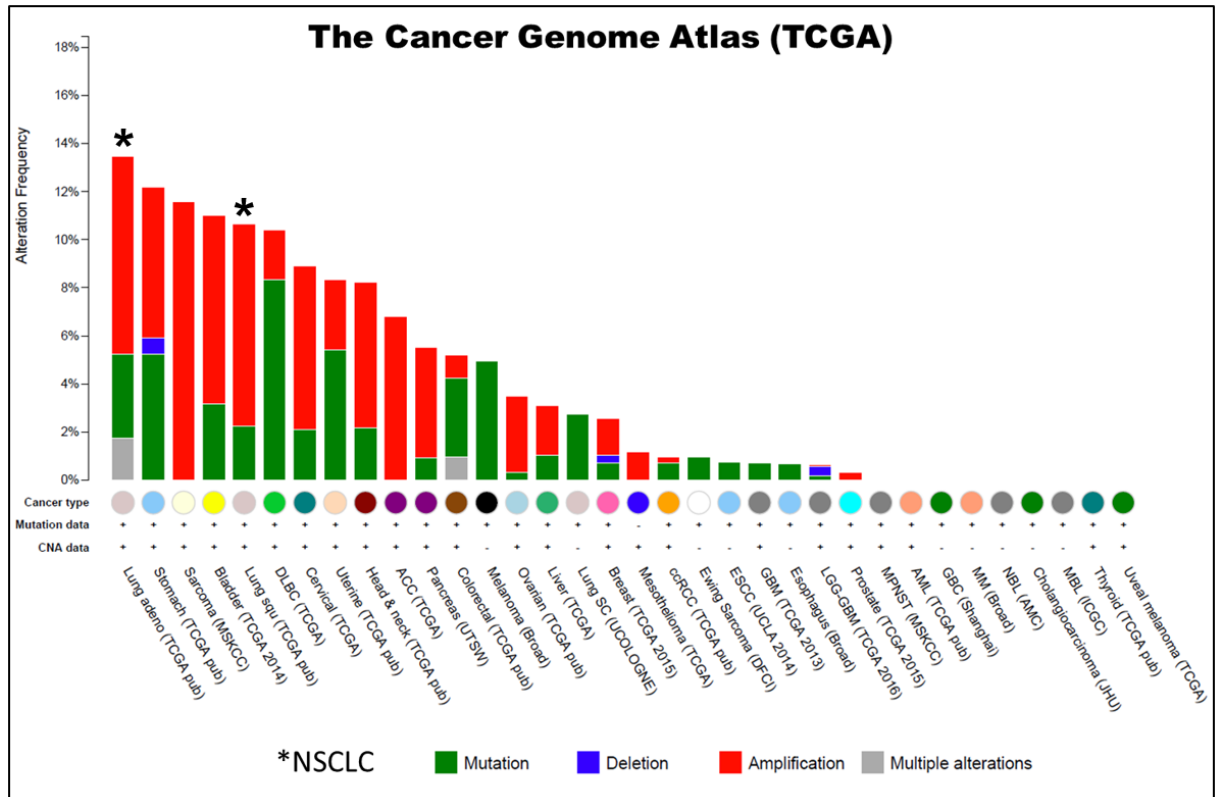


Figure 9. Cross-cancer mutational frequency of *RICTOR* in the TCGA database. cBioPortal query across various cancer types for *RICTOR* DNA mutation frequencies. Alteration frequency is displayed as a histogram across reported cancer studies. NSCLC datasets are marked with an asterisk, showing lung adenocarcinoma as the most frequently mutated tumor type. Database accessed on November 18, 2016.

3.2 *RICTOR* mRNA expression is higher in *RICTOR* amplified than non-amplified NSCLC

We next evaluated the correlation between *RICTOR* amplification and *RICTOR* gene expression in our two datasets. There was a significant direct correlation between *RICTOR* gene amplification and *RICTOR* mRNA expression in the early stage TCGA dataset, and a trend seen in the advanced stage BATTLE-2 lung adenocarcinoma cases (Figure 10). Of note, when we performed this analysis including all NSCLC subtypes from the BATTLE-2 cases (total of 159 cases with DNA NGS profiling), there was statistical significance of direct correlation between *RICTOR* gene amplification and *RICTOR* mRNA expression (data not shown), suggesting that the sample size in the BATTLE-2 adenocarcinoma was too small to reach statistical significance.

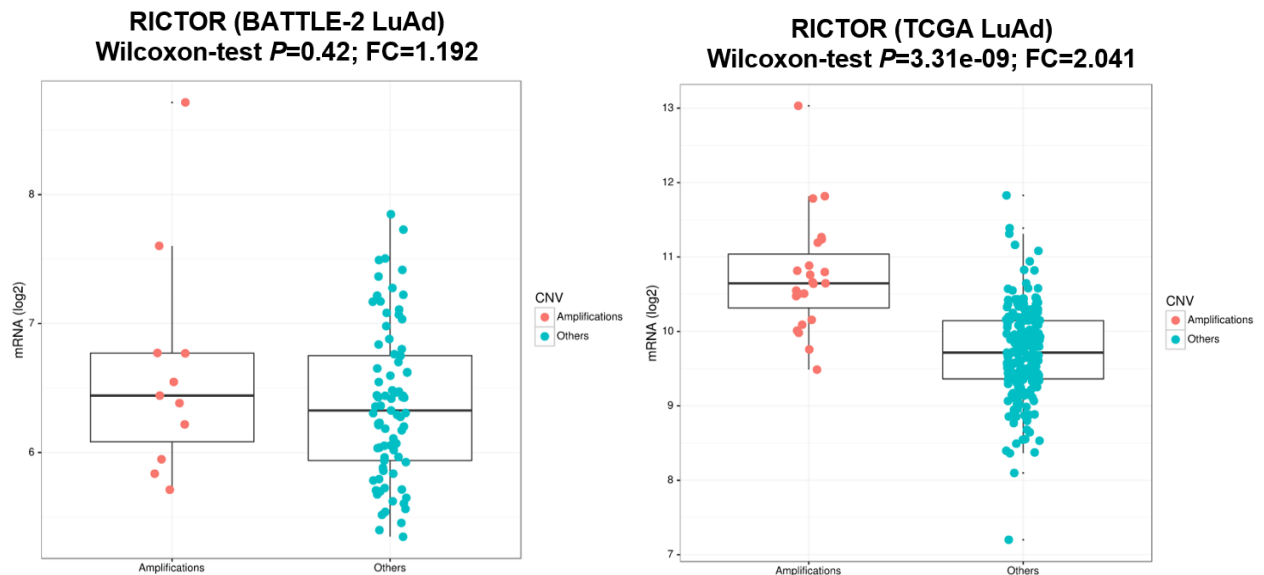


Figure 10. Correlation of *RICTOR* amplification to mRNA gene expression in lung adenocarcinoma cases. Correlation of *RICTOR* amplified vs. non-amplified cases to *RICTOR* mRNA (log₂) expression levels in BATTLE-2 (n=92) (left) and

TCGA (n=230) (right) datasets. *Red circle = amplified RICTOR case; blue circle = non-amplified RICTOR case.*

3.3 Associating *RICTOR* mRNA expression to clinical outcome

To determine the association of *RICTOR* alterations to clinical outcome, we performed a univariate overall survival (OS) analysis of *RICTOR* mRNA expression in lung adenocarcinoma patients using the Cox proportional hazards model. As shown in Table 1, there is significantly worse overall survival in patients with advanced stage lung adenocarcinoma in the BATTLE-2 cases (OS, hazard ratio [HR]: 1.73, 95% confidence interval [CI]: 1.23-2.42, $P=0.0015$). We also saw a worse prognosis in our early stage surgically resected lung adenocarcinoma cases from the PROSPECT dataset (OS, HR: 1.54, 95% CI: 1.03-2.29, $P=0.0337$); however, no significance was seen in patients from the TCGA dataset.

Table 1. Univariate overall survival analysis of *RICTOR* mRNA expression in lung adenocarcinoma patients by Cox proportional hazards model

Study	HR (95% CI)	P-value
BATTLE-2 Trial (n=107)	1.73 (1.23-2.42)	0.0015
PROSPECT (n=151)	1.54 (1.03-2.29)	0.0337
TCGA (n=496)	1.05 (0.81-1.37)	0.675

Abbreviations: HR, hazard ratio; CI, confidence interval.

3.4 Surveying the co-mutational landscape of *RICTOR* alterations

We next explored the co-mutational landscape of *RICTOR*-altered cases using the TCGA lung adenocarcinoma dataset to determine enrichment of specific pathway

alterations that are known to be aberrantly regulated in lung cancers. We surveyed the percent alterations (mutations and/or copy number changes) in several key genes that play important roles in mediating pathways such as receptor tyrosine kinase (RTK) signaling, mTOR signaling, MAPK signaling, and oxidative stress response. The specific gene alterations and frequencies are listed in Table 2. As depicted in Figure 11, there were significantly higher *PTEN* co-mutant cases in the *RICTOR*-altered group, suggestive of a hyperactive PI3K/RICTOR/AKT pathway. Interestingly, there was mutual exclusivity between *RICTOR* alterations and *STK11* mutations in both the TCGA and BATTLE-2 datasets. We found an enrichment of alterations (mutations and/or amplifications) in several key genes of the MAPK pathway in *RICTOR*-altered cases compared to the rest. There was a notably high percentage of *KRAS*, *NF1*, *BRAF/CRAF* alterations in the *RICTOR*-altered cases. These data suggest that RICTOR expression could be an important co-oncogenic driver in lung cancer progression, and thus we focused our efforts on characterizing the importance of RICTOR, specifically in *KRAS* mutant settings.

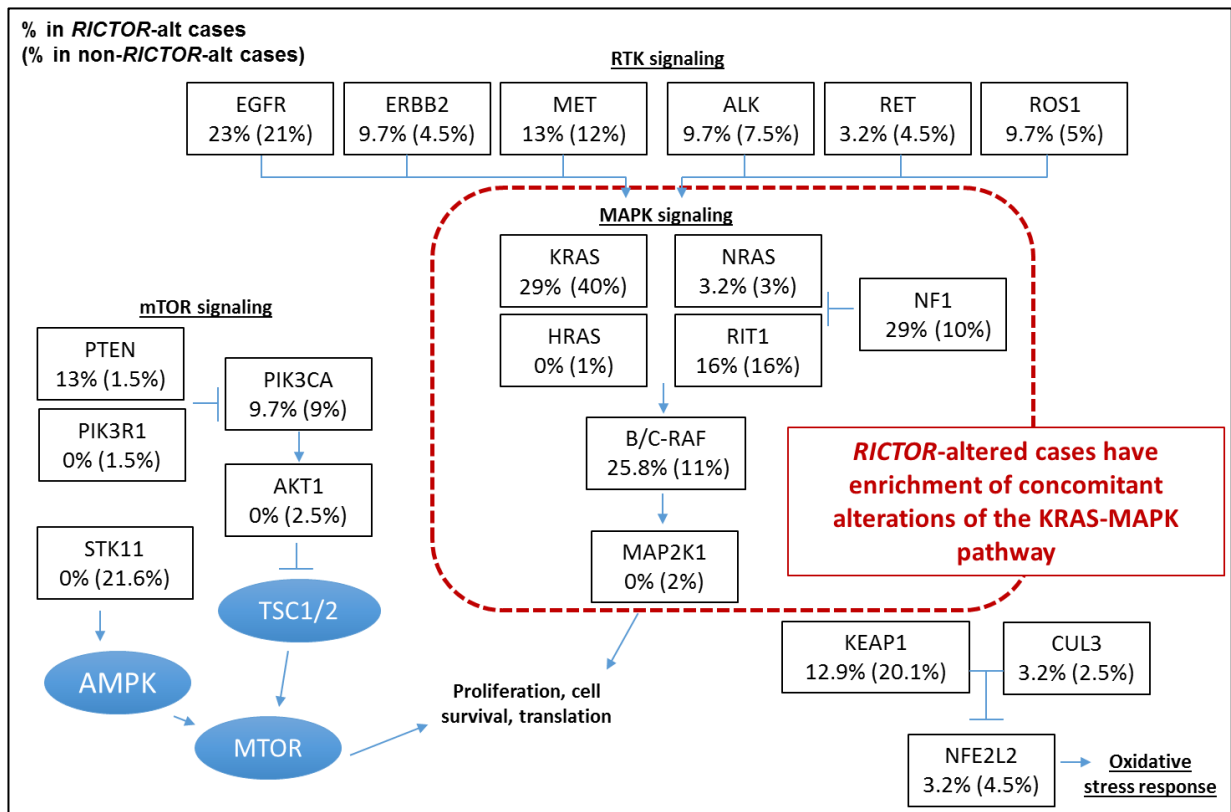


Figure 11. Surveying the co-mutational landscape of *RICTOR*-altered cases.

Selected pathways are shown with percentages of gene alterations (mutations and/or copy number changes) extracted from the lung adenocarcinoma dataset of the cBioPortal for Cancer Genomics. The percentages of gene alterations in *RICTOR*-altered cases (outside parenthesis) are compared to non-altered cases (inside parenthesis).

Table 2. List of co-mutant genes and their frequency of alterations (TCGA LuAd)

Gene	Type of Alt	# in RICTOR alt (%) (out of 31)	# in RICTOR un-alt (%) (out of 199)	Log ratio	p-value	q-value	Tendency
<i>EGFR</i>	mut	4 (12.9%)	29 (14.57%)	-0.18	0.531	0.865	Mut exclusivity
	del	0 (0.00%)	1 (0.50%)	<-10	0.865	0.865	Mut exclusivity
	amp	3 (9.68%)	12 (6.03%)	0.68	0.328	0.801	Co-occurrence
<i>ERBB2</i>	mut	2 (6.45%)	4 (2.01%)	1.68	0.187	0.733	Co-occurrence
	amp	1 (3.23%)	5 (2.51%)	0.36	0.585	0.865	Co-occurrence
<i>MET</i>	mut	1 (3.23%)	18 (9.05%)	-1.49	0.24	0.733	Mutual exclusivity
	del	0 (0.00%)	1 (0.50%)	<-10	0.865	0.865	Mutual exclusivity
	amp	3 (9.68%)	5 (2.51%)	1.95	0.0777	0.629	Co-occurrence
<i>ALK</i>	mut	3 (9.68%)	15 (7.54%)	0.36	0.448	0.865	Co-occurrence
<i>RET</i>	mut	1 (3.23%)	8 (4.02%)	-0.32	0.652	0.865	Mutual exclusivity
	del	0 (0.00%)	1 (0.50%)	<-10	0.865	0.865	Mutual exclusivity
<i>ROS1</i>	mut	3 (9.68%)	9 (4.52%)	1.1	0.209	0.733	Co-occurrence
	del	0 (0.00%)	1 (0.50%)	<-10	0.865	0.865	Mutual exclusivity
<i>KRAS</i>	mut	8 (25.81%)	67 (33.67%)	-0.38	0.257	0.748	Mutual exclusivity
	del	0 (0.00%)	1 (0.50%)	<-10	0.865	0.865	Mutual exclusivity
	amp	1 (3.23%)	12 (6.03%)	-0.9	0.455	0.865	Mutual exclusivity
<i>NRAS</i>	mut	0 (0.00%)	1 (0.50%)	<-10	0.865	0.865	Mutual exclusivity
	del	0 (0.00%)	4 (2.01%)	<-10	0.558	0.865	Mutual exclusivity
	amp	1 (3.23%)	1 (0.50%)	2.68	0.252	0.703	Co-occurrence
<i>HRAS</i>	mut	0 (0.00%)	1 (0.50%)	<-10	0.865	0.865	Mutual exclusivity
	del	0 (0.00%)	1 (0.50%)	<-10	0.865	0.865	Mutual exclusivity
<i>RIT1</i>	mut	0 (0.00%)	5 (2.51%)	<-10	0.482	0.865	Mutual exclusivity
	amp	5 (16.13%)	27 (13.57%)	0.25	0.439	0.865	Co-occurrence
<i>NF1</i>	mut	9 (29.03%)	18 (9.05%)	1.68	3.93E-03	0.324	Co-occurrence
	del	0 (0.00%)	1 (0.50%)	<-10	0.865	0.865	Mutual exclusivity

	amp	0 (0.00%)	1 (0.50%)	<-10	0.865	0.865	Mutual exclusivity
<i>BRAF</i>	mut	4 (12.90%)	18 (9.05%)	0.51	0.342	0.83	Co-occurrence
	amp	3 (9.68%)	3 (1.51%)	2.68	0.0336	0.475	Co-occurrence
<i>RAF1</i>	mut	1 (3.23%)	1 (0.50%)	2.68	0.252	0.733	Co-occurrence
<i>MAP2K1</i>	mut	0 (0.00%)	3 (1.51%)	<-10	0.646	0.865	Mutual exclusivity
	amp	0 (0.00%)	1 (0.50%)	<-10	0.865	0.865	Mutual exclusivity
<i>KEAP1</i>	mut	4 (12.90%)	36 (18.09%)	-0.49	0.338	0.83	Mutual exclusivity
	del	0 (0.00%)	4 (2.01%)	<-10	0.558	0.865	Mutual exclusivity
<i>CUL3</i>	mut	1 (3.23%)	3 (1.51%)	1.1	0.442	0.865	Co-occurrence
	del	0 (0.00%)	1 (0.50%)	<-10	0.865	0.865	Mutual exclusivity
	amp	0 (0.00%)	1 (0.50%)	<-10	0.865	0.865	Mutual exclusivity
<i>NFE2L2</i>	mut	0 (0.00%)	4 (2.01%)	<-10	0.558	0.865	Mutual exclusivity
	amp	1 (3.23%)	5 (2.51%)	0.36	0.585	0.865	Co-occurrence
<i>PTEN</i>	mut	2 (6.45%)	1 (0.50%)	3.68	0.0485	0.612	Co-occurrence
	amp	2 (6.45%)	2 (1.01%)	2.68	0.0888	0.629	Co-occurrence
<i>PIK3R1</i>	mut	0 (0.00%)	2 (1.01%)	<-10	0.748	0.865	Mutual exclusivity
	del	0 (0.00%)	3 (1.51%)	<-10	0.646	0.865	Mutual exclusivity
<i>PIK3CA</i>	mut	1 (3.23%)	14 (7.04%)	-1.12	0.372	0.863	Mutual exclusivity
	del	0 (0.00%)	1 (0.50%)	<-10	0.865	0.865	Mutual exclusivity
	amp	2 (6.45%)	3 (1.51%)	2.1	0.136	0.629	Co-occurrence
<i>AKT1</i>	mut	0 (0.00%)	2 (1.01%)	<-10	0.748	0.865	Mutual exclusivity
	del	0 (0.00%)	1 (0.50%)	<-10	0.865	0.865	Mutual exclusivity
	amp	0 (0.00%)	2 (1.01%)	<-10	0.748	0.865	Mutual exclusivity
<i>STK11</i>	mut	0 (0.00%)	40 (20.10%)	<-10	1.67E-03	0.262	Mutual exclusivity
	del	0 (0.00%)	3 (1.51%)	<-10	0.646	0.865	Mutual exclusivity

TCGA cBioPortal calculates Log ratio = Log₂ based ratio of (% in altered / % in unaltered);

p-value derived from Fisher Exact Test; q-value derived from Benjamini-Hochberg procedure.

Chapter 4

Results

4.1 Selection and mutational background of RICTOR cell line panel

In order to study the oncogenic effects imposed by RICTOR, we established a RICTOR cell line panel by first screening 57 NSCLC cell lines to detect *RICTOR* copy number variations (CNVs) by utilizing a single nucleotide polymorphism (SNP) array (Figure 12). We selected seven *RICTOR* amplified (highlighted in red arrows) and five non-amplified cell lines (highlighted in black arrows) that span diverse co-mutational backgrounds, including several lines that harbor *KRAS*, *PTEN*, *PIK3CA*, *STK11*, and/or *EGFR* mutations. The mutational background of the cell line panel used in our studies is summarized in Table 3. *RICTOR* amplified cell lines chosen were H23, H3122, H1792, H2009, H1650, H2172, H2126 and non-amplified cell lines were HCC193, H1819, A549, CALU6, and HCC44.

Moreover, in order to perform experiments that require extended duration for completion, we established several stable inducible sh*RICTOR* cell line models (Figure 13). These cell lines possess puromycin resistance and inducible red fluorescence protein (RFP) expression for selection and visualization of transduction efficiency, respectively. Upon administration of doxycycline, we see a significant reduction in the RICTOR protein expression levels in the selected cell lines.

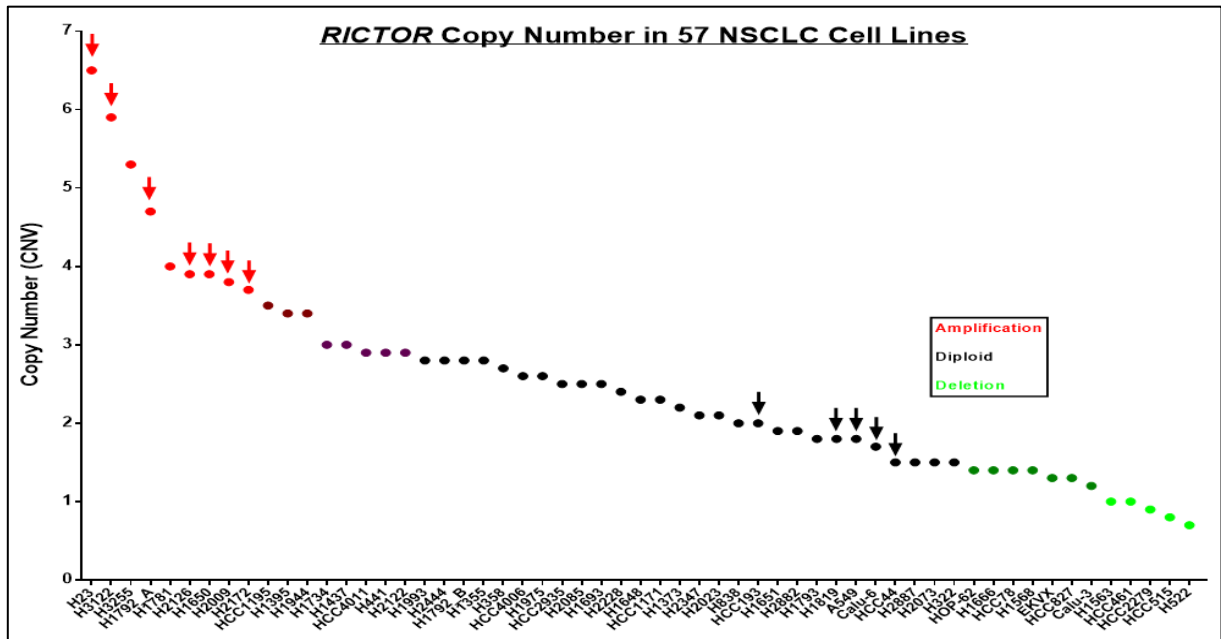


Figure 12. Selection of RICTOR cell line panel used for *in vitro* studies. Whole genome single nucleotide polymorphism (SNP) array profiling was obtained for 57 NSCLC cell lines to determine *RICTOR* amplified (copy number variation (CNV) ≥ 3.5) and non-amplified cell lines (CNV ~ 2). Seven *RICTOR* amplified cell lines (red arrows) and five *RICTOR*-non-amplified cell lines (black arrows) were selected. Copy number variation (CNV) values: red = amplified; black = diploid; green = deletion.

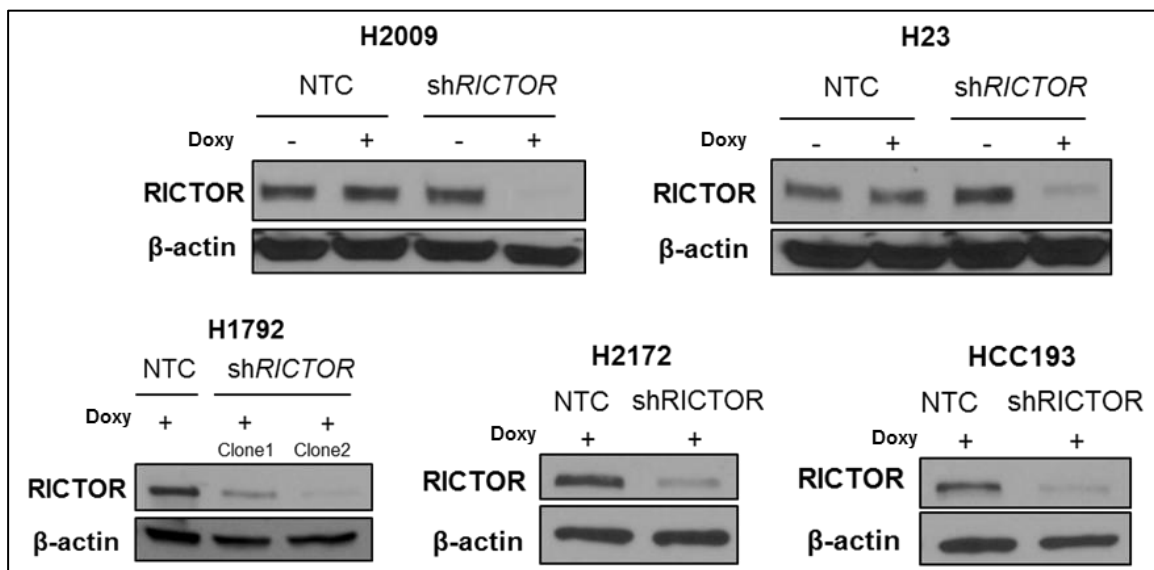


Figure 13. Establishment of inducible sh*RICTOR* cell line models. Several cell lines from the RICTOR cell line panel were used to establish *tet*-ON inducible

sh*RICTOR* cell line models. pTRIPZ plasmid (Dharmacon) was used to stably transduce the indicated cell lines, and puromycin and RFP was used for positive clone selection. Doxycycline was used to stably knock down *RICTOR* in the cells, following dose and time optimization. Ideal knockdown was seen after doxycycline administration (2 µg/mL) for 96-144 hours depending on the cell line. Non-targeting control (NTC) was used as a doxycycline and transduction negative control, and β-actin used as a loading control for Western blotting.

Table 3. Mutational profile of RICTOR NSCLC cell line panel.

	Cell line	<i>KRAS</i>	<i>EGFR</i>	<i>STK11</i>	<i>PIK3CA</i>	<i>PTEN</i>	<i>EML4/ALK</i>
<i>RICTOR</i> amplified	H2172	WT	WT	WT	WT	WT	WT
	H2126	WT	WT	Mut	WT	WT	WT
	H23	mut - G12C	WT	Mut	WT	Mut	WT
	H3122	WT	WT	WT	WT	WT	Mut
	H1792	mut - G12C	WT	WT	WT	WT	WT
	H1650	WT	Mut	WT	Mut	Mut	WT
	H2009	mut - G12A	WT	WT	WT	WT	WT
<i>RICTOR</i> non-amplified	HCC193	WT	WT	WT	WT	WT	WT
	H1819	WT	WT	WT	WT	WT	WT
	A549	mut - G12S	WT	Mut	WT	WT	WT
	Calu6	mut - Q61K	WT	WT	WT	WT	WT
	HCC44	mut - G12C	WT	Mut	WT	WT	WT

4.2 RICTOR signaling in *RICTOR* amplified versus non-amplified cell lines

After selecting our cell lines that carry additional secondary mutations, representative of the complex heterogeneity of NSCLC, we wanted to assess the signaling patterns associated with these cells at basal level. Figure 14 shows western blotting analysis of the signaling patterns seen in the amplified (shown in red) versus the non-amplified (shown in black) cell lines. We noticed several key

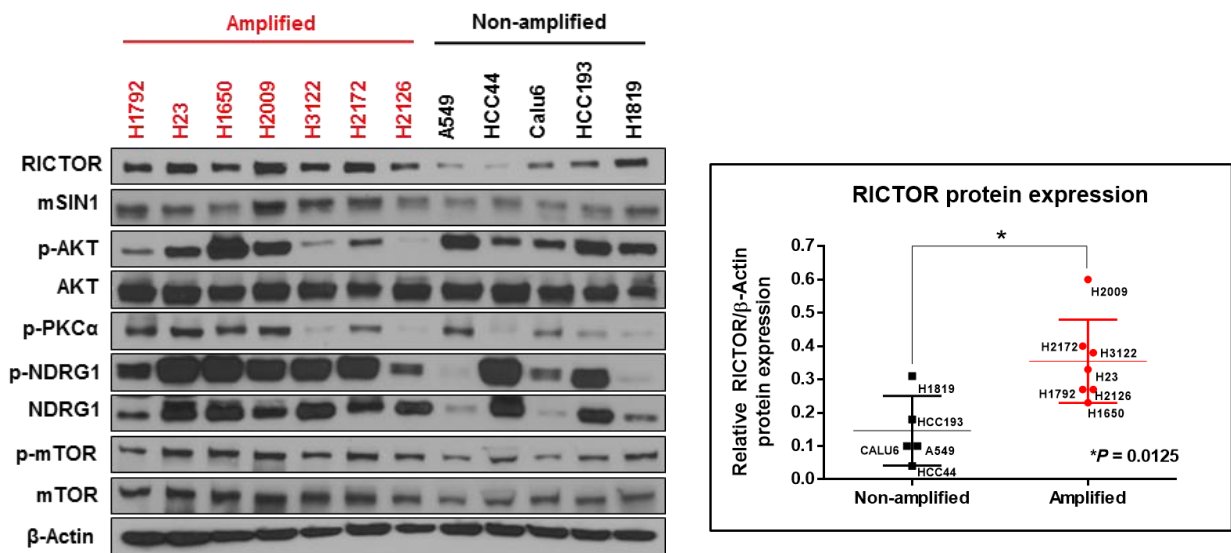


Figure 14. Comparison of signaling and RICTOR expression in amplified versus non-amplified cell lines. (Left) Cell lysates from 12 NSCLC cell lines (amplified or non-amplified for *RICTOR*) were examined by Western blotting. Total and phospho-specific antibodies used were for levels of RICTOR, mSIN1, p-AKT (S473), AKT, p-PKCα (S657), p-NDRG1 (T346), NDRG1, p-mTOR (S2481), mTOR, and β-Actin as loading control. (Right) Quantification of relative RICTOR/β-Actin protein expression from densitometric analysis of western blot panel. *, $P = 0.01$.

trends that became apparent. First, RICTOR protein expression was significantly higher in the *RICTOR* amplified cell lines compared to the non-amplified cell lines. Densitometric analysis of relative RICTOR/ β -Actin protein expression from the Western blot is shown on the right, and shows significantly higher RICTOR protein expression (*, $P = 0.01$). This is in concordance with our clinical analysis data from the TCGA and BATTLE-2 cohorts, showing that *RICTOR* amplification directly correlates with an overall higher *RICTOR* mRNA expression, suggesting that amplification of this gene drives the overexpression of the protein product. Next, we discovered that the expression of the mTORC2 component, mSIN1, is elevated in *RICTOR* amplified cells, suggesting increased rate of mTORC2 complex formation and potential activity (124). Additionally, increased mTORC2 activity markers were seen in our amplified cells, marked by an overall increase in p-PKC α S657 levels and elevated phosphorylation of N-myc downstream regulated gene 1 (p-NDRG1 T346), which serves as a surrogate marker for SGK1 activity (43). Interestingly, although mTORC2 is predominately responsible for the phosphorylation of AKT on S473 leading to full activation, our RICTOR amplified cell lines displayed variable degrees of basal AKT activity levels compared to our non-amplified cells. This could be attributed to the complex heterogeneity of these cell lines that induce signaling to the often-deregulated PI3K/AKT/mTOR pathway. Also, other AKT regulators have been shown to influence AKT activation such as DNA-dependent protein kinase (DNA-PK), ILK1, protein kinase C β II (PKC β II), PH domain leucine-rich repeat protein phosphatase (PHLPP), and ataxia-telangiectasia mutant (ATM), all shown to reflect the various cellular contexts in which AKT activity may be modulated (26, 125, 126).

4.3 *RICTOR* knockdown decreases colony formation and anchorage-independent growth in amplified cells

We next sought to determine the phenotypic consequences of *RICTOR* knockdown *in vitro*. We utilized our established stably transduced doxycycline (doxy)-inducible sh*RICTOR* cell lines that are either amplified or not for *RICTOR*. Following *RICTOR* knockdown in our cell lines, colony formation potential was assessed after 2 to 3 weeks and resulted in a significant reduction of colony growth in all 3 of our *RICTOR* amplified cell lines (H23, H2009, H1792), as measured by relative percentage of colony area compared to non-targeting control (NTC) (*, $P < 0.05$) (Figure 15, top). We did not see an effect in our non-amplified cell lines A549 and HCC193, suggesting that *RICTOR* amplifications provide a survival advantage to NSCLC cells driven by increased *RICTOR* expression. Additionally, when we performed an anchorage-independent growth assay to test the transformative ability of *RICTOR* by plating H23 cells on soft agarose and treating either NTC or sh*RICTOR* cells with doxycycline to stably knock down *RICTOR*, there was complete abrogation of colony formation following *RICTOR* inhibition, again suggesting that *RICTOR* contributes proliferative properties to cells (Figure 15, bottom).

4.4 *RICTOR* knockdown decreases cell proliferation in part through G₀/G₁ cell cycle arrest

Since we witnessed a dramatic reduction in the colony formation potential of cells following *RICTOR* knockdown, it was of interest to determine the precise role that *RICTOR* plays in regulating cell survival and/or proliferation. We therefore performed a cell proliferation assay by culturing cells in the presence or absence of

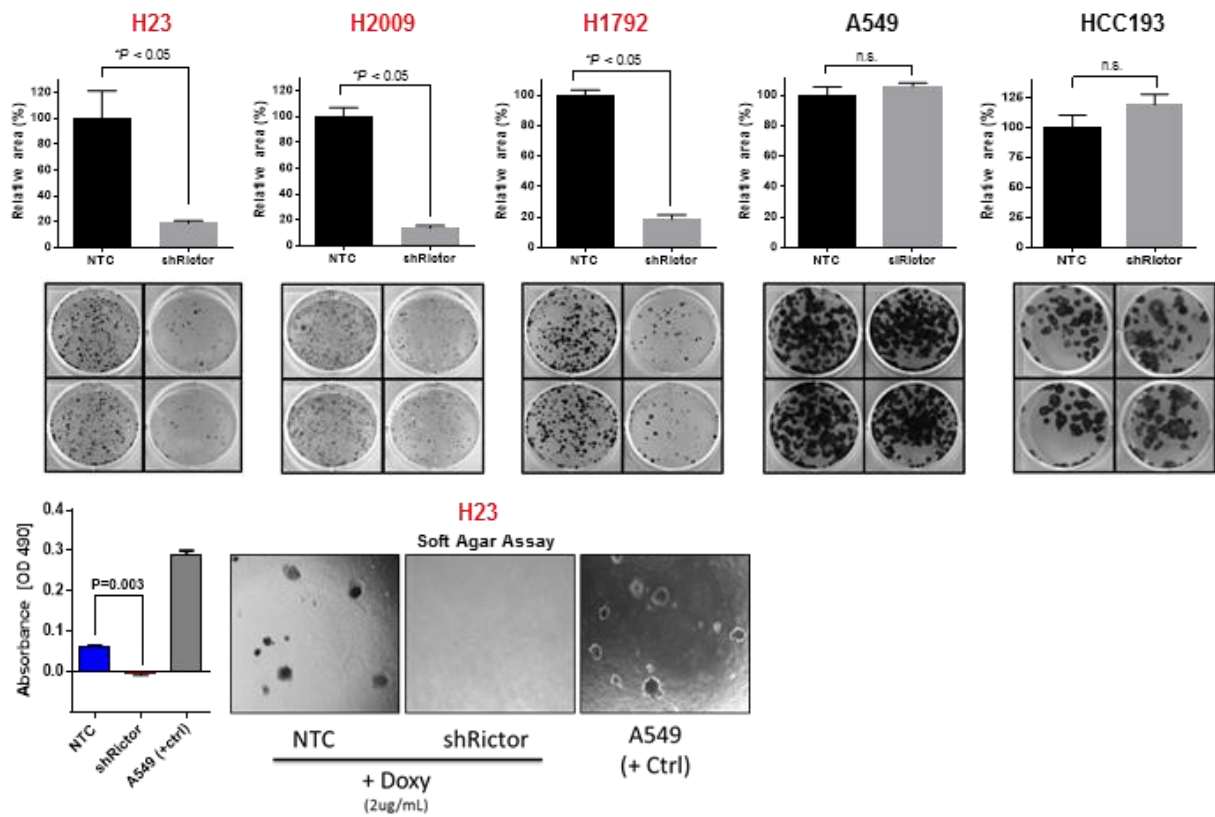


Figure 15. *RICTOR* knockdown decreases colony formation and anchorage-independent growth in amplified cells. (Top) Colony formation assay of 3 *RICTOR* amplified cell lines (H23, H2009, H1792) and 2 non-amplified cell lines (A549, HCC193) comparing *RICTOR* knockdown to non-targeting control. Data are graphed as the mean percentage \pm percent SD. (Bottom) Anchorage-independent growth assay in soft agar of stably transduced H23 cell line with *RICTOR* knockdown (A549 serves as positive control). *, $P < 0.05$; n.s. = not significant.

doxycycline to induce *RICTOR* knockdown for an extended duration of time, and quantified total cell numbers at 4, 8, 12, and 16 days of incubation (Figure 16A). Results demonstrate that reducing RICTOR levels in the three cell lines tested markedly reduced the total cell numbers in as early as 4 to 8 days, and reduced the cell numbers by over 75% in all 3 cell types by day 16, yielding similar results to the colony formation assay (Figure 15). Moreover, we assessed whether this reduction in cell number was due to cell cycle changes. H23, H2009, and H1792 cell lines were cultured for 8 days with or without doxycycline, and stained with Propidium iodide (PI) for FACS cell cycle analysis. As seen in Figure 16B, *RICTOR* knockdown resulted in a slight G₀/G₁ cell cycle arrest in all 3 cell lines tested. Quantification of the cell cycle phases was performed and shows an increase of 10%, 11.7%, 4.9% G₀/G₁ cell cycle arrest in the sh*RICTOR* cells compared to NTC cells of H23, H1792, and H2009, respectively (Figure 16C). Previous reports have linked RICTOR/mTORC2 to the regulation of the cell cycle through modulation of cyclin-D1 levels (115, 127-129). To test this, we performed Western blotting analysis on the H23 cell line to check for p-AKT, p-MEK1/2, and cyclin-D1 levels (Figure 16D) following *RICTOR* knockdown via siRNA. We witnessed a slight decrease in the levels of Cyclin-D1 following *RICTOR* siRNA, providing a potential explanation of the modest increase seen in the G₀/G₁ cell cycle arrest.

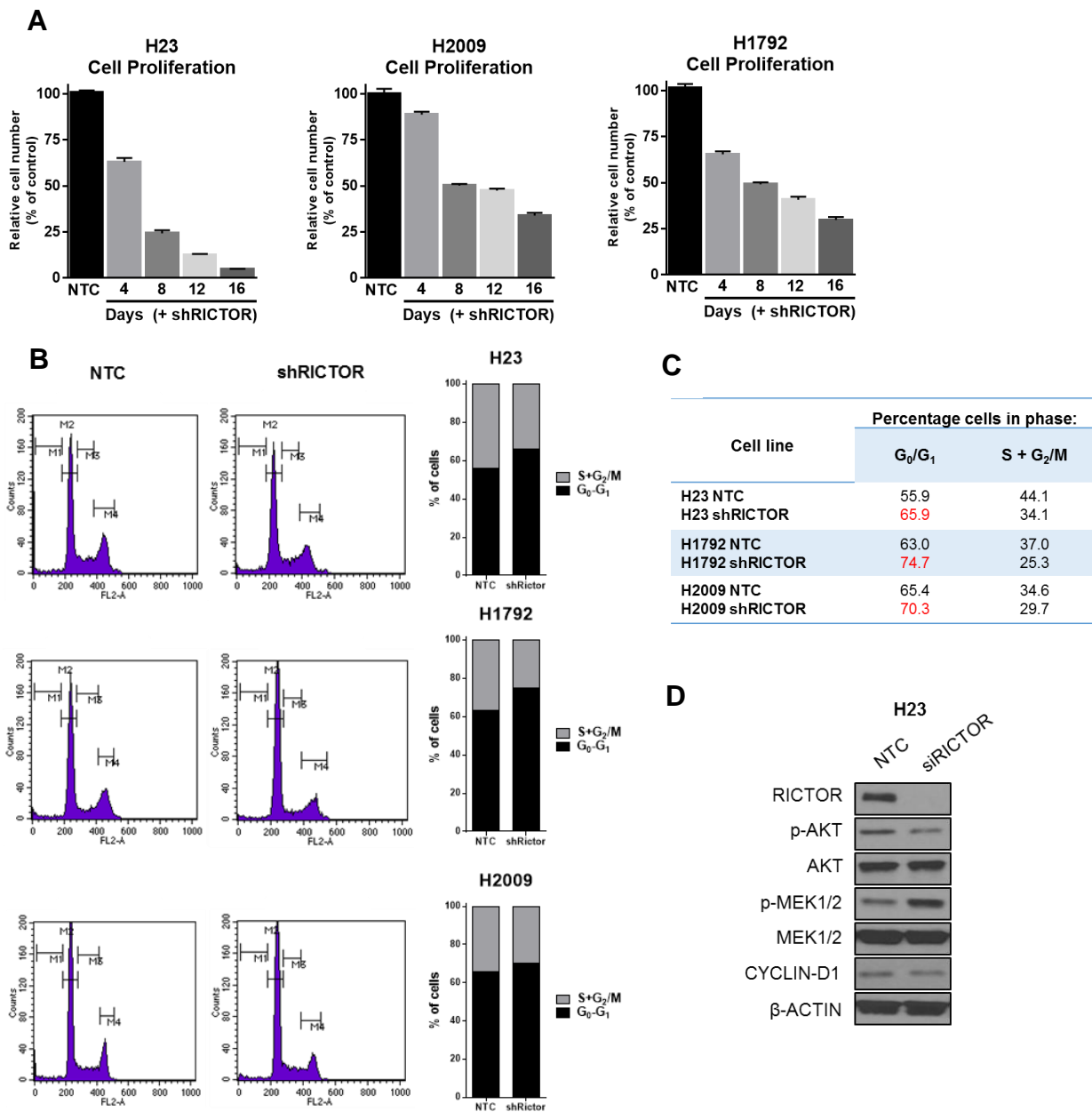


Figure 16. *RICTOR* knockdown decreases the cell proliferative capacity. (A)

Quantification of the relative cell number counts of shRICTOR cells relative to NTC cells at the indicated time points following doxycycline treatment. Complete cell counts were performed following 4, 8, 12, 16 days of incubation and shown as percentage relative to NTC. (B, C) Flow cytometry histograms and quantification of the phases of cell cycle in NTC versus shRICTOR cells following Propidium iodide (PI) staining and FACS sorting after 8 days of incubation. (D) Western blotting analysis of representative H23 cell line showing decreased cyclin-D1 expression.

4.5 *RICTOR* knockdown reduces the migration and invasion capacity of *RICTOR* amplified NSCLC cells

To determine whether *RICTOR* plays a role in mediating migration and invasion of NSCLC cells, we utilized transwell *in vitro* migration and invasion assay chambers. These assays allow for the quantification of migratory and invasive cells that are able to move through specified pores of a filter membrane chamber placed in media containing a chemoattractant (e.g. FBS). After the cells were incubated for 24 hours, the number of H23, H2009, and H1792 cells (*RICTOR* amplified, *KRAS* mutant cell lines) that migrated through the membranes of the chambers were significantly lower following *RICTOR* knockdown (>50%) in both serum reduced and normal serum conditions ($P \leq 0.001$) compared to NTC cells (Figure 17, top). Interestingly, H2172 and H2126 (*RICTOR* amplified, *KRAS* wild-type cell lines) had a very poor basal migrative capacity, seen by the number of migratory control (NTC) cells quantified even in the absence of *RICTOR* knockdown (Figure 17, bottom). The results indicate that *RICTOR* knockdown reduces the migratory capability of *RICTOR* amplified NSCLC cell lines that possess *KRAS* co-mutations.

Similarly, the invasive capability was assessed using a Matrigel coated membrane filter chamber. After incubation of cells for 48 hours in either serum reduced or normal serum conditions, the number of cells that invaded through the membranous matrix were quantified. As seen in Figure 18 (top), H23, H2009, and H1792 cells had a significant reduction in the number of invasive cells following *siRICTOR* compared to NTC in both serum reduced and full serum conditions ($P \leq 0.001$). H2009 had the most dramatic reduction in invasive ability (>80%) followed by H23 (>61%) and H1792 (>44%). Of note, similar to the migrative capacities, the

RICTOR amplified *KRAS* wild-type cell lines H2172 and H2126 had a very poor basal invasive capability, once again emphasizing the potential importance of mutant *KRAS* perhaps serving as a co-oncogenic driver with *RICTOR* to fuel these tumorigenic properties in these cell types. Taken together, these results show that *RICTOR* knockdown suppresses the migration and invasion efficiency of select NSCLC cell types.

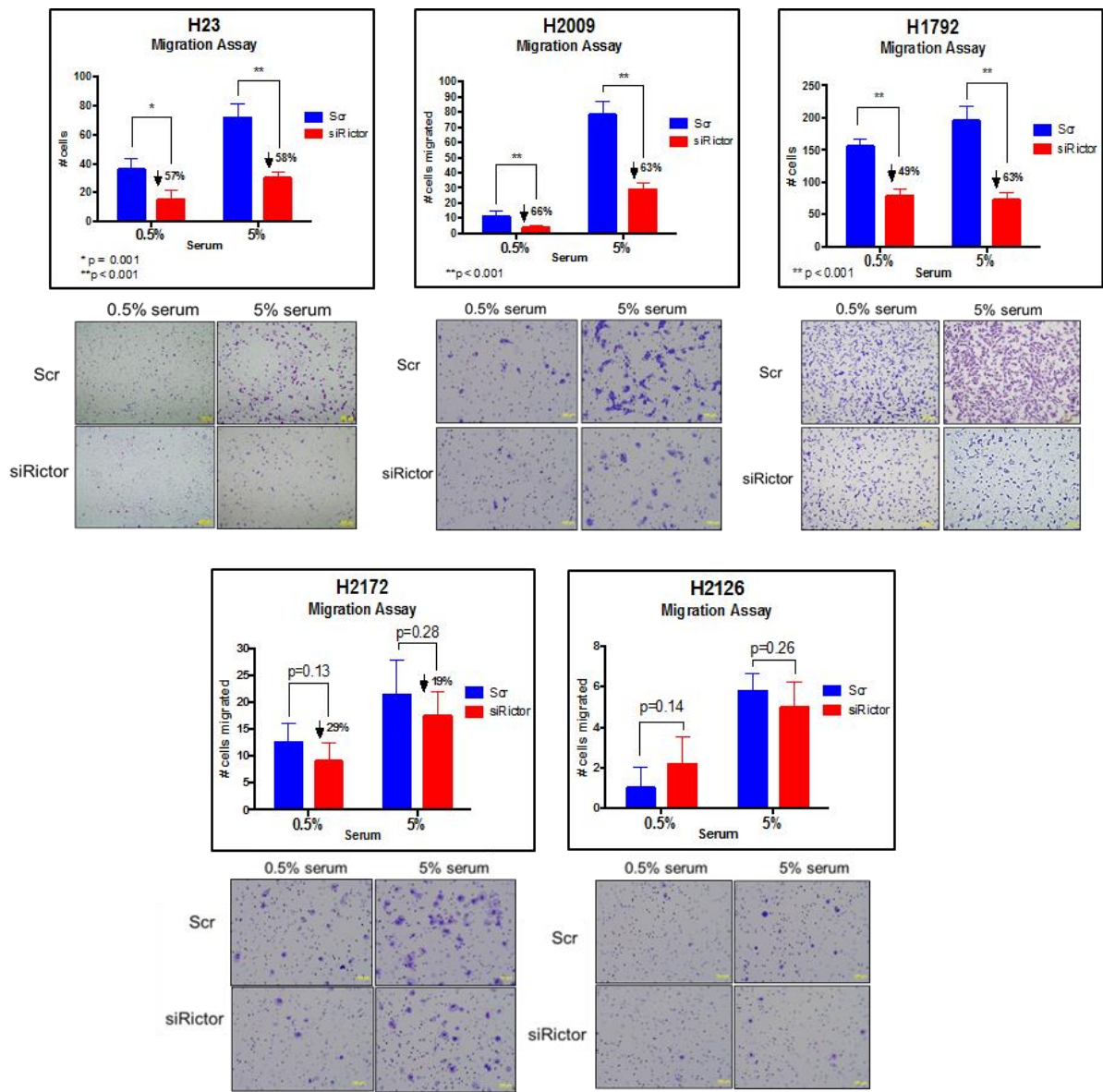


Figure 17. *RICTOR* knockdown reduces migration potential in *RICTOR* amplified cell lines. Cell migration was assessed using transwell chambers with 8µm pore polyethylene terephthalate (PET) membrane filters. Cells were incubated in either reduced serum (0.5%) or normal serum (5%) for 24 hours. Representative visual images of the stained surfaces are shown. The results presented are an average of five random microscopic fields at 10X of the number of cells stained and counted. Data shown are of the means \pm standard error of the means (SEM) of data from at least 3 independent experiments. * $P = 0.001$; ** $P < 0.001$.

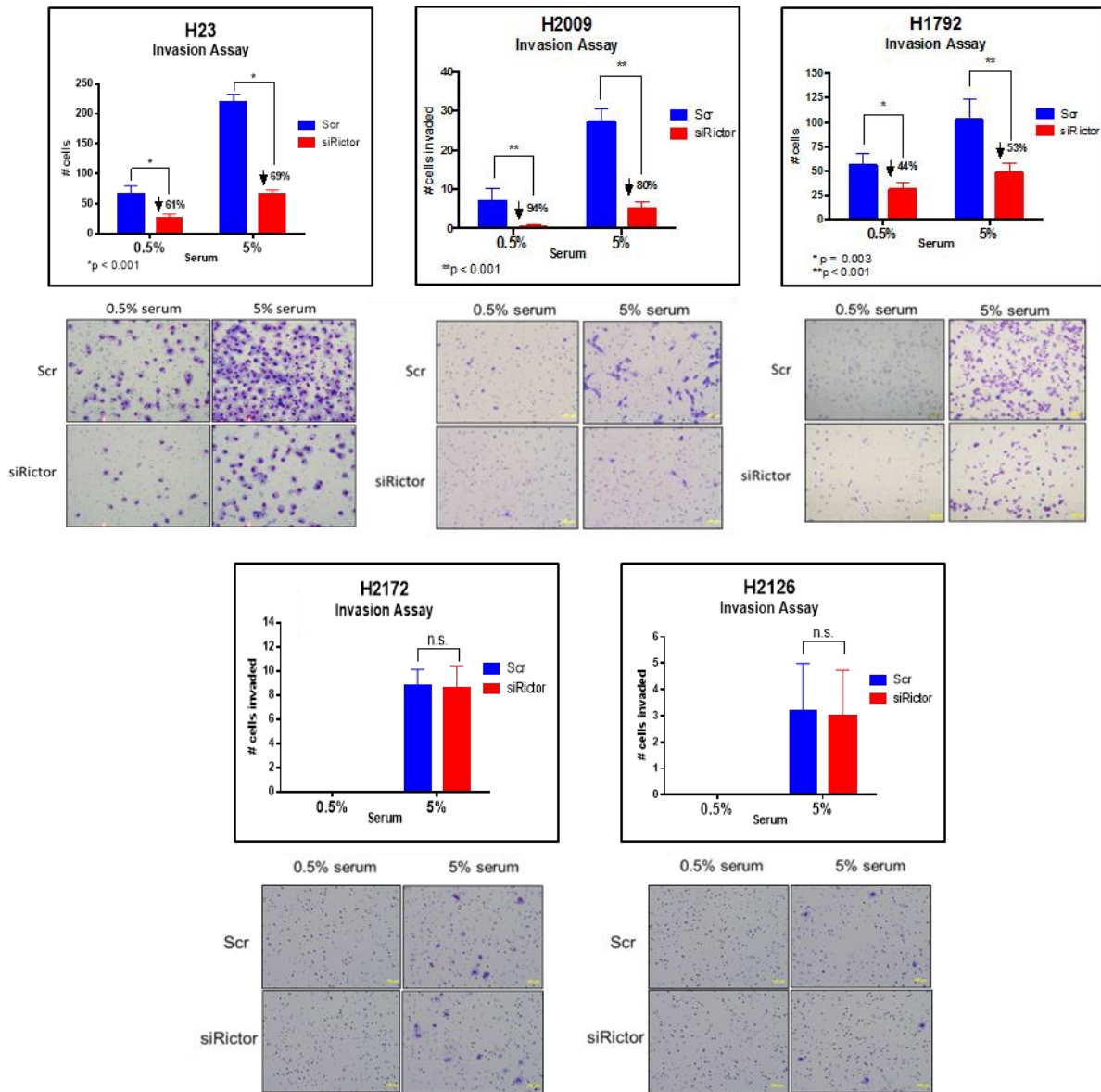


Figure 18. *RICTOR* knockdown reduces invasion potential in *RICTOR* amplified cell lines. Cell invasion was assessed using modified transwell chambers coated with growth factor reduced Matrigel with 8µm pore polyethylene terephthalate (PET) membrane filters. Cells were incubated in either reduced serum (0.5%) or normal serum (5%) for 48 hours. Representative visual images of the stained surfaces are shown. The results presented are an average of five random microscopic fields at 10X of the number of cells stained and counted. Data shown are of the means ± standard error of the means (SEM) of data from at least 3 independent experiments. * $P < 0.01$; ** $P < 0.001$; ns=not significant.

4.6 *RICTOR* knockdown results in reduced tumorigenicity *in vivo*

Our data thus far suggests that RICTOR serves as an important oncogene involved in promoting various malignant phenotypes such as colony formation, migration and invasion. We wanted to investigate the role of RICTOR *in vivo* by use of murine xenografts engrafted with our established inducible sh*RICTOR* lung adenocarcinoma cell lines H1792 and H23. There was a significant reduction in H1792 and H23 xenograft tumor growth following continuous induction of *RICTOR* knockdown by doxycycline administration compared to mouse control groups without treatment by 6 weeks (*, $P < 0.05$) (Figure 19 A, B). To assess the molecular signaling patterns following RICTOR blockade *in vivo*, we extracted total protein lysates from the tumor tissues of both the doxycycline treated and control groups from H1792 xenografts and performed Western blotting analysis. As seen in Figure 19C, RICTOR expression was significantly reduced in the +Doxy group and resulted in overall decreased p-AKT levels, in concordance with our *in vitro* results. In addition, p-MEK1/2 and p-ERK1/2 levels were elevated in the *RICTOR* knockdown tumors, indicative of the compensatory mechanisms seen *in vitro* in our *KRAS* mutant cell lines. Taken together, genetic blockade of *RICTOR* is associated with growth inhibition *in vivo*, further supporting RICTOR's role as an oncogenic driver in NSCLC.

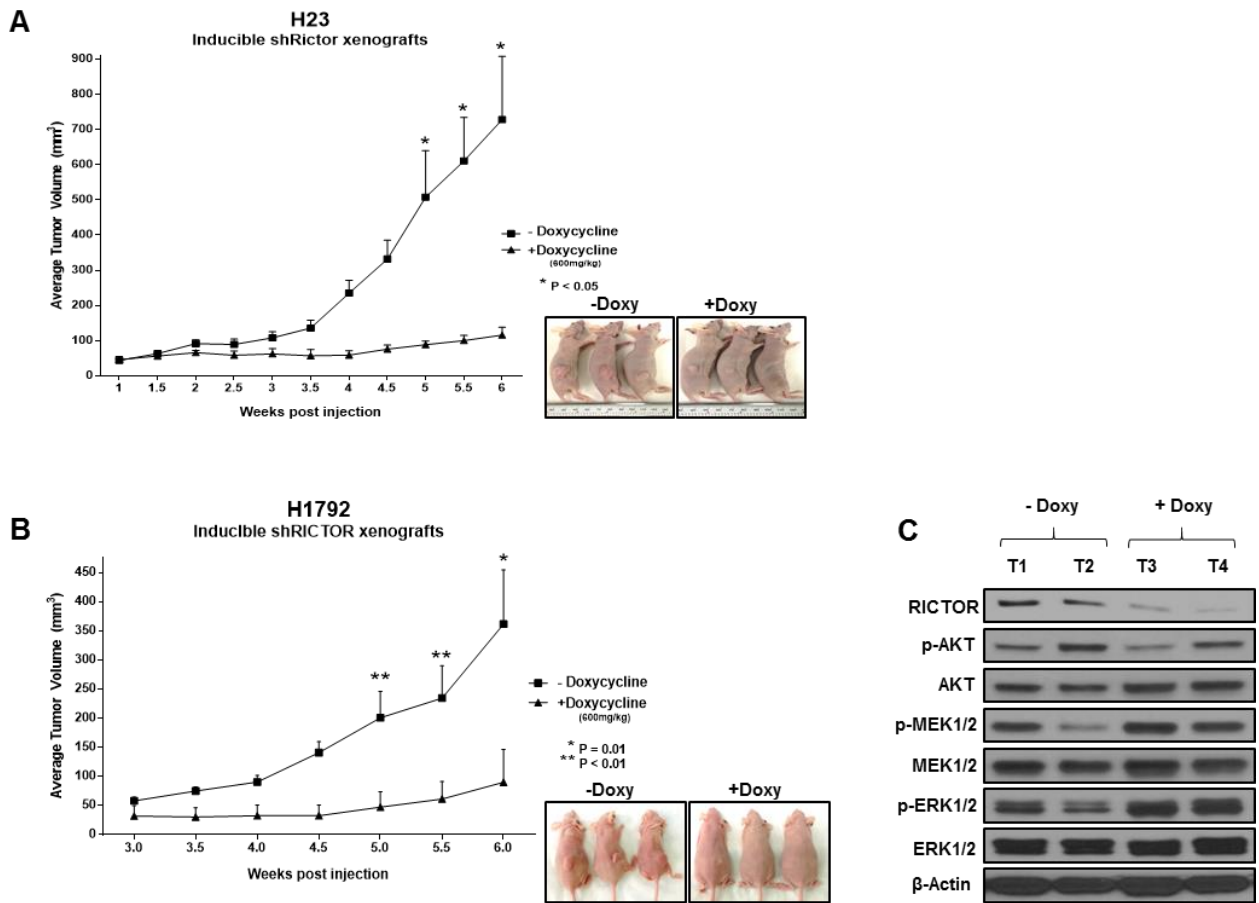


Figure 19. *RICTOR* knockdown using *RICTOR* shRNA results in reduced tumorigenicity *in vivo*. (A, B) Athymic nude mice were inoculated with H1792 or H23 sh*RICTOR* cell lines and were fed with either doxycycline (+Doxy, 600mg/kg) or control diet (-Doxy). Tumor volumes were measured twice weekly. Data points are presented as the mean tumor volume \pm SEM. Representative images of xenograft tumors from each group before tumor harvesting are shown. *, $P = 0.01$; **, $P < 0.01$. (C) Lysates extracted from H1792 tumor xenografts were subjected to Western blot analysis with the indicated antibodies, showing *RICTOR* knockdown.

Chapter 5

Results

5.1 Compensatory MAPK signaling activation following RICTOR inhibition in *KRAS* mutant settings

Our clinical analysis of *RICTOR*-altered cases from the TCGA dataset demonstrated an enrichment of MAPK pathway alterations (Figure 11). Thus, we wanted to determine possible changes in the cell signaling patterns of the RAS/RAF/MEK pathway affected by RICTOR. We performed knockdown studies via siRNA in several cell lines from our panel that harbor either *RICTOR* amplifications and/or *KRAS* mutations. Western blot analysis indicated that *RICTOR* siRNA effectively knocked down RICTOR protein expression levels in the respective samples (Figure 20A). Interestingly, si*RICTOR* treatment in *RICTOR* amplified NSCLC cell lines that harbor *KRAS* mutations (H23, H2009, H1792) resulted in a compensatory increased activation of the MAPK pathway seen by elevated levels of phosphorylated MEK (p-MEK1/2) compared to non-targeting control (NTC) treatment (Figure 20A). As expected, we saw a reduction in the full activation of AKT S473 (p-AKT) in these cells after *RICTOR* knockdown, associated with reduced mTORC2 activity. To determine if this compensation occurs specifically in *KRAS* mutant settings, we performed si*RICTOR* treatment on *RICTOR* amplified but *KRAS* wild-type cell lines (H1650, H2126, H2172), and results confirmed there was no significant increase in the p-MEK1/2 levels. Of note, p-AKT levels were not reduced following RICTOR inhibition in H1650 (*EGFR*, *PIK3CA*, *PTEN* mutant) and H2126 (*LKB1* mutant), which could be a result of their secondary mutations known to stimulate the PI3K/AKT/mTOR pathway.

Interestingly, a similar compensatory MAPK pathway activation was seen in *RICTOR* non-amplified but *KRAS* mutant cell lines (A549, HCC44), but not in *KRAS* wild-type cell lines (H1819, HCC193), suggesting that *RICTOR* amplification is not necessary for driving this compensatory mechanism.

To further test our hypothesis that mutant *KRAS* is important in mediating this compensatory mechanism following *RICTOR* blockade, we performed double knockdown studies via siRNA targeting *RICTOR* and *KRAS* alone, or in combination. As seen in Figure 20B, in two of our *RICTOR* amplified *KRAS* mutant cell lines (H23, H1792), Western blotting results of si*RICTOR* showed an elevated activation of p-MEK1/2, whereas si*KRAS* alone actually reduced the p-MEK1/2 levels and hence decreased MAPK pathway activity. When concomitant targeting of si*RICTOR* and si*KRAS* occurred, there was no increase in p-MEK1/2 levels, suggesting that there is an important interplay between *RICTOR* and mutant *KRAS*. Collectively, these findings suggest that there is a fine tuned balance of pro-survival signaling mechanisms in *RICTOR/KRAS*-altered settings, such that when the *RICTOR* pathway is blocked the cells tip the pro-survival balance to the parallel oncogenic MAPK pathway mediated by mutant *KRAS*, through increased activation of p-MEK1/2 (Figure 20C). These data expose a unique therapeutic vulnerability in this specific setting where dual pathway targeted therapy approaches could be beneficial.

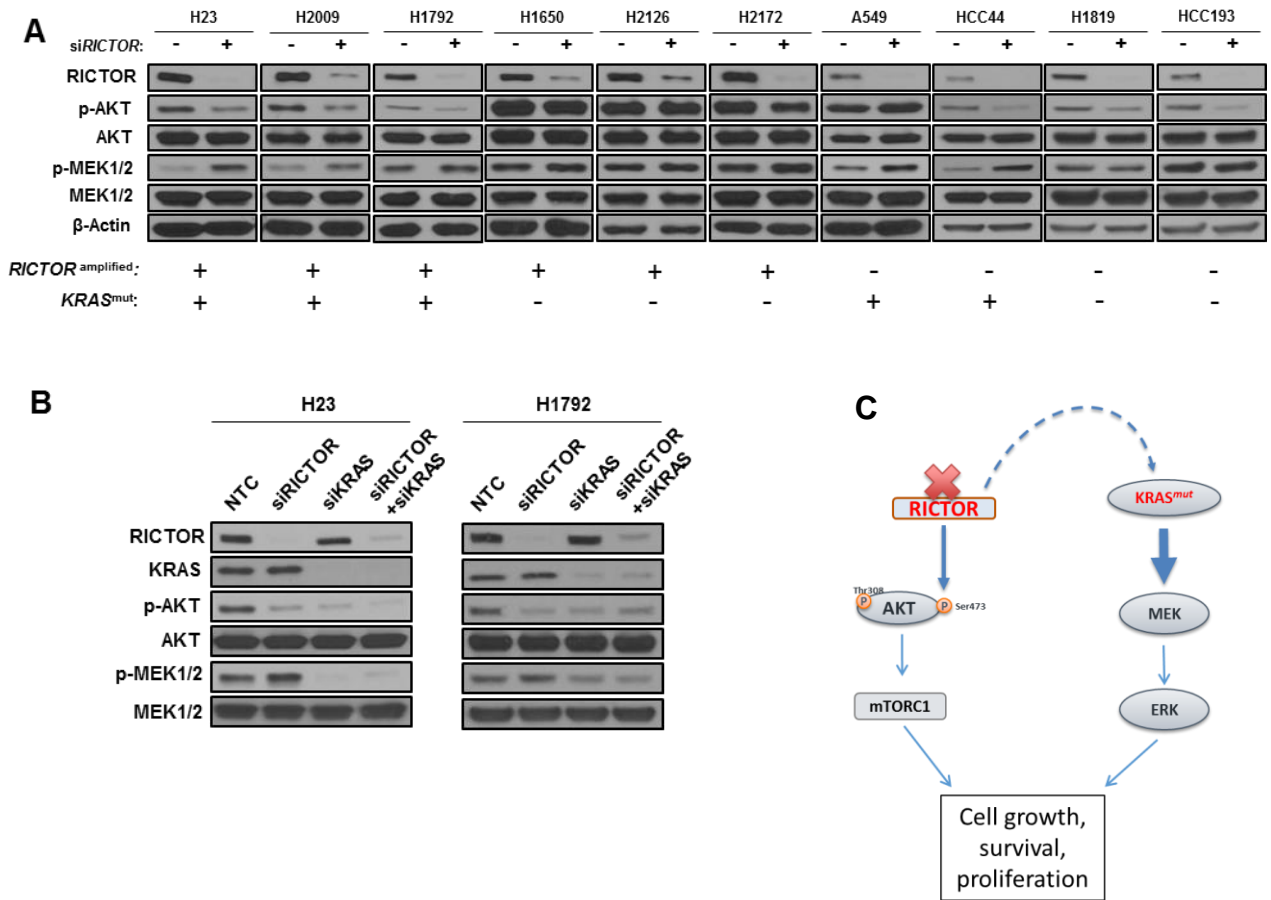


Figure 20. Compensatory MAPK signaling activation following *RICTOR*

knockdown in *KRAS* mutant settings. (A) A panel of 6 *RICTOR* amplified and 4 non-amplified NSCLC cell lines that are *KRAS* wildtype or mutant were transfected with siRNAs specific for RICTOR or scrambled negative control for 72 hours and cell lysates were analyzed by Western blotting for the specified proteins. (B) H23 and H1792 cells were transfected with siRNAs specific for RICTOR, *KRAS*, or scrambled negative control for 72 hours and cell lysates were analyzed by Western blotting for the specified proteins. (C) Potential model of compensatory mechanism between RICTOR and mutant *KRAS*.

5.2 Compensatory MEK1/2 activation following *RICTOR* knockdown may be mediated through de-repression of inhibitory CRAF phosphorylation

We next wanted to elucidate a potential mechanism behind the compensatory upregulation of p-MEK1/2, which occurs following RICTOR inhibition. We treated our H23 cell line (*RICTOR* amplified, *KRAS* mutant) with either siRNA directed against RICTOR or various mTOR/MAPK pathway inhibitors targeting mTORC1 (everolimus), mTORC1/2 (AZD2014), MEK1/2 (AZD6244, selumetinib), or a combination of AZD2014 and AZD6244 (Figure 21A). Whole-cell lysates were then extracted and probed with phosphorylation-specific antibodies for various PI3K/AKT/mTOR and MAPK pathway activation markers and Western blotting analysis was performed. In first assessing the full activation of AKT (p-AKT S473) under the different treatment conditions, si*RICTOR* treatment reduced the p-AKT levels as expected, with similar results seen after treatment with the dual mTORC1/2 inhibitor, AZD2014. Treatment with the mTORC1 inhibitor everolimus, however, increased the activity of AKT as previously reported (130, 131), most likely through attenuation of upstream feedback inhibition of IGF-1 receptor. To further confirm the specificity of the drugs and the subsequent downregulation of mTORC1 pathway activity, the p-S6RP levels were measured and were shown to be completely inhibited with everolimus or AZD2014 treatment, but unchanged with the selective MEK1/2 inhibitor AZD6244, confirming that each drug was working selectively and inhibiting its respective pathway.

Additionally, to reconfirm the compensatory activation of p-MEK1/2 after RICTOR inhibition, treatment of H23 cells with si*RICTOR* significantly increased the p-MEK1/2 levels compared to parental or NTC cells, as previously shown (Figure 20A, B). Moreover, when AZD6244 was used to block MEK1/2 signaling, we saw a

significant reduction in the downstream p-ERK1/2 levels, reinforcing the specificity and downregulation of the MAPK pathway activity with this drug. Expectedly, there was also a dramatic increase in the p-MEK1/2 levels, as previously reported (132, 133). This is because selumetinib does not disrupt the phosphorylated activation loop sites of MEK1/2, and therefore, treatment with this MEK inhibitor relieves a negative feedback loop mediated through ERK1/2. When p-ERK1/2 levels decrease, the relief of the feedback loop allows stronger activation of upstream components and ultimately reactivates phosphorylated MEK1/2 levels.

Moreover, we evaluated the effects of the treatments on the levels of p-CRAF S259, a site previously reported to be an inhibitory phosphorylation mediated directly by AKT (49, 54, 55). Our hypothesis was that the compensatory activation of p-MEK1/2 following *RICTOR* knockdown is mediated through de-repression of the inhibitory CRAF phosphorylation as a result of decreased activation of AKT, leading to a more active CRAF involved in transduction of mutant *KRAS* signaling (Figure 21A). A proposed model of this interaction is illustrated in Figure 21C. Densitometric quantification of p-CRAF shows that si*RICTOR* decreased p-CRAF S259 by an average of 34% compared to parental and NTC H23 cells (Figure 21B). Conversely, the specific mTORC1 inhibitor, everolimus, did not yield a significant reduction, likely due to the hyperactivation of p-AKT; however, the combination of everolimus with si*RICTOR* had an average 43% reduction of p-CRAF S259, similar to si*RICTOR* alone. Interestingly, treatment with the dual mTORC1/2 inhibitor, AZD2014, only decreased the p-CRAF levels by an average of 23%. This could suggest that RICTOR may have a more important interplay with AKT, independent of its interaction with mTORC2, in modulating AKT activity and ultimately regulating CRAF activation

through mutant KRAS. Alternatively, the lower reduction of p-CRAF seen by AZD2014 could be due to the specificity of AZD2014's inhibitory mechanism on the mTOR kinase directly, and not RICTOR, suggesting that there is a unique and specific interplay between RICTOR and KRAS/CRAF. This also brings forward the idea of developing a specific RICTOR inhibitor.

Additionally, in comparing the various targeted drugs and their effects on cell viability, apoptosis was measured via the detection of cleaved PARP levels (Cl-PARP) across the panel of drug treatments. In concordance with our proposed hypothesis that a dual pathway inhibition strategy targeting both, the mTOR and MAPK pathways, is an effective solution in *RICTOR/KRAS*-altered molecular settings, our results here show that the greatest apoptotic induction is seen when using AZD2014 in combination with AZD6244 (Figure 21A). When *RICTOR* alone is knocked down, we do not see significant upregulation of cleaved PARP even though p-AKT levels decrease, suggesting that the compensatory activation of the MAPK pathway, through upregulated p-MEK1/2, is allowing the cells to sustain viability by promoting alternate survival mechanisms, as evidenced in section 5.3 below.

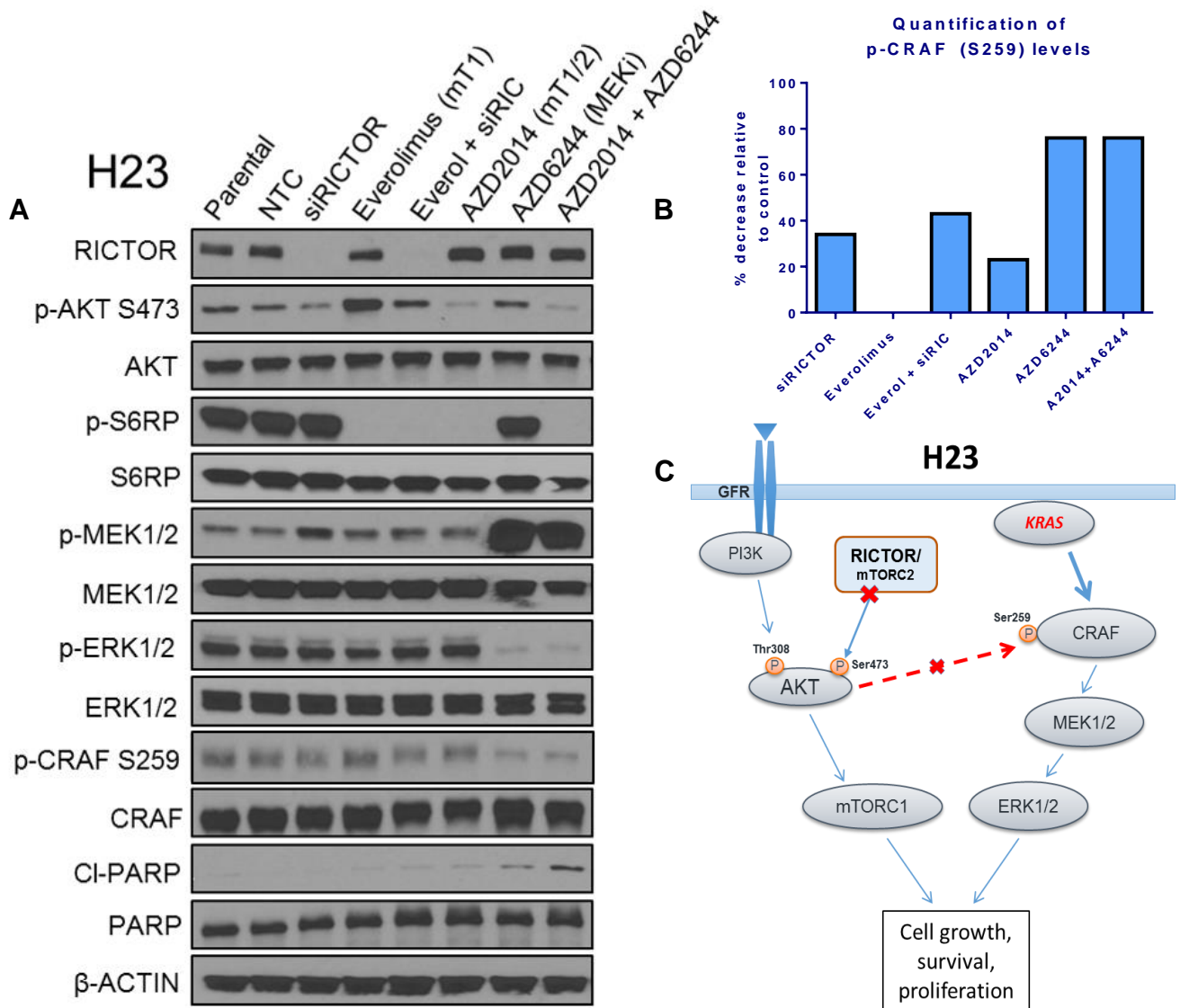


Figure 21. Compensatory MEK1/2 activation following *RICTOR* knockdown may be mediated through de-repression of inhibitory CRAF phosphorylation.

(A) H23 cells were treated with the indicated siRNAs for a total of 72 hours and compounds were administered for 24 hours (all at 1 μ M, except AZD6244 at 5 μ M) before cells were harvested. Western blot analyses was performed and densitometric quantification done using Image Studio Lite 5.0 software and bands were normalized to the respective β -Actin control bands. (B) Percent inhibition of p-CRAF S259 plotted per sample relative to the average of Parental and NTC samples. (C) Model illustrating the proposed mechanism of p-MEK1/2 activation following *RICTOR* knockdown in *KRAS* mutant cells.

5.3 Human p-MAPK array reveals *RICTOR* knockdown affects the activity of several mediators of cellular stress and survival pathways.

We next subjected our *RICTOR* amplified, *KRAS* mutant cell line, H23, to a human p-MAPK array which allows us to monitor the phosphorylation levels of 26 kinases. We treated H23 cells with NTC or si*RICTOR* for 72 hours, and following whole-cell lysis, incubated the lysates with the phosphorylation specific array. Figure 22A shows differences of band intensities (in duplicates) for 26 different kinases involved in the major MAPK pathways. Western blotting was performed separately on the NTC and si*RICTOR* lysates to confirm effective *RICTOR* knockdown (Figure 22B). Only kinases that were differentially activated (phosphorylated) were marked with corresponding numbers and ultimately quantified to evaluate difference in activity (Figure 22C). Densitometric quantification found several MAPK-related kinases that were downregulated following *RICTOR* knockdown. Notably, we found decrease in phosphorylation levels of CREB (S133), HSP27 (S78/82), and p38a (T180/Y182). Interestingly, these MAPK pathway effectors are found to play broad roles as key mediators of cellular stress response, survival, and proliferation (47, 134-136). These results open several possible mechanisms by which *RICTOR*, either through an mTORC2-dependent or independent process, is able to contribute to the oncogenic properties of NSCLC revealed by our work, by mediating the MAPK pathway(s). Future experiments are still needed to fully decipher these potential mechanisms.

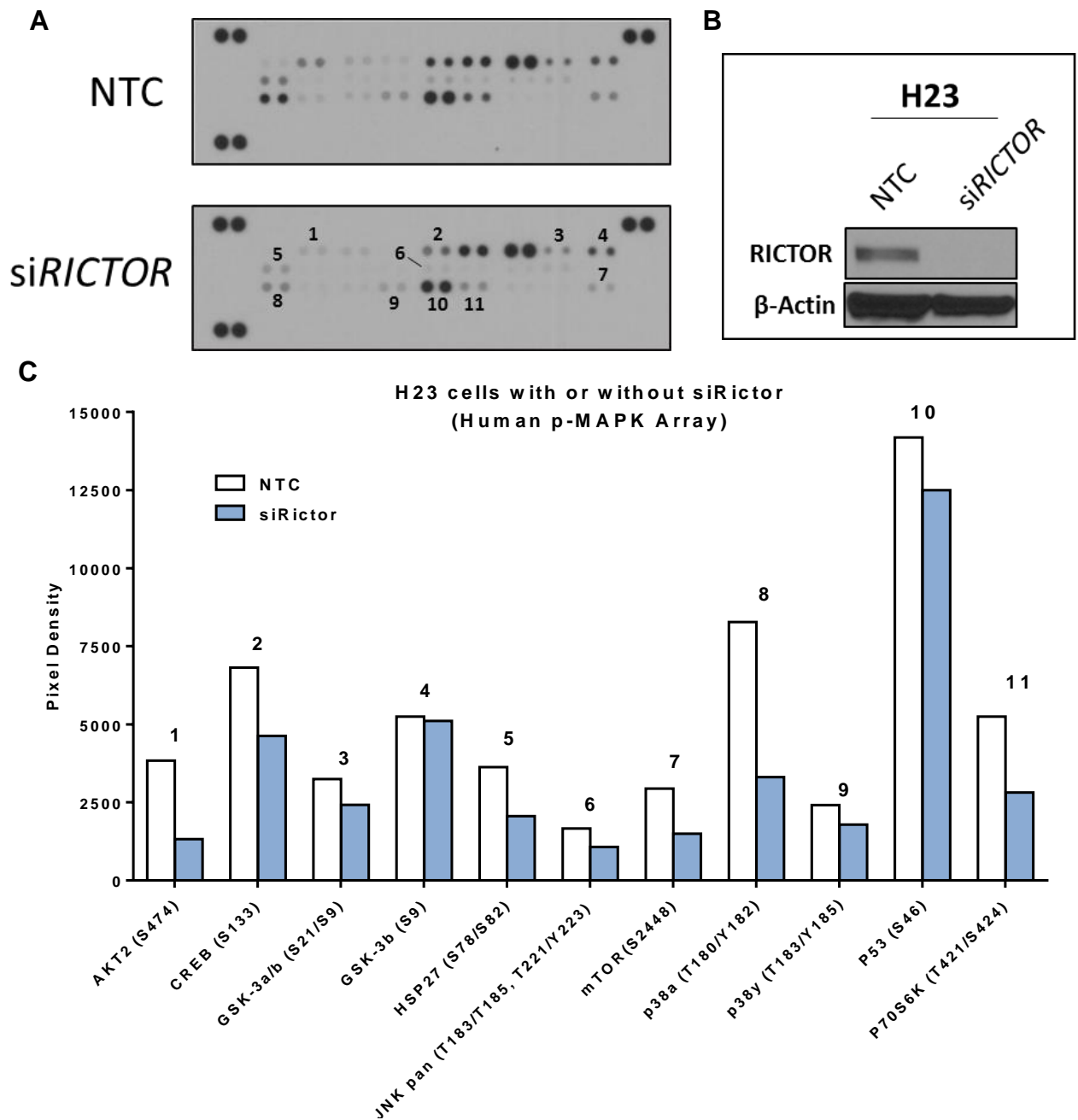


Figure 22. Human p-MAPK array reveals RICTOR is linked to several

mediators of cellular stress and survival. (A) Whole-cell extracts from H23 cells, treated with a NTC or siRICTOR for 72 hours, were incubated with the Human p-MAPK array, and phosphorylation status of 26 kinases was captured from a 5 minute exposure to X-ray film. (B) Western blotting analysis of lysates used for array shows knockdown efficiency of siRICTOR. (C) Densitometric quantification of selected phospho-kinases (in duplicates) marked by corresponding numbers.

Chapter 6

Results

6.1 *RICTOR* knockdown enhances the pharmacologic efficacy of MAPK pathway inhibition in *RICTOR/KRAS-altered* NSCLC cell lines

To exploit the compensatory MAPK pathway activation seen following *RICTOR* signaling inhibition, we evaluated the effect of blocking the MEK-ERK signaling pathway via pharmacologic agents alone or in combination with genetic *RICTOR* blockade, in specific *KRAS* co-mutational settings *in vitro*. We tested two currently available allosteric MEK1/2 inhibitors, selumetinib (AZD6244) and trametinib (GSK1120212), either alone or in combination with sh*RICTOR* treatment in three *RICTOR* amplified, *KRAS* mutant sh*RICTOR* inducible cell lines via MTT assay (Figure 23A). Pharmacologic disruption of signaling in the MEK-ERK pathway by selumetinib (5 μ M) or trametinib (0.05 μ M) alone rendered all three cell lines resistant (> 50% viability) at the selected doses. However, the response was more marked in the presence of sh*RICTOR* in combination with MEK1/2 targeted therapy, seen by a significant reduction in cell viability compared to either inhibitor alone ($P < 0.0001$).

We next checked the signaling effects induced by the MEK1/2 inhibitors with or without *RICTOR* knockdown by Western blotting analysis in the representative H23 cell line (Figure 23B). Single treatment with either MEK inhibitors or combined with sh*RICTOR* suppressed AKT and MAPK signaling pathways (seen by reduced p-AKT and p-ERK levels, respectively) in a dose-dependent manner. In concordance with the aforementioned cell viability results, there was a substantial increase in the cleaved PARP (cl-PARP) levels detected in samples treated with concomitant MEK inhibitors

and shRICTOR compared to MEK inhibition alone, signifying reduced cell viability as a result of increased apoptosis.

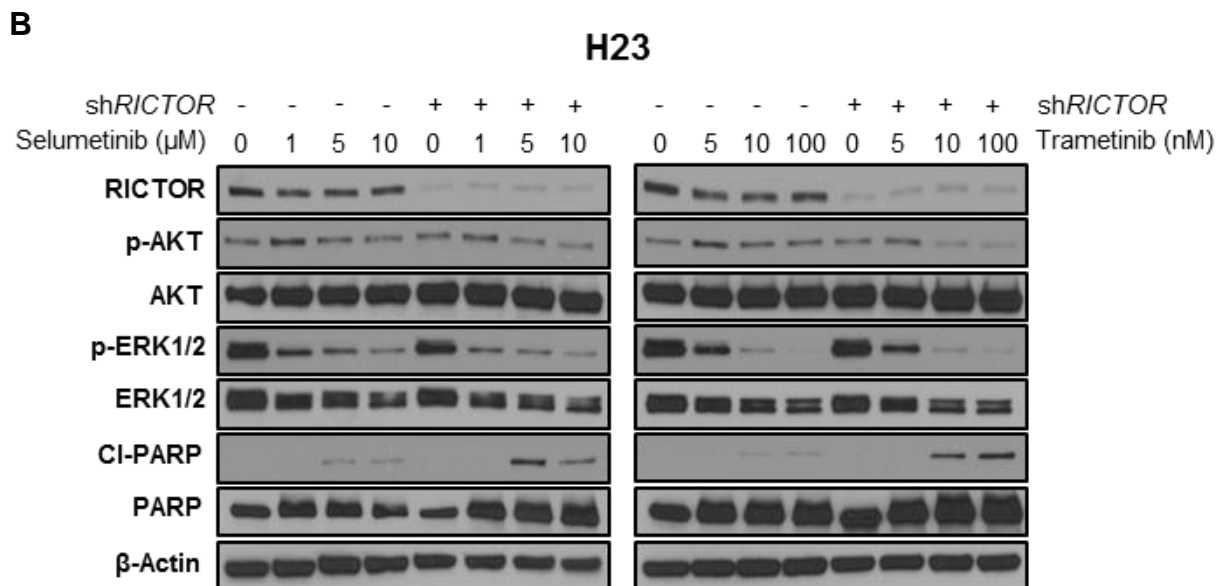
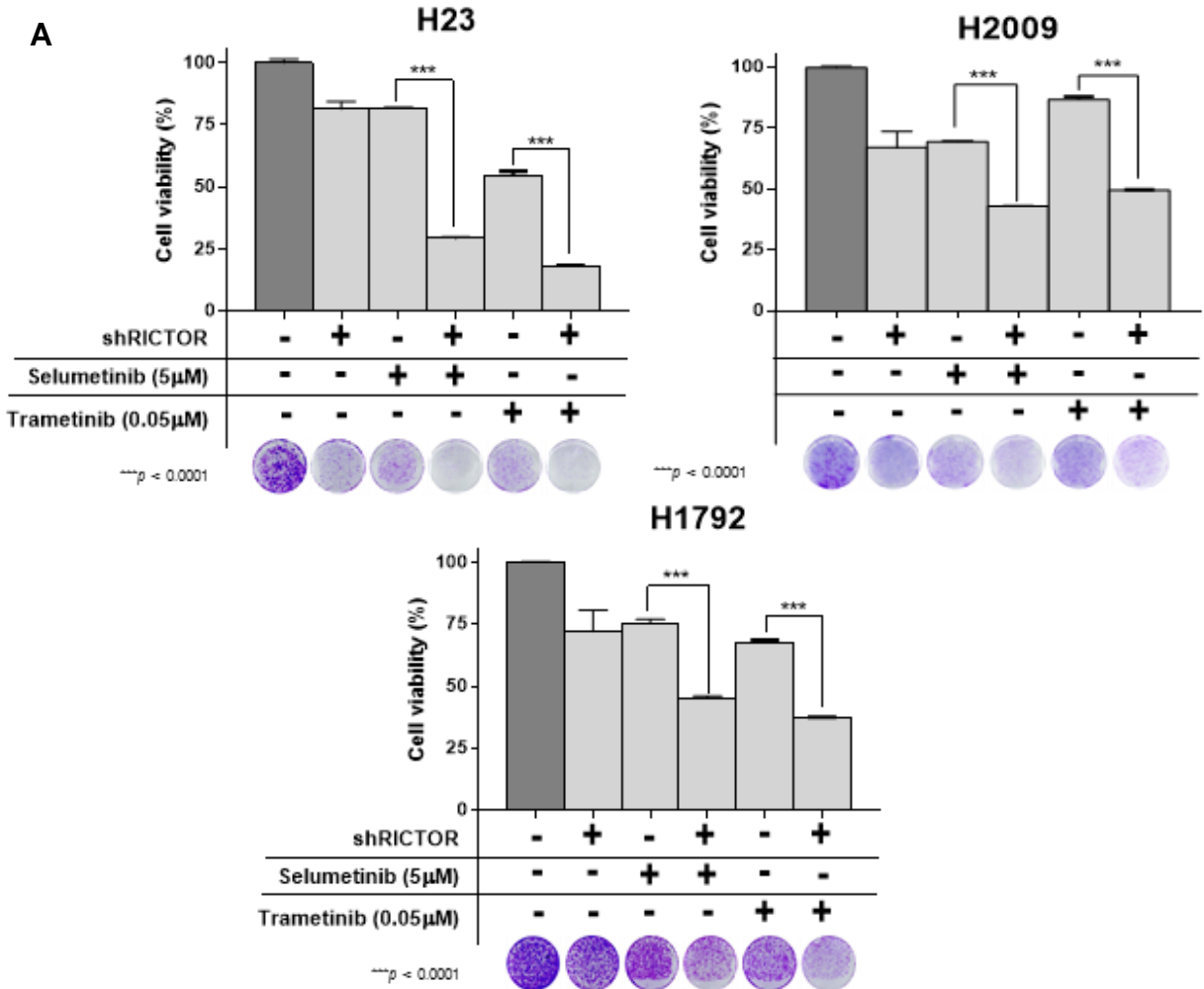


Figure 23. *RICTOR* knockdown enhances the pharmacologic efficacy of MAPK pathway inhibition in *RICTOR/KRAS-altered* NSCLC cell lines.

(A) Inducible sh*RICTOR* NSCLC cell lines were cultured in the presence or absence of 2µg/mL doxycycline to induce sh*RICTOR* knockdown, alone or in combination with either selumetinib (AZD6244, 5µM) or trametinib (0.05µM). After 7 to 10 days of treatment, cell viability was measured by MTT assay and compared between sh*RICTOR* alone and in combination with MEK1/2 inhibitors. Separate wells were stained with crystal violet on the same day to visualize and complement cell viability data. Data are graphed as the mean percentage ± percent SD. ***, $P < 0.0001$.

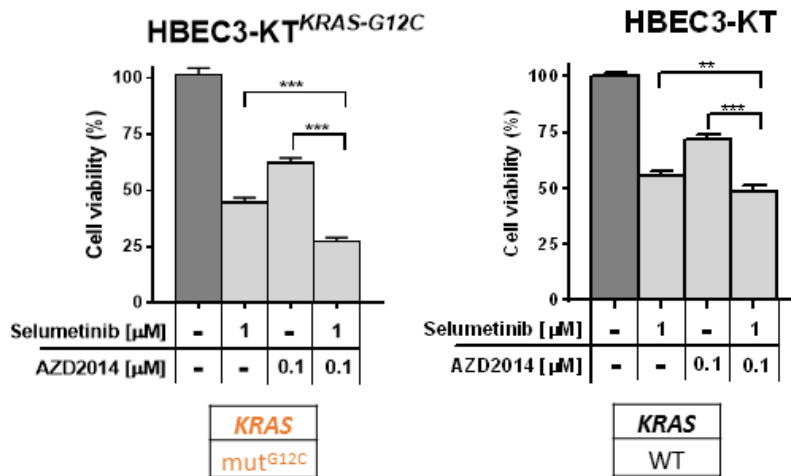
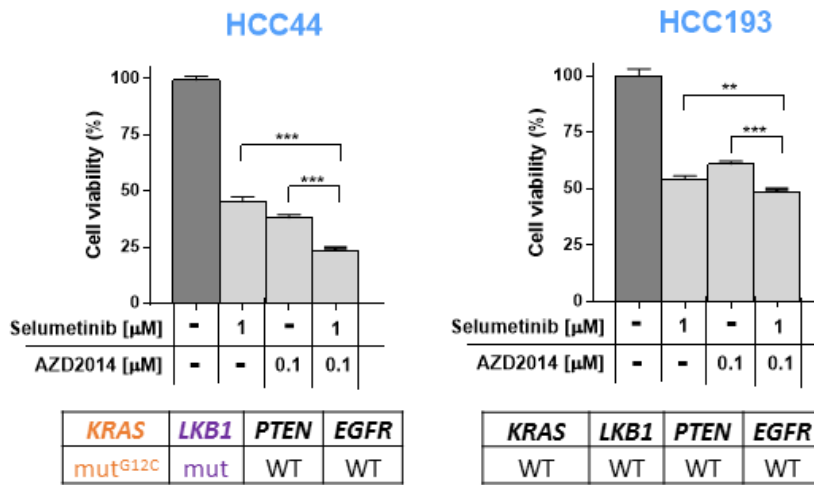
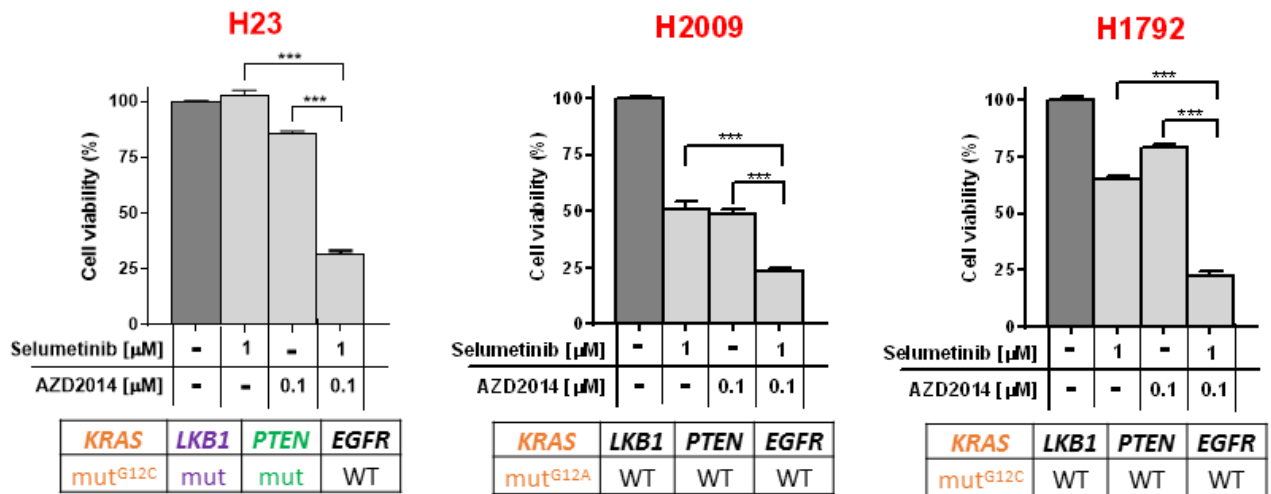
(B) Western blot analysis of inducible H23 cell line treated with increased doses of selumetinib (left, 1, 5, 10 µM) or trametinib (right, 5, 10, 100 nM) alone or in combination with 2µg/mL doxycycline to induce sh*RICTOR* knockdown for a total 6 days. Total and phospho-specific antibodies used were for levels of RICTOR, p-AKT (S473), AKT, p-ERK1/2 (T202/Y204), ERK1/2, cleaved-PARP, PARP, and β-Actin as loading control.

6.2 Combined mTORC1/2 and MEK inhibition is an effective therapeutic approach in *RICTOR/KRAS*-altered settings and results in synergistic anti-tumor effects *in vitro*

We next wanted to investigate the efficacy of our dual pathway inhibition approach by use of two currently available pharmacologic inhibitors either alone or in combination across several *RICTOR* amplified or non-amplified NSCLC cell lines that carry various secondary mutations in the PI3K/AKT/mTOR and/or MAPK pathways. We performed an MTT assay after treating cells with selumetinib and/or the dual catalytic mTORC1/2 inhibitor AZD2014 (currently in phase II clinical trials) at the specified doses (Figure 24). In H23, H2009, and H1792 (*RICTOR* amplified, *KRAS* mutant) cell lines, concomitant targeting of mTORC1/2 and MEK resulted in approximately 75% reduction of cell viability in all three cell types. Of note, H23 also harbors *LKB1* and *PTEN* mutations, which could explain why this cell line is more resistant to either single agent treatment when compared to H2009 or H1792. We then tested our inhibitors in two *RICTOR* non-amplified cell lines, HCC44 and HCC193, which are *KRAS* mutant or wild-type, respectively. In HCC44 cells, combined selumetinib and AZD2014 treatment decreased cell viability by over 75%; however, HCC193 cell lines were relatively resistant to either agent alone or the combination (> 50% cell viability). To further confirm that this dual pathway inhibition is most effective specifically in *KRAS* co-mutant settings, we used the isogenic human bronchial epithelial cell lines (HBECs) previously described (137, 138), that either have *KRAS* wild-type (HBEC3-KT) or *KRAS* G12C mutation (HBEC3-KT-G12C). Our results indicated that in concordance with the aforementioned data in NSCLC cell lines, HBEC3-KT cells with *KRAS* mutation are significantly more sensitive to the dual

pathway blockade of selumetinib with AZD2014 (~75% reduction in cell viability) compared to the *KRAS* wild-type cells which were more resistant (~50% viability).

In addition, we assessed whether the combination therapy of both drugs resulted in synergistic, additive, or antagonistic effects across a range of therapeutic doses by MTS assay. H23, H2009, H1792 (*RICTOR* amplified, *KRAS* mutant) cell lines were treated with various concentrations of AZD2014 (0.024-12.5 μ M) and a fixed set of selumetinib doses (2.3, 4.6, 9.3, or 18.7 μ M) for 96 hours (Figure 25). We calculated the combination index (CI) values based on the previously described Chou-Talalay model (139) using ComboSyn software (ComboSyn Inc, Paramus, NJ). The CI parameters used were: CI = 0-0.9, synergism; CI = 0.9-1.1, additive effect; CI > 1.1, antagonism. In all three representative cell lines, optimal drug dose combinations that impose synergistic effects were found. H23 showed the highest level of synergism in the range of AZD2014 (0.024-0.781 μ M) combined with selumetinib (2.3 or 4.6 μ M), whereas increasing the AZD2014 and/or selumetinib combination doses outside of these ranges resulted in a loss of synergy and caused an additive or antagonistic effect. In H2009, we found consistent synergism across most of the combination dose ranges used, and in H1792 the synergistic and/or additive effects were observed in the range of AZD2014 (0.195-6.25 μ M) combined with selumetinib (2.3-18.7 μ M). Collectively, these findings suggest that a dual pathway inhibition approach is warranted in specific NSCLC settings where *RICTOR/KRAS* alterations exist, and that careful consideration should be given when combination dosing is performed to render most effective synergistic anti-tumor effects.



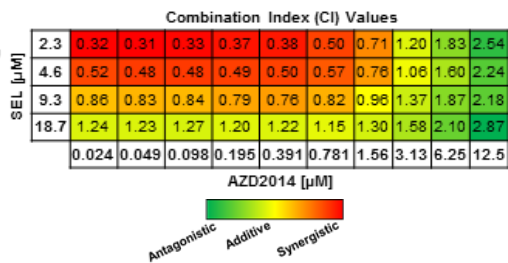
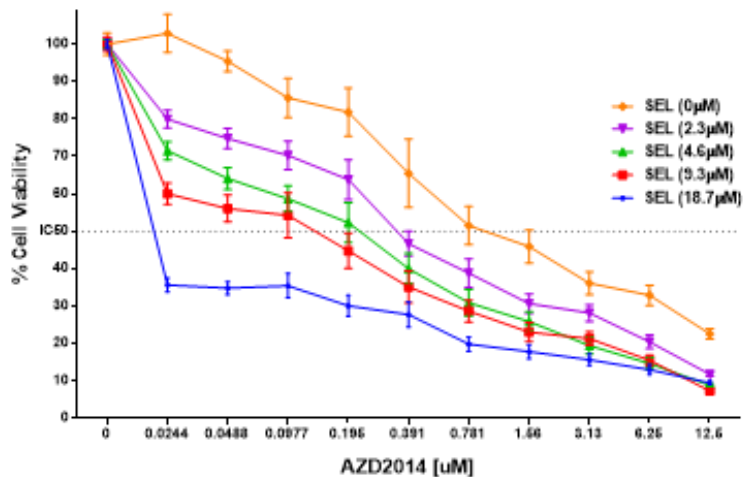
■ RICTOR amplified NSCLC cells
■ RICTOR non-amplified NSCLC cells
■ HBEC (Immortalized Human Bronchial Epithelial Cells)

Selumetinib: (MEK1/2 inhibitor)
 AZD2014: (mTORC1/2 inhibitor)

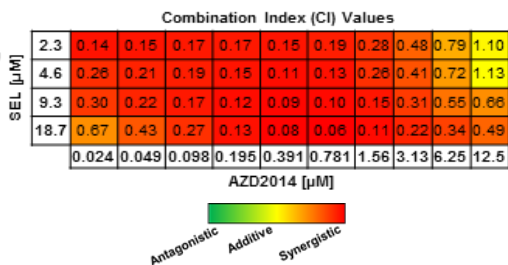
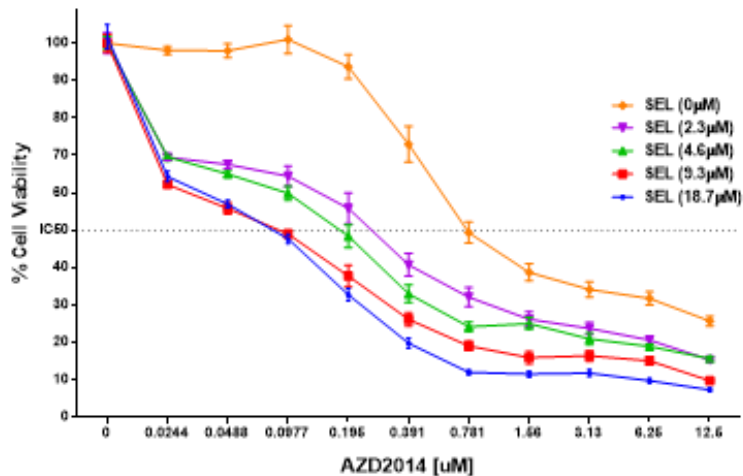
Figure 24. Combined mTORC1/2 and MEK1/2 inhibition is an effective therapeutic approach in *RICTOR/KRAS*-altered *in vitro* settings.

Five NSCLC cell lines (3 *RICTOR* amplified (red), 2 *RICTOR*-non-amplified (blue)) and two immortalized human bronchial epithelial cell lines (HBECs, black) were treated with DMSO (control), selumetinib (1 μ M), AZD2014 (0.1 μ M), or the combination selumetinib (1 μ M) with AZD2014 (0.1 μ M). Mutation status of *KRAS*, *LKB1*, *PTEN*, and *EGFR* are shown below each cell line. After 72 hours of treatment, cell viability was compared to control DMSO cells and measured by MTT assay. Data are graphed as the mean percentage \pm percent SD. **, $P < 0.01$; ***, $P < 0.0001$.

H23



H2009



H1792

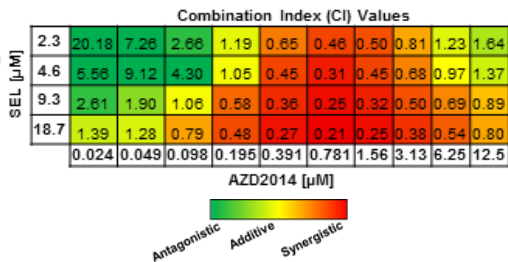
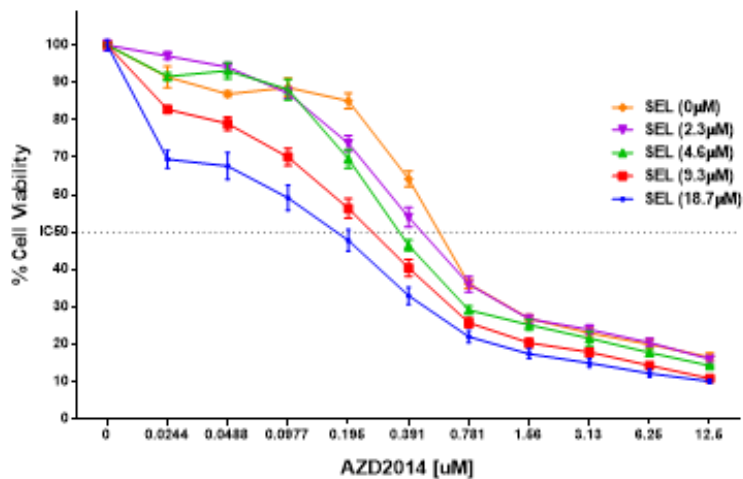


Figure 25. AZD2014 and selumetinib act synergistically to block mTOR and MAPK pathway signaling *in vitro*.

Three NSCLC (*RICTOR* amplified, *KRAS* mutant) cell lines were incubated with increasing concentrations of AZD2014 (0.024-12.5 μ M) and a fixed dose of selumetinib (0, 2.3, 4.6, 9.3, 18.7 μ M) for 96 hours. Controls were treated with DMSO only. Cell viability was analyzed by MTS assay. Data are graphed as the mean percentage \pm percent SD. Combination index (CI) values were calculated using ComboSyn software (ComboSyn Inc, Paramus, NJ). The CI parameters used were: CI = 0-0.9, synergism; CI = 0.9-1.1, additive effect; CI > 1.1, antagonism.

6.3 Comparative effects of mTORC1/2 and MEK1/2 pathway inhibition *in vivo*

To determine whether the synergistic effects seen *in vitro* translated into anti-tumorigenic effects *in vivo*, we utilized our stably transduced inducible sh*RICTOR* cell line H1792 (*RICTOR* amplified, *KRAS* mutant) to subcutaneously establish tumor xenografts in mice. Once tumors reached a palpable size of 150 to 200 mm³, the animals were randomized into five treatment arms: vehicle (1% tween-80, *bid*), selumetinib (25mg/kg, *bid*), selumetinib (25mg/kg, *bid*) + doxycycline feed (600mg/kg), AZD2014 (15mg/kg, *qd*), and selumetinib + AZD2014 (equivalent dosages used as per individual inhibitor treatments). Dose administration via oral gavage was performed for a total of 22 days continuously, with tumor volumes and mouse body weights recorded twice weekly (Figure 26 A, B).

Results show that in comparison to the vehicle (control) group, mice receiving selumetinib with AZD2014 had the most enhanced antitumor effects compared to single-agent treatment groups. Similarly, we saw a significant reduction of tumor growth in the selumetinib with sh*RICTOR* (+Doxy) treatment arm compared to control, although the utilization of the abovementioned combination drugs still had a more pronounced reduction in tumor volume. Interestingly, in concordance with our *in vitro* H1792 cell viability MTT data (Figure 24), selumetinib treatment alone resulted in an increased reduction of cell viability/tumor growth compared to single agent AZD2014 treatment, suggesting that this particular *KRAS* mutant setting (*KRAS*^{G12C}) is more sensitive to MEK1/2 inhibition than mTORC1/2, despite having amplification of *RICTOR* present. Furthermore, to determine whether these effects were seen without detrimental consequences on the health and well-being of the experimented animals, body weight of animals was measured several times a week (Figure 26B). No

significant loss of body weight or visible signs of declined health were witnessed during the duration of any of the treatments.

Following the last treatment dose, tumors were extracted after 3 hours proceeding the final dose administration, and tumor lysates were prepared as described in materials and methods section. Representative samples from each treatment arm were subject to Western blotting analysis (Figure 26C). Results revealed that the treatments alone and the combination inhibited their direct targets of each inhibitor. The treatment groups incorporating selumetinib effectively blocked downstream p-ERK1/2 signaling, AZD2014 had a marked reduction in the downstream mTORC1/2 effectors p-AKT, p-S6RP and p-4EBP1, and sh*RICTOR* induction with doxycycline showed a reduction in the total RICTOR protein levels. Collectively, these findings suggest that AZD2014 in combination with selumetinib result in significant anti-tumor effects mediated through mTORC1/2 and MEK dual pathway inhibition, and is an effective therapeutic strategy in *RICTOR/KRAS*-altered NSCLC.

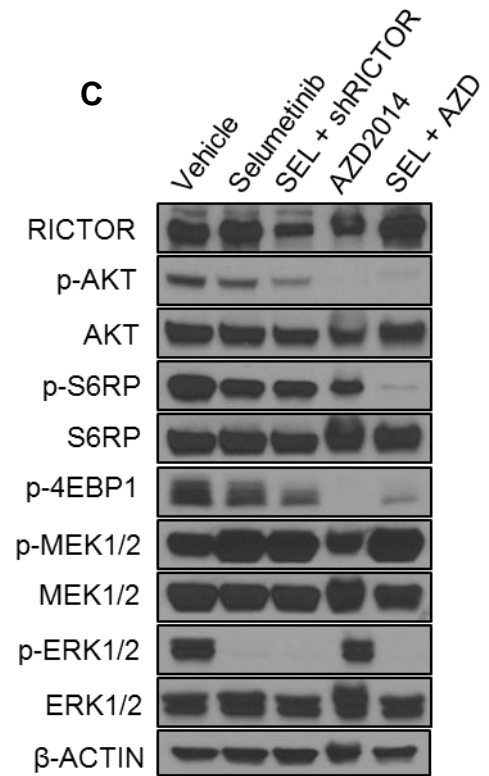
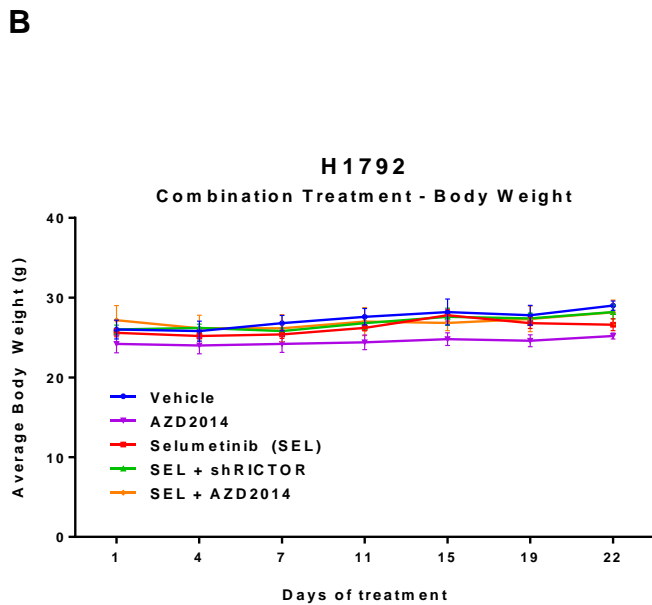
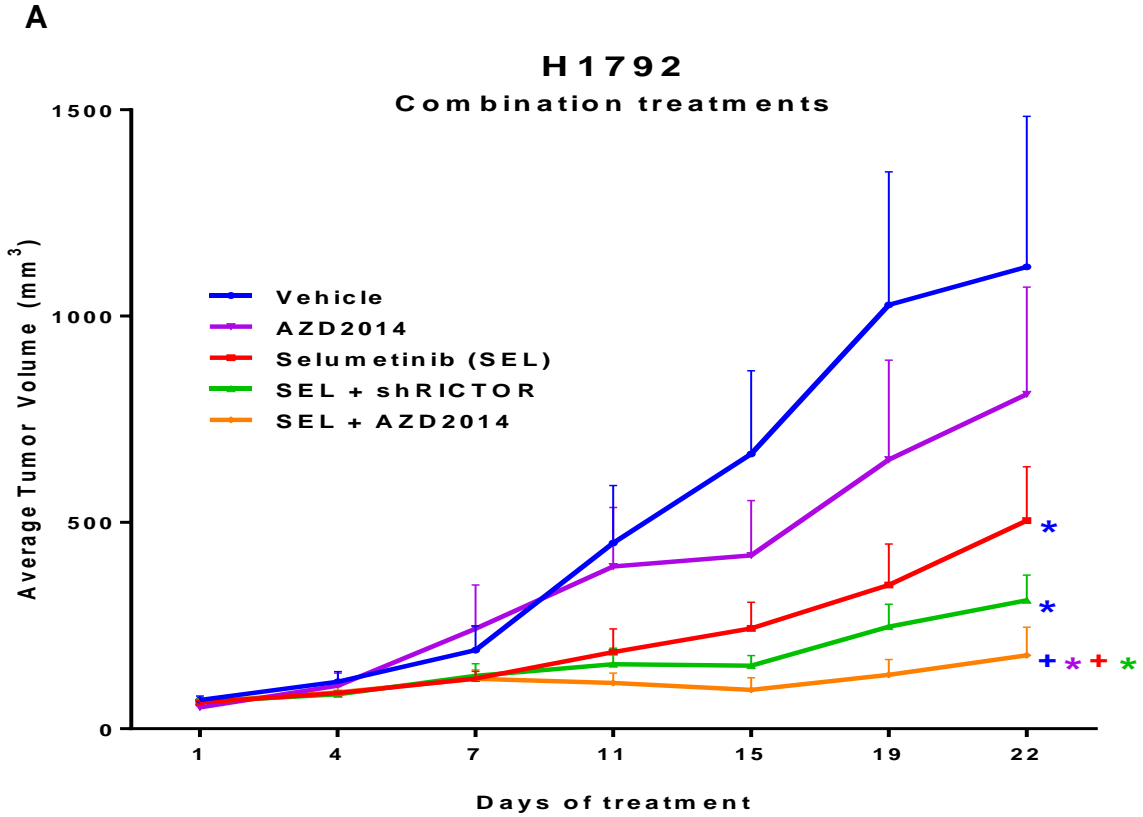


Figure 26. Selumetinib in combination with sh*RICTOR* or AZD2014 results in the strongest anti-tumor activity *in vivo*.

(A) Athymic nude mice were inoculated subcutaneously with the inducible H1792 sh*RICTOR* cell line. Once tumor volumes reached an average of 150 to 200 mm³, mice were randomized to each treatment group and given the respective treatments via oral gavage daily for a total of 22 days. Tumor volumes were measured twice weekly, and data points are presented as the mean tumor volume \pm SEM. Colored asterisks represent significant difference of that treatment from a different treatment resembled by its respective line color. (*, $P < 0.05$; +, $P < 0.01$). (B) Average body weight of mice is displayed for each treatment arm, and measured twice weekly. (C) Western blot analysis showing the levels of indicated proteins in tumor lysates harvested 3 hours after last drug treatment on day 22.

Chapter 7

Discussion, Conclusions, and Future Directions

Lung cancer is the leading cause of cancer-related mortality worldwide, with a dismal five year survival of less than 16% and over 1.5 million deaths annually (140). Despite improvement in early detection strategies and standard treatment options, it continues to have a poor prognosis. What were once considered a single disease entity, lung tumors are now comprised of discrete genetically and clinically distinct subtypes. NSCLC is the most prevalent type of lung cancer, and the last decade has seen significant effort invested in the advent of rapid genomic profiling that led to development of molecular-targeted therapy that inhibit key oncogenic drivers such as *EGFR*, *ALK*, and *RAF*, resulting in dramatic responses in patients (5). However, even though responses are seen initially, these targeting agents rarely promote complete or durable antitumor effects especially in unselected patients, leading to acquired resistance mechanisms and relapse. Further, effective therapeutic options still lack for lung tumors driven by other key mutations such as in oncogenic *KRAS* (~30%) and those with untargetable oncogenic drivers that are yet to be discovered (123, 141). Moreover, it is now evident more than ever that clinical trials performed in the absence of sufficient molecular and genetic stratification lead to poor response rates in patients.

In this study, we aimed to identify novel actionable genetic alterations in lung cancer by utilizing genomic profiling data from the BATTLE-2 clinical trial that targets advanced stage chemorefractory NSCLC patients. We identified *RICTOR* alterations (amplifications and/or mutations) to be present in 17.4% (16/92) of advanced stage

NSCLC patients, including 11.9% amplifications (11/92) and 5.4% mutations (5/92). Mutations in the *RICTOR* gene have not been previously characterized, and thus the precise functional significance of these mutations is yet to be determined. To date, only one correlative study was found from literature searches highlighting a specific *RICTOR* polymorphism (rs6878291) associated to clinical benefit and that serves as an independent risk factor for progression-free survival in a cohort of Chinese NSCLC patients treated with platinum-based chemotherapy (142) . However, the exact functional significance of this SNP is unknown and further validation is needed in an independent cohort to draw any major conclusions from this study. Interestingly, mutations in the *RICTOR* gene identified from the BATTLE-2 patients were all mutually exclusive from *RICTOR* gene amplifications. We also surveyed early-stage lung adenocarcinoma cases using the TCGA dataset, and identified a total 13.4% (31/230) of *RICTOR*-altered cases, which included 10% amplifications (23/230) and 5.2% mutations (12/230). When we utilized the cBioPortal dataset analysis tool to identify the frequency of *RICTOR* alterations across numerous different tumor types, we found that alterations in this gene are also found in other cancers and are not exclusive to lung tumors. However, the highest frequency of alterations was found in NSCLC, particularly in lung adenocarcinoma. Further, in contrast to our advanced stage BATTLE-2 cases, we identified 4 early stage cases in the TCGA dataset that had concomitant *RICTOR* gene amplifications and mutations. These data might suggest that advanced-stage tumors do not require concomitant alterations in the *RICTOR* gene to drive the involved pro-tumorigenic processes, whereas some early stage tumors require concomitant mutations. Also, it is not clear which alteration type—*RICTOR* amplification or mutation—is more important in the oncogenic process

or in terms of response to specific targeted therapies. An example of the importance of this difference was shown in a report analyzing mutations versus amplifications of the gene, *KIT*, in melanomas, and found that patients with *KIT* mutations had responses to the tyrosine kinase inhibitor, imatinib, whereas those with amplifications had no response (143). As noted above, a closer examination of the functional significance of these mutations is required to fully decipher their implications in NSCLC tumorigenesis. Experimental approaches such as site-directed mutagenesis or targeted CRISPR-Cas9 approaches *in vitro* can be utilized to aid in such studies.

Gene amplifications refer to the increase in copy number levels of a gene within the genomic DNA of a cell. Amplification of a gene typically involves the overexpression of the gene product, consequently leading to selective advantages for tumor cell growth. We were interested to evaluate the correlation between *RICTOR* amplification and *RICTOR* gene expression in our two datasets. Our findings show that there was a significant direct correlation between *RICTOR* gene amplification and *RICTOR* mRNA expression in the early stage TCGA dataset, and a trend seen in the advanced stage BATTLE-2 lung adenocarcinoma cases. It is important to note that when we performed this analysis including all NSCLC subtypes from the BATTLE-2 cases (total of 159 cases that were subjected to DNA NGS profiling), there was statistical significance of direct correlation between *RICTOR* gene amplification and *RICTOR* mRNA expression (data not shown). These differences in significance could be due to either the smaller sample size of *RICTOR* amplified lung adenocarcinoma cases being a limitation factor, or that in other NSCLC subtypes (e.g. small-cell lung carcinomas), increased *RICTOR* copy number levels definitively drive the mRNA expression of *RICTOR* in those tumor histotypes. Another possibility could be

differences in epigenetic and micro-RNA (miRNA) regulatory mechanisms in these tumors. One such example is a study that found that DNA hypermethylation silences miR-218 in oral squamous cell carcinoma, which directly targets RICTOR and suppresses its expression and activity (112). Another study showed that the downregulation of miR-153 resulted in increased RICTOR mRNA and protein expression and tumorigenic activity, explaining the upregulation of RICTOR seen in human glioma tissues and cell lines (144).

We next wanted to determine the association of *RICTOR* alterations to prognosis using our clinical datasets. Since we have mutation data from our BATTLE-2 and TCGA datasets, we checked whether there is association between dichotomizing *RICTOR* amplified, mutated, or altered (combining amplified/mutated) cases versus non-altered cases, and correlated these parameters to overall survival and progression-free survival (data not shown). Results yielded a lack of statistical significance between all these analyses, most likely due to inadequate statistical power as a result from the limited number of mutant cases. Since we found an overall direct correlation between *RICTOR* amplification and mRNA expression, we next analyzed whether levels of *RICTOR* mRNA expression associated to outcome in our datasets. For this analysis, in addition to our BATTLE-2 (advanced stage) and TCGA (early stage) cases, we utilized the PROSPECT cases, a dataset our laboratory possesses, which is comprised of early stage surgically resected lung adenocarcinoma tumors, in which we have mRNA expression and clinical outcome data. We performed a univariate overall survival analysis of *RICTOR* mRNA expression using the Cox proportional hazards model. We found a significantly worse overall survival in patients with advanced stage lung adenocarcinoma in the BATTLE-

2 cases. We also noted poor prognosis in our early stage surgically resected lung adenocarcinoma cases from the PROSPECT dataset; however, no significance was seen in patients from the TCGA dataset. One possible explanation could be that in heavily pre-treated advanced stage cases (BATTLE-2), RICTOR serves a more dominant role in driving malignant phenotypes of tumors and has an important interplay with co-oncogenes such as *KRAS*, ultimately leading to a worse survival of patients due to the severity of mutational burden. Similarly, although the PROSPECT cases are still considered early stage cases relative to the BATTLE-2 cohort, these tumors are more advanced compared to the TCGA lung adenocarcinomas. On the contrary, in the TCGA cases, the mutational load is lower due to the early stage and less treatment exposure, and therefore RICTOR serves more as a secondary driver and requires, in some cases, to harbor concomitant mutations and amplifications in *RICTOR* to perhaps drive cancer progression. Although the true prognostic implications of RICTOR remain unclear in the context of NSCLC, a more expanded analysis of larger study cohorts may provide more conclusive information on RICTOR's predictive and prognostic role. To date, RICTOR's association with prognosis has been proposed in some tumor types with differing conclusions. For instance, RICTOR mRNA and protein expression was determined to be an independent prognostic factor for endometrial carcinoma (145). Also, *RICTOR* mRNA expression was identified as an independent prognostic indicator for disease-free survival in patients with hepatocellular carcinoma (146). Conversely, elevated *RICTOR* mRNA expression was found in normal breast tissues, lower tumor grade, and correlated with a significantly better disease-free and overall survival (147).

A recent study by Cheng *et al.* highlighted *RICTOR* amplification as a distinct subset of lung cancer patients, and reported *RICTOR* amplifications in 8.4% of lung adenocarcinomas from an independent cohort (Foundation Medicine, Inc.) (117). Of these, 11% of the cases harbored *RICTOR* amplification as the sole potentially actionable target out of a targeted gene panel. In concordance with our data, the study highlighted the oncogenic role of RICTOR by showing that RICTOR inhibition resulted in reduced cancer cell growth and cell survival in NSCLC cells amplified for *RICTOR*. Moreover, their data indicated that dual mTORC1/2 inhibition was effective against *RICTOR* amplified lung cancer cells. They further reported one patient (harboring *RICTOR* amplification as the single actionable genomic alteration found) that underwent treatment with dual mTORC1/2 therapy, and had over 18 months of tumor stabilization. Although the strategy of dual mTORC1/2 therapy for *RICTOR* amplified cases seems reasonable in settings where the only major oncogenic actionable driver is RICTOR, our data presented here suggest that this treatment strategy may not be as effective in lung tumors where other genomic aberrations are present.

To gain insight into the co-mutational landscape that exists in *RICTOR*-altered cases, we utilized the cBioPortal platform to survey the TCGA dataset for enrichment of specific pathway alterations that are known to be deregulated in lung cancers. We examined the frequency of alterations (mutations and/or copy number changes) in genes known to mediate key pathways, including tyrosine kinase (RTK) signaling, mTOR signaling, MAPK signaling, and oxidative stress response. Of great interest, we found co-mutational enrichment of alterations in genes involved in the oncogenic MAPK pathway, including *KRAS*, *NF1*, *BRAF*, and *CRAF*. The elevated frequency of

these co-mutations suggested that RICTOR could potentially serve as an important co-oncogenic driver in lung cancer progression in specific molecular settings. *KRAS* has been an orphan target, and numerous attempts in its direct and even indirect targeting have failed (88). Therefore, a great shift in focus over the years has occurred to study and potentially inhibit downstream or parallel effector pathways and molecules. Additionally, characterizing the genomic landscape of *KRAS* mutant lung tumors is critical to better determine co-driver alterations that when identified and appropriately targeted, can re-sensitize RAS-driven tumors to the given therapeutic modalities. These results tailored our experimental efforts and focus on characterizing the significance of RICTOR in the context of NSCLC, specifically in a *KRAS* co-mutational setting

Our *in vitro* cell line models were carefully selected to reflect the heterogeneity of NSCLC and specific mutations in the MAPK pathway. Cell lines selected were either *RICTOR* amplified or non-amplified, and included various co-mutations in *KRAS*, *PTEN*, *PIK3CA*, *STK11*, and/or *EGFR*. Similar to our clinical findings that *RICTOR* amplified cases directly correlated with *RICTOR* mRNA expression, we found that our *RICTOR* amplified cell lines had a significantly higher RICTOR protein expression compared to non-amplified cell lines. This is supportive of the idea that amplification of this gene drives the overexpression of the protein product, perhaps leading to increased malignant effects.

Since RICTOR's roles in tumorigenesis are actively emerging, both dependent and independent of the mTORC2 complex, we sought to characterize the phenotypic consequences of modulating the levels of RICTOR in our *in vitro* cell line panel to better understand RICTOR in the context of NSCLC. We found that *RICTOR*

knockdown significantly reduces the clonogenic and anchorage-independent growth of *RICTOR* amplified cells. In assessing its role on the tumorigenic potential in a more physiologically relevant *in vivo* settings, we found that knocking down *RICTOR* in H1792 and H23 (*RICTOR* amplified, *KRAS* mutant) xenografts significantly abrogated the tumorigenicity of these cells in nude mice. These results are in concordance with other studies showing that in various tumor types, including gliomas, bladder, ovarian, and prostate cancers, *RICTOR* contributes oncogenic properties (103, 117, 148, 149).

Moreover, when we performed migration and invasion assays, we found that *RICTOR* knockdown in *RICTOR* amplified cell lines significantly abrogated the migrative and invasive capacity of these cells. *RICTOR*'s role in migration and/or invasion has been previously reported. For example, several reports have shown that in glioma and bladder cancer cell lines, the genetic silencing of *RICTOR* significantly reduced cell growth, migration and invasion (103, 148). In addition, Lamouille *et al.* have shown that the mTORC2 complex is an essential downstream mediator of TGF- β signaling, affecting cellular migration (through regulation of focal adhesions in response to paxillin expression), invasion (through induction of MMP9 expression), and cancer cell dissemination (through EMT-associated cytoskeletal and gene expression changes) (150). Moreover, the *RICTOR*/mTOR complex has been reported to modulate the activity of PKC α in regulating the actin cytoskeleton to impair cell motility (41); however, this mechanism could be cell type specific, as another study was unable to determine similar findings upon treatment with classic PKC inhibitors to reverse this phenotype (151). Instead, their findings suggested that *RICTOR* interacts and specifically regulates PKC ζ activation to induce cancer cell metastasis in an mTORC2-independent manner (151). On the contrary, Das *et al.*

reported that suppression of RICTOR actually resulted in an increased invasive capacity of glioma cells by enhancing the expression of MMP9 through a RAF1-MEK-ERK mediated pathway (152). Perhaps one of the more convincing pieces of evidence shedding light on RICTOR's independent role on regulating cell migration was elucidated in a study showing that loss of RICTOR leads to the induction of RhoGDI2, which disrupts cell migration via the inhibition of RAC1 and CDC42 GTPase activity (106). Both of these GTPases have been shown to regulate cell motility and the actin cytoskeleton (153). Interestingly, in our studies, the trend of downregulation of cell migration and invasion following RICTOR abrogation was observed specifically in *RICTOR* amplified cell lines that also carried concomitant *KRAS* mutations (H23, H2009, and H1792). We did not observe this trend in *RICTOR* amplified but *KRAS* wildtype cell lines (H2172, H2126). *KRAS* has been previously linked to regulating migration and invasion in various cancer types. Specifically, mutant *KRAS* has been shown to promote invasion and metastasis in pancreatic cancer through regulation of GTPase pathways involving RhoGAP5, RalA, and CAV-1 (154). Additionally, Sunaga *et al.* showed that oncogenic *KRAS* in NSCLC induces interleukin-8 overexpression to promote cell migration (155). Although the mechanism underlying the role of RICTOR, specifically in the context of mutant *KRAS*, in regulating migration and invasion was outside of the scope of this project, it would be interesting to show which, if any, of these previously reported mechanisms occur in our cell types, and whether mutant *KRAS* has a direct involvement in mediating these phenotypes in our cell types.

Furthermore, to better understand the phenotypic consequences described thus far, we wanted to evaluate if RICTOR affects cell proliferation. From our

experimental results, we found that silencing RICTOR in our amplified cell lines resulted in a significant reduction in cell number over time. Also, we found that there was a slight increase in G₀/G₁ cell cycle arrest as seen in our FACS cell cycle experiments. Western blotting analysis further confirmed that there was a decrease of cyclin D1 levels following *RICTOR* knockdown in the H23 cell line tested. Other studies have linked the regulatory effects of RICTOR/mTORC2 to cell cycle progression. For instance, depletion of RICTOR resulted in increased G₁ phase arrest caused by downregulation of cyclin D1, resulting in reduced proliferation and anchorage-independent growth in pancreatic and breast cancer cell lines (115). In agreement, a similar link was described in melanoma cells overexpressed with RICTOR which led to increased proliferation, colony formation, and cyclin D1 expression (127). Similarly, in hepatocellular carcinoma cells, targeted inhibition of RICTOR, but not RAPTOR, promoted G₀/G₁ cell cycle arrest and was explained by the reduced phosphorylation of p-AKT S473 levels, suggesting that hydrophobic motif phosphorylation of AKT may be required for the maintenance of cyclin D1 expression (129). There could be various mechanisms by which RICTOR's effects on cell cycle progression are mediated. One mechanistic basis of the reduction of cyclin D1 was shown in a study that pinpointed to the inhibition of mTORC2 triggering a proteasome-mediated cyclin D1 degradation via a GSK3-dependent manner, and suggested that specifically RICTOR, as part of mTORC2, is responsible for increasing the stability of cyclin D1 (128). This study further highlighted that although AKT is known to positively regulate cyclin D1 stability through the negative phosphorylation and inactivation of GSK3 (156), the reduced levels of cyclin D1 are independent of AKT. Other studies have reported that mTORC2 targeting suppresses cyclin D1 translation by inhibiting

the recruitment of *cyclin D1* mRNA to polysomes in certain leukemia cells (157, 158), since the downstream AKT/mTORC1 translational repressor, 4E-BP1, is known to be involved in the regulation of cap-dependent mRNA translation and can also be deactivated upon mTORC2 inhibition (29, 159). However, further investigation is needed to precisely decipher the relationship between RICTOR/mTORC2, AKT, and 4E-BP1 in cell cycle progression.

The consequences of RICTOR inhibition from our studies clearly highlighted the significance of this oncogene in the context of NSCLC. We next wanted to characterize the cell signaling patterns associated with RICTOR in our cell line panel. Our findings demonstrated that exclusively in *KRAS* co-mutational backgrounds, knockdown of *RICTOR* resulted in a compensatory increased activation of phosphorylated MEK1/2 levels compared to controls. We further discovered that this compensation occurs in both *RICTOR* amplified and non-amplified settings, suggesting that regardless of the increased expression of RICTOR in amplified cells, there is an important interplay between RICTOR and mutant *KRAS* in mediating crosstalk mechanisms between the mTOR/AKT and RAS/MEK pathways. Our *in vitro* work further uncovered that when we perform concomitant knockdown of *RICTOR* and *KRAS*, there is no increase in p-MEK levels, suggesting that mutant *KRAS* is required for this compensatory mechanism to occur.

To further define a potential mechanism mediating this crosstalk between these two parallel oncogenic pathways, we tested the hypothesis that the compensatory activation of p-MEK1/2 following RICTOR blockade is mediated through the de-repression of the inhibitory CRAF S259 phosphorylation as a result of decreased activation of AKT, leading to a more active CRAF involved in transduction of mutant

KRAS signaling. Previous reports have identified this negative crosstalk mechanism between AKT and CRAF in certain cellular contexts (49, 54, 55). In our tested H23 cell line, we found that genetic inhibition of *RICTOR* decreased p-AKT levels and as a result, reduced the phosphorylation of CRAF S259, suggestive of increased CRAF activity. When we tested the mTORC1 inhibitor everolimus, we did not find a significant reduction in the phosphorylation levels of CRAF, in line with the displayed elevated p-AKT levels, and in agreement with previously described AKT feedback loops following mTORC1 inhibition (130, 131). When we combined si*RICTOR* in combination with everolimus, there was a similar reduction of p-CRAF S259 levels as si*RICTOR* alone, displaying the lack of mTORC1 contribution to this crosstalk mechanism. Interestingly, treatment with our dual mTORC1/2 inhibitor, AZD2014, had only a slight effect on decreasing the inhibitory p-CRAF levels, despite having a pronounced reduction in p-AKT levels. These data suggest that RICTOR may have a unique interplay with AKT in mediating the CRAF cross-talk activity, independent of mTORC1 and mTORC2. Similar to our finding, a study by Das *et al.* showed that RICTOR ablation enhanced the phosphorylation of MEK, ERK, and also increased the CRAF kinase activity in glioma cells (152). In further support of the preliminary evidence shown here, there have been several reports signifying the importance of CRAF in the context of mutant *KRAS*. For example, in *KRAS*-driven NSCLC, CRAF, rather than BRAF, was determined to be the critical effector in mediating *KRAS* signaling (160). Similarly, Karreth *et al.* has shown that *KRAS*^{G12D} mutations elicit their oncogenic effects primarily through CRAF in a lung cancer mouse model, whereas BRAF is dispensable (161). Voice *et al.* has shown that of all the human RAS homologs tested, *KRAS* was revealed to be the most significant activator of CRAF *in*

vivo (162). In line with this, Lito *et al.* showed convincing evidence that in *KRAS* mutant tumors, effective MEK inhibition (and essentially MAPK pathway downregulation) requires the disruption of CRAF mediated MEK activation (163). Taken together, although our preliminary mechanistic findings here suggest a possible link between RICTOR/AKT-mediated regulations of CRAF activity in a *KRAS* mutant setting, further investigation is warranted. For example, it would be interesting to study the effects of genetic or targeted inhibition of AKT in this setting to conclusively confirm this negative crosstalk. Furthermore, it would be important to perform immunoprecipitation experiments to see if RICTOR, AKT, and/or CRAF directly bind in this particular cell line, and whether other mTORC2 components are involved. This will elucidate whether RICTOR is acting upon AKT independently of mTORC2 in this cell type, as prior studies have shown this to be a possibility (108, 109). Lastly, since this experiment was performed in one cell line (H23, *RICTOR* amplified, *KRAS/STK11/PTEN* mutant), it would be imperative to expand this study in other cell lines, particularly those that do not possess *RICTOR* amplification and/or the other listed co-mutations. This would shed light as to which specific genomic landscape the crosstalk occurs in, as it is well established that the complex heterogeneity of even cell lines results in differential signaling mechanisms.

As we continued to explore the cell signaling effects mediated by RICTOR in our *RICTOR* amplified cell lines, we performed a phospho-MAPK proteomic array on our H23 cell line to compare si*RICTOR* versus control cells. We found that RICTOR inhibition decreased the phosphorylation and activation levels of p38 α , CREB, and HSP27. Interestingly, these kinases have broad roles in mediating cellular stress response, survival, and/or proliferation, in which some of the signaling pathways and

functionalities overlap, especially since these kinases can, in fact, regulate one another (47, 134). Notably, the most significant difference in phosphorylation was seen in p38 α , which has been reported to have both tumor suppressive and oncogenic roles, depending on the cellular context. Although some reports have shown prosurvival functionalities, many others have associated this kinase with the induction of apoptosis during cellular stress (47). Another report confirmed similar results as ours, showing that in mice in which *RICTOR* is conditionally knocked out in the liver, phospho-proteomic profiling identified a significant reduction in the p38 MAPK levels *in vivo* (164). In connection to our abovementioned cyclin D1 downregulation and slight increase in cell cycle arrest after RICTOR inhibition, p38 has been shown to negatively regulate cell cycle progression by inducing a G₁/S checkpoint in response to osmotic stress, reactive oxygen species, and cell senescence stimuli (136). Specifically, p38 has been connected with reducing the levels of cyclin D1 either through an indirect transcriptional repression mechanism (165, 166), or through direct phosphorylation of cyclin D1, resulting in ubiquitination and proteosomal degradation (135). These data suggest that there could be a link between RICTOR and p38 α in modulating the cell cycle progression and cellular stress response in the NSCLC cell lines tested. Accordingly, accumulating evidence has shown that RICTOR/mTORC2 is linked to the regulation of metabolic stress, inflammatory response, and energy balance in various contexts (167-170). Furthermore, it is interesting to note that since we determined a compensatory activation of p-MEK following RICTOR inhibition, it is plausible that this activated MEK could bypass ERK and interact with p38 α to mediate alternate survival pathways such as autophagy. A study by Wang *et al.* demonstrated that MEK may play a more

important role by bypassing ERK and regulating BECLIN-1 expression to induce autophagy, emphasizing a non-canonical MEK-ERK signaling pathway (171). In line with this assumption, genetic ablation or targeted inhibition of p38 α was shown to cause cell cycle arrest and autophagic cell death in colorectal cancer cells (172). A more detailed mechanistic study assessing various markers of autophagy, senescence, proliferation, and/or apoptosis is needed to fully ascertain the mechanism by which we see a reduction in colony formation, cell counts, and tumorigenicity following RICTOR inhibition in our pre-clinical NSCLC models.

The PI3K/AKT/mTOR and RAS/RAF/MEK/ERK signaling pathways are critical integrators of mechanisms mediating cell survival, proliferation, differentiation, metabolism, and invasion/migration in response to extracellular stimuli. Various targeted therapies have been developed directed at each of these major oncogenic pathways (173, 174). However, it is now clear that monotherapeutic targeting of effectors of these pathways result in resistance mechanisms such as re-activation of feedback loops and cross-talk mechanisms. Thus, these acquired bypass mechanisms are to blame for the lack of therapeutic efficacy and relapse often seen in patients, and therefore prompt the use of combinatorial therapeutic strategies. Our *in vitro* and *in vivo* data suggest that RICTOR blockade results in a compensatory activation of the MAPK pathway, specifically in *KRAS* co-mutational settings. We show that in both *RICTOR* amplified and non-amplified NSCLC cell lines, *RICTOR* knockdown increases p-MEK levels only when the cells harbor *KRAS* mutations. This is important as mutations in *KRAS* have been identified in 20-30% of lung cancers and are known to serve as crucial drivers of this malignancy, leading to poorer prognosis and resistance to chemo- and targeted therapies, yet *KRAS* still remains an

orphan target in NSCLC and other tumors (3, 175). To date, direct targeting of aberrant KRAS activation has been unsuccessful despite significant research efforts (176). We exploited this resistance mechanism as a therapeutic vulnerability and therefore tested a dual pathway inhibition approach by use of a catalytic mTORC1/2 inhibitor (AZD2014) and allosteric MEK1/2 inhibitor (selumetinib). Our results suggest this combination renders a highly synergistic anti-tumor effect in our *RICTOR/KRAS*-altered NSCLC cell lines both *in vitro* and *in vivo*.

Combination strategies with other inhibitors targeting both pathways have been proposed and reported, but with varying efficacy and in differing genomic subsets. A study by *Meng et al.* found that combining selumetinib with an AKT inhibitor (MK2206) had a significant synergistic effect on tumor growth *in vitro* and *in vivo* in NSCLC (177). However, they found no correlation between mutational status of *KRAS*, *EGFR*, *BRAF*, or *PI3K* to sensitivity to either drug. Moreover, a study reported that activation of the PI3K pathway strongly influences sensitivity to MEK inhibition in *RAS* mutant cells, and thus suggest a combination therapy of PI3K and MEK inhibitors for tumors with concomitant mutations of *KRAS* and *PIK3CA* (178). However, the role of RICTOR in *PI3K* co-mutational settings is yet to be determined.

Similar to our proposed strategy, a recent *in vitro* study signified the rationale of combined inhibition of MEK and mTOR signaling in *KRAS* mutant NSCLC (179). They assessed a panel of EGFR/ALK wildtype NSCLC cell lines that are either *KRAS* mutant or wildtype, and have shown that inhibition of mTOR is dominantly responsible for the majority of growth inhibition in the combination therapy of mTORC1/2 inhibitor (AZD2014) with MEK1/2 inhibitor (trametinib), and the combination is more effective in *KRAS* mutant lines. Interestingly, our *in vitro* data testing selumetinib and AZD2014 in

KRAS mutant cells did not define a clear dominant trend between which drug has the more potent effect on cell viability, perhaps due to the diverse co-mutational nature of the RICTOR cell line panel. This could also be due to the differences in the MEK inhibitor used (selumetinib vs. trametinib), which are known to have differing mechanisms of action. Additionally, our *in vivo* data using the H1792 xenograft model actually showed that selumetinib had a more enhanced anti-tumor effect as a single agent compared to the mTORC1/2 inhibitor AZD2014, suggesting that this particular *KRAS* mutant cell line (*KRAS*^{G12C}) is more sensitive to MEK1/2 inhibition than mTORC1/2, despite having amplification of *RICTOR* present.

Nevertheless, these reports and others underscore the combinatorial rationale of dual pathway inhibition presented here. It would be of interest to elucidate, however, whether the development of specific pharmacologic targeting of RICTOR would prove beneficial in defined patient populations, namely in *RICTOR* amplified cases, exclusive of other major driver mutations. This would prove beneficial considering that RICTOR is known to function independently of the mTORC2 complex, regulating other effectors involved in tumor progression. However, in the patient cohort that we are targeting here, we believe that dual mTORC1/2 inhibitors, such as AZD2014, are still warranted further clinical testing in combination with MEK inhibitors, such as selumetinib, as this approach prevents the compensatory feedback we described in our study, and other mechanisms often seen by single mTORC1 inhibitors known to induce hyperactivation of PI3K-AKT (180). Moreover, although previous reports suggest limited clinical benefits from mTORC1/2 inhibitors, proper patient selection in lung cancer patients is needed to fully exploit this therapeutic option (181). Lastly, although combination therapy might be highly effective in cancer patients, there are

great limitations in regards to toxicity. In our proposed strategy specifically, the mTOR and MAPK signaling pathways regulate important physiological functions in non-malignant cells, and thus, an extended treatment setting targeting both pathways might not be feasible. It is therefore important to assess various dosing strategies (e.g. intermittent versus continuous treatment) to fully define the maximal tolerated frequency/doses with the lowest toxicity profile.

In conclusion, our study uncovers defined molecular settings by which we believe can impose clinical benefit to *KRAS* mutant NSCLC by screening for concomitant *RICTOR* alterations that will determine potential benefit from dual mTOR/MAPK pathway inhibition. Excitingly, an ongoing clinical trial termed “TORCMEK” (NCT02583542) is recruiting patients with advanced cancers, including triple-negative breast cancer and NSCLC (*KRAS* mutant vs. wild-type tumors), to assess feasible dose levels and clinical activity of combining AZD2014 in combination with selumetinib. Despite that these targeting agents have been utilized in other clinical trials as single agents or in combination with alternative drugs, this specific combination has not been tested in the clinical setting. On the basis of our studies, it would be of interest to identify if any potential responders to this combination harbored *RICTOR* and/or *KRAS* alterations.

Chapter 8

Appendix

The manuscript described below has been submitted for publication and includes the data presented in the results section of this dissertation.

Title:

Concomitant targeting of the mTOR/MAPK pathways: novel therapeutic strategy in subsets of *RICTOR/KRAS*-altered non-small cell lung cancer

Authors:

Dennis Ruder, Vassiliki Papadimitrakopoulou, Kazuhiko Shien, Carmen Behrens, Neda Kalhor, J. Jack Lee, Waun Ki Hong, Ximing Tang, Luc Girard, John D. Minna, Li Shen, Lixia Diao, Jing Wang, Huiqin Chen, Veera Baladandayuthapani, Barbara Mino, Pamela Villalobos, Jaime Rodriguez-Canales, Nana E. Hanson, James Sun, Vincent Miller, Garrett Frampton, Roy S. Herbst, Ignacio I. Wistuba and Julie G. Izzo

Bibliography

1. Siegel RL, Miller KD, Jemal A. Cancer statistics, 2016. *CA Cancer J Clin.* 2016;66(1):7-30. doi: 10.3322/caac.21332. PubMed PMID: 26742998.
2. Herbst RS, Heymach JV, Lippman SM. Lung cancer. *N Engl J Med.* 2008;359(13):1367-80. doi: 10.1056/NEJMra0802714. PubMed PMID: 18815398.
3. Chan BA, Hughes BG. Targeted therapy for non-small cell lung cancer: current standards and the promise of the future. *Transl Lung Cancer Res* 2015. p. 36-54.
4. Thunnissen E, van der Oord K, den Bakker M. Prognostic and predictive biomarkers in lung cancer. A review. *Virchows Archiv : an international journal of pathology.* 2014;464(3):347-58. Epub 2014/01/15. doi: 10.1007/s00428-014-1535-4. PubMed PMID: 24420742.
5. Tsao AS, Scagliotti GV, Bunn PA, Jr., Carbone DP, Warren GW, Bai C, de Koning HJ, Yousaf-Khan AU, McWilliams A, Tsao MS, Adusumilli PS, Rami-Porta R, Asamura H, Van Schil PE, Darling GE, Ramalingam SS, Gomez DR, Rosenzweig KE, Zimmermann S, Peters S, Ignatius Ou SH, Reungwetwattana T, Janne PA, Mok TS, Wakelee HA, Pirker R, Mazieres J, Brahmer JR, Zhou Y, Herbst RS, Papadimitrakopoulou VA, Redman MW, Wynes MW, Gandara DR, Kelly RJ, Hirsch FR, Pass HI. Scientific Advances in Lung Cancer 2015. *J Thorac Oncol.* 2016;11(5):613-38. Epub 2016/03/26. doi: 10.1016/j.jtho.2016.03.012. PubMed PMID: 27013409.
6. Solomon BJ, Mok T, Kim DW, Wu YL, Nakagawa K, Mekhail T, Felip E, Cappuzzo F, Paolini J, Usari T, Iyer S, Reisman A, Wilner KD, Tursi J, Blackhall F. First-line crizotinib versus chemotherapy in ALK-positive lung cancer. *N Engl J Med.*

2014;371(23):2167-77. Epub 2014/12/04. doi: 10.1056/NEJMoa1408440. PubMed PMID: 25470694.

7. Mok TS, Wu YL, Thongprasert S, Yang CH, Chu DT, Saijo N, Sunpaweravong P, Han B, Margono B, Ichinose Y, Nishiwaki Y, Ohe Y, Yang JJ, Chewaskulyong B, Jiang H, Duffield EL, Watkins CL, Armour AA, Fukuoka M. Gefitinib or carboplatin-paclitaxel in pulmonary adenocarcinoma. *N Engl J Med*. 2009;361(10):947-57. Epub 2009/08/21. doi: 10.1056/NEJMoa0810699. PubMed PMID: 19692680.

8. Cancer Genome Atlas Research N. Comprehensive molecular profiling of lung adenocarcinoma. *Nature*. 2014;511(7511):543-50. Epub 2014/08/01. doi: 10.1038/nature13385. PubMed PMID: 25079552; PMCID: PMC4231481.

9. Weinstein IB, Begemann M, Zhou P, Han EK, Sgambato A, Doki Y, Arber N, Ciaparrone M, Yamamoto H. Disorders in cell circuitry associated with multistage carcinogenesis: exploitable targets for cancer prevention and therapy. *Clinical cancer research : an official journal of the American Association for Cancer Research*. 1997;3(12 Pt 2):2696-702. Epub 1999/03/06. PubMed PMID: 10068276.

10. Hanahan D, Weinberg RA. Hallmarks of cancer: the next generation. *Cell*. 2011;144(5):646-74. Epub 2011/03/08. doi: 10.1016/j.cell.2011.02.013. PubMed PMID: 21376230.

11. Dearden S, Stevens J, Wu YL, Blowers D. Mutation incidence and coincidence in non small-cell lung cancer: meta-analyses by ethnicity and histology (mutMap). *Annals of oncology : official journal of the European Society for Medical Oncology / ESMO*. 2013;24(9):2371-6. Epub 2013/06/01. doi: 10.1093/annonc/mdt205. PubMed PMID: 23723294; PMCID: PMC3755331.

12. Alamgeer M, Ganju V, Watkins DN. Novel therapeutic targets in non-small cell lung cancer. *Current opinion in pharmacology*. 2013;13(3):394-401. Epub 2013/04/24. doi: 10.1016/j.coph.2013.03.010. PubMed PMID: 23608109.
13. Barouch-Bentov R, Sauer K. Mechanisms of drug resistance in kinases. *Expert Opin Investig Drugs*. 2011;20(2):153-208. doi: 10.1517/13543784.2011.546344. PubMed PMID: 21235428; PMCID: PMC3095104.
14. Lovly CM, Shaw AT. Molecular pathways: resistance to kinase inhibitors and implications for therapeutic strategies. *Clinical cancer research : an official journal of the American Association for Cancer Research*. 2014;20(9):2249-56. doi: 10.1158/1078-0432.CCR-13-1610. PubMed PMID: 24789032; PMCID: PMC4029617.
15. Shea M, Costa DB, Rangachari D. Management of advanced non-small cell lung cancers with known mutations or rearrangements: latest evidence and treatment approaches. *Ther Adv Respir Dis*. 2016;10(2):113-29. doi: 10.1177/1753465815617871. PubMed PMID: 26620497.
16. Thorpe LM, Yuzugullu H, Zhao JJ. PI3K in cancer: divergent roles of isoforms, modes of activation and therapeutic targeting. *Nature reviews Cancer*. 2015;15(1):7-24. Epub 2014/12/24. doi: 10.1038/nrc3860. PubMed PMID: 25533673; PMCID: PMC4384662.
17. Yuan TL, Cantley LC. PI3K pathway alterations in cancer: variations on a theme. *Oncogene*. 2008;27(41):5497-510. Epub 2008/09/17. doi: 10.1038/onc.2008.245. PubMed PMID: 18794884; PMCID: PMC3398461.
18. Rodon J, Dienstmann R, Serra V, Tabernero J. Development of PI3K inhibitors: lessons learned from early clinical trials. *Nature reviews Clinical oncology*.

2013;10(3):143-53. Epub 2013/02/13. doi: 10.1038/nrclinonc.2013.10. PubMed PMID: 23400000.

19. Engelman JA. Targeting PI3K signalling in cancer: opportunities, challenges and limitations. *Nature reviews Cancer*. 2009;9(8):550-62. Epub 2009/07/25. doi: 10.1038/nrc2664. PubMed PMID: 19629070.

20. Pal I, Mandal M. PI3K and Akt as molecular targets for cancer therapy: current clinical outcomes. *Acta pharmacologica Sinica*. 2012;33(12):1441-58. Epub 2012/09/18. doi: 10.1038/aps.2012.72. PubMed PMID: 22983389; PMCID: PMC4001841.

21. Sarbassov DD, Guertin DA, Ali SM, Sabatini DM. Phosphorylation and regulation of Akt/PKB by the rictor-mTOR complex. *Science*. 2005;307(5712):1098-101. doi: 10.1126/science.1106148. PubMed PMID: 15718470.

22. Attoub S, Arafat K, Hammadi NK, Mester J, Gaben AM. Akt2 knock-down reveals its contribution to human lung cancer cell proliferation, growth, motility, invasion and endothelial cell tube formation. *Sci Rep*. 2015;5:12759. doi: 10.1038/srep12759. PubMed PMID: 26234648; PMCID: PMC4522680.

23. Datta SR, Dudek H, Tao X, Masters S, Fu H, Gotoh Y, Greenberg ME. Akt phosphorylation of BAD couples survival signals to the cell-intrinsic death machinery. *Cell*. 1997;91(2):231-41. PubMed PMID: 9346240.

24. Linnerth-Petrik NM, Santry LA, Petrik JJ, Wootton SK. Opposing functions of Akt isoforms in lung tumor initiation and progression. *PloS one*. 2014;9(4):e94595. doi: 10.1371/journal.pone.0094595. PubMed PMID: 24722238; PMCID: PMC3983215.

25. Vadlakonda L, Dash A, Pasupuleti M, Anil Kumar K, Reddanna P. The Paradox of Akt-mTOR Interactions. *Frontiers in oncology*. 2013;3:165. doi: 10.3389/fonc.2013.00165. PubMed PMID: 23802099; PMCID: 3687210.
26. Fayard E, Tintignac LA, Baudry A, Hemmings BA. Protein kinase B/Akt at a glance. *Journal of cell science*. 2005;118(Pt 24):5675-8. doi: 10.1242/jcs.02724. PubMed PMID: 16339964.
27. Kim D, Sun M, He L, Zhou QH, Chen J, Sun XM, Bepler G, Sebti SM, Cheng JQ. A small molecule inhibits Akt through direct binding to Akt and preventing Akt membrane translocation. *The Journal of biological chemistry*. 2010;285(11):8383-94. doi: 10.1074/jbc.M109.094060. PubMed PMID: 20068047; PMCID: PMC2832988.
28. Sonenberg N, Gingras AC. The mRNA 5' cap-binding protein eIF4E and control of cell growth. *Current opinion in cell biology*. 1998;10(2):268-75. Epub 1998/04/30. PubMed PMID: 9561852.
29. Gingras AC, Gygi SP, Raught B, Polakiewicz RD, Abraham RT, Hoekstra MF, Aebersold R, Sonenberg N. Regulation of 4E-BP1 phosphorylation: a novel two-step mechanism. *Genes & development*. 1999;13(11):1422-37. Epub 1999/06/11. PubMed PMID: 10364159; PMCID: PMC316780.
30. Ma XM, Blenis J. Molecular mechanisms of mTOR-mediated translational control. *Nature reviews Molecular cell biology*. 2009;10(5):307-18. Epub 2009/04/03. doi: 10.1038/nrm2672. PubMed PMID: 19339977.
31. Jastrzebski K, Hannan KM, Tchoubrieva EB, Hannan RD, Pearson RB. Coordinate regulation of ribosome biogenesis and function by the ribosomal protein S6 kinase, a key mediator of mTOR function. *Growth factors (Chur, Switzerland)*.

2007;25(4):209-26. Epub 2007/12/20. doi: 10.1080/08977190701779101. PubMed PMID: 18092230.

32. Manning BD, Cantley LC. United at last: the tuberous sclerosis complex gene products connect the phosphoinositide 3-kinase/Akt pathway to mammalian target of rapamycin (mTOR) signalling. *Biochemical Society transactions*. 2003;31(Pt 3):573-8. Epub 2003/05/30. doi: 10.1042/. PubMed PMID: 12773158.

33. Populo H, Lopes JM, Soares P. The mTOR Signalling Pathway in Human Cancer. *International journal of molecular sciences*. 2012;13(2):1886-918. doi: 10.3390/ijms13021886. PubMed PMID: 22408430; PMCID: 3291999.

34. Bracho-Valdes I, Moreno-Alvarez P, Valencia-Martinez I, Robles-Molina E, Chavez-Vargas L, Vazquez-Prado J. mTORC1- and mTORC2-interacting proteins keep their multifunctional partners focused. *IUBMB Life*. 2011;63(10):896-914. doi: 10.1002/iub.558. PubMed PMID: 21905202.

35. Dobashi Y, Watanabe Y, Miwa C, Suzuki S, Koyama S. Mammalian target of rapamycin: a central node of complex signaling cascades. *Int J Clin Exp Pathol*. 2011;4(5):476-95. PubMed PMID: 21738819; PMCID: 3127069.

36. Laplante M, Sabatini DM. mTOR signaling at a glance. *Journal of cell science*. 2009;122(Pt 20):3589-94. Epub 2009/10/09. doi: 10.1242/jcs.051011. PubMed PMID: 19812304; PMCID: PMC2758797.

37. Hung CM, Garcia-Haro L, Sparks CA, Guertin DA. mTOR-dependent cell survival mechanisms. *Cold Spring Harbor perspectives in biology*. 2012;4(12). Epub 2012/11/06. doi: 10.1101/cshperspect.a008771. PubMed PMID: 23124837; PMCID: PMC3504431.

38. Morselli E, Galluzzi L, Kepp O, Vicencio JM, Criollo A, Maiuri MC, Kroemer G. Anti- and pro-tumor functions of autophagy. *Biochimica et biophysica acta*. 2009;1793(9):1524-32. doi: 10.1016/j.bbamcr.2009.01.006. PubMed PMID: 19371598.
39. Choi KS. Autophagy and cancer. *Experimental & molecular medicine*. 2012;44(2):109-20. doi: 10.3858/emm.2012.44.2.033. PubMed PMID: 22257886; PMCID: 3296807.
40. Liu B, Bao JK, Yang JM, Cheng Y. Targeting autophagic pathways for cancer drug discovery. *Chinese journal of cancer*. 2013;32(3):113-20. doi: 10.5732/cjc.012.10010. PubMed PMID: 22835386.
41. Sarbassov DD, Ali SM, Kim DH, Guertin DA, Latek RR, Erdjument-Bromage H, Tempst P, Sabatini DM. Rictor, a novel binding partner of mTOR, defines a rapamycin-insensitive and raptor-independent pathway that regulates the cytoskeleton. *Current biology : CB*. 2004;14(14):1296-302. doi: 10.1016/j.cub.2004.06.054. PubMed PMID: 15268862.
42. Ikenoue T, Inoki K, Yang Q, Zhou X, Guan KL. Essential function of TORC2 in PKC and Akt turn motif phosphorylation, maturation and signalling. *EMBO J*. 2008;27(14):1919-31. doi: 10.1038/emboj.2008.119. PubMed PMID: 18566587; PMCID: 2486275.
43. Garcia-Martinez JM, Alessi DR. mTOR complex 2 (mTORC2) controls hydrophobic motif phosphorylation and activation of serum- and glucocorticoid-induced protein kinase 1 (SGK1). *The Biochemical journal*. 2008;416(3):375-85. doi: 10.1042/BJ20081668. PubMed PMID: 18925875.

44. Chapuis N, Tamburini J, Green AS, Willems L, Bardet V, Park S, Lacombe C, Mayeux P, Bouscary D. Perspectives on inhibiting mTOR as a future treatment strategy for hematological malignancies. *Leukemia*. 2010;24(10):1686-99. Epub 2010/08/13. doi: 10.1038/leu.2010.170. PubMed PMID: 20703258.
45. Dhillon AS, Hagan S, Rath O, Kolch W. MAP kinase signalling pathways in cancer. *Oncogene*. 2007;26(22):3279-90. Epub 2007/05/15. doi: 10.1038/sj.onc.1210421. PubMed PMID: 17496922.
46. Pratilas CA, Solit DB. Targeting the mitogen-activated protein kinase pathway: physiological feedback and drug response. *Clinical cancer research : an official journal of the American Association for Cancer Research*. 2010;16(13):3329-34. Epub 2010/05/18. doi: 10.1158/1078-0432.ccr-09-3064. PubMed PMID: 20472680; PMCID: PMC2912210.
47. Cargnello M, Roux PP. Activation and function of the MAPKs and their substrates, the MAPK-activated protein kinases. *Microbiology and molecular biology reviews : MMBR*. 2011;75(1):50-83. Epub 2011/03/05. doi: 10.1128/membr.00031-10. PubMed PMID: 21372320; PMCID: PMC3063353.
48. Aksamitiene E, Kiyatkin A, Kholodenko BN. Cross-talk between mitogenic Ras/MAPK and survival PI3K/Akt pathways: a fine balance. *Biochemical Society transactions*. 2012;40(1):139-46. Epub 2012/01/21. doi: 10.1042/bst20110609. PubMed PMID: 22260680.
49. Mendoza MC, Er EE, Blenis J. The Ras-ERK and PI3K-mTOR pathways: cross-talk and compensation. *Trends in biochemical sciences*. 2011;36(6):320-8. doi: 10.1016/j.tibs.2011.03.006. PubMed PMID: 21531565; PMCID: PMC3112285.

50. Bandyopadhyay S, Chiang C, Srivastava J, Gersten M, White S, Bell R, Kurschner C, Martin CH, Smoot M, Sahasrabudhe S, Barber DL, Chanda SK, Ideker T. A Human MAP Kinase Interactome. *Nat Methods*. 2010;7(10):801-5. PubMed PMID: 20936779; PMCID: 2967489.
51. Pilot-Storck F, Chopin E, Rual JF, Baudot A, Dobrokhotov P, Robinson-Rechavi M, Brun C, Cusick ME, Hill DE, Schaeffer L, Vidal M, Goillot E. Interactome mapping of the phosphatidylinositol 3-kinase-mammalian target of rapamycin pathway identifies deformed epidermal autoregulatory factor-1 as a new glycogen synthase kinase-3 interactor. *Molecular & cellular proteomics : MCP*. 2010;9(7):1578-93. Epub 2010/04/07. doi: 10.1074/mcp.M900568-MCP200. PubMed PMID: 20368287; PMCID: PMC2938100.
52. Yu CF, Liu ZX, Cantley LG. ERK negatively regulates the epidermal growth factor-mediated interaction of Gab1 and the phosphatidylinositol 3-kinase. *The Journal of biological chemistry*. 2002;277(22):19382-8. Epub 2002/03/16. doi: 10.1074/jbc.M200732200. PubMed PMID: 11896055.
53. Hoeflich KP, O'Brien C, Boyd Z, Cavet G, Guerrero S, Jung K, Januario T, Savage H, Punnoose E, Truong T, Zhou W, Berry L, Murray L, Amler L, Belvin M, Friedman LS, Lackner MR. In vivo antitumor activity of MEK and phosphatidylinositol 3-kinase inhibitors in basal-like breast cancer models. *Clinical cancer research : an official journal of the American Association for Cancer Research*. 2009;15(14):4649-64. Epub 2009/07/02. doi: 10.1158/1078-0432.ccr-09-0317. PubMed PMID: 19567590.

54. Moelling K, Schad K, Bosse M, Zimmermann S, Schweneker M. Regulation of Raf-Akt Cross-talk. *The Journal of biological chemistry*. 2002;277(34):31099-106. Epub 2002/06/06. doi: 10.1074/jbc.M111974200. PubMed PMID: 12048182.
55. Zimmermann S, Moelling K. Phosphorylation and regulation of Raf by Akt (protein kinase B). *Science*. 1999;286(5445):1741-4. Epub 1999/11/27. PubMed PMID: 10576742.
56. Dhillon AS, Meikle S, Yazici Z, Eulitz M, Kolch W. Regulation of Raf-1 activation and signalling by dephosphorylation. *EMBO J*2002. p. 64-71.
57. Guan KL, Figueroa C, Brtva TR, Zhu T, Taylor J, Barber TD, Vojtek AB. Negative regulation of the serine/threonine kinase B-Raf by Akt. *The Journal of biological chemistry*. 2000;275(35):27354-9. Epub 2000/06/28. doi: 10.1074/jbc.M004371200. PubMed PMID: 10869359.
58. Dumaz N, Marais R. Protein kinase A blocks Raf-1 activity by stimulating 14-3-3 binding and blocking Raf-1 interaction with Ras. *The Journal of biological chemistry*. 2003;278(32):29819-23. Epub 2003/06/13. doi: 10.1074/jbc.C300182200. PubMed PMID: 12801936.
59. Kodaki T, Woscholski R, Hallberg B, Rodriguez-Viciana P, Downward J, Parker PJ. The activation of phosphatidylinositol 3-kinase by Ras. *Current biology : CB*. 1994;4(9):798-806. Epub 1994/09/01. PubMed PMID: 7820549.
60. Rodriguez-Viciana P, Warne PH, Dhand R, Vanhaesebroeck B, Gout I, Fry MJ, Waterfield MD, Downward J. Phosphatidylinositol-3-OH kinase as a direct target of Ras. *Nature*. 1994;370(6490):527-32. Epub 1994/08/18. doi: 10.1038/370527a0. PubMed PMID: 8052307.

61. Suire S, Hawkins P, Stephens L. Activation of phosphoinositide 3-kinase gamma by Ras. *Current biology : CB.* 2002;12(13):1068-75. Epub 2002/07/18. PubMed PMID: 12121613.
62. Zoncu R, Efeyan A, Sabatini DM. mTOR: from growth signal integration to cancer, diabetes and ageing. *Nature reviews Molecular cell biology.* 2011;12(1):21-35. Epub 2010/12/16. doi: 10.1038/nrm3025. PubMed PMID: 21157483; PMCID: PMC3390257.
63. Manning BD, Cantley LC. AKT/PKB signaling: navigating downstream. *Cell.* 2007;129(7):1261-74. Epub 2007/07/03. doi: 10.1016/j.cell.2007.06.009. PubMed PMID: 17604717; PMCID: PMC2756685.
64. Biggs WH, 3rd, Meisenhelder J, Hunter T, Cavenee WK, Arden KC. Protein kinase B/Akt-mediated phosphorylation promotes nuclear exclusion of the winged helix transcription factor FKHR1. *Proceedings of the National Academy of Sciences of the United States of America.* 1999;96(13):7421-6. Epub 1999/06/23. PubMed PMID: 10377430; PMCID: PMC22101.
65. Tang ED, Nunez G, Barr FG, Guan KL. Negative regulation of the forkhead transcription factor FKHR by Akt. *The Journal of biological chemistry.* 1999;274(24):16741-6. Epub 1999/06/08. PubMed PMID: 10358014.
66. Rena G, Guo S, Cichy SC, Unterman TG, Cohen P. Phosphorylation of the transcription factor forkhead family member FKHR by protein kinase B. *The Journal of biological chemistry.* 1999;274(24):17179-83. Epub 1999/06/08. PubMed PMID: 10358075.
67. Sengupta S, Peterson TR, Sabatini DM. Regulation of the mTOR complex 1 pathway by nutrients, growth factors, and stress. *Molecular cell.* 2010;40(2):310-22.

Epub 2010/10/23. doi: 10.1016/j.molcel.2010.09.026. PubMed PMID: 20965424;
PMCID: PMC2993060.

68. Scrima M, De Marco C, Fabiani F, Franco R, Pirozzi G, Rocco G, Ravo M, Weisz A, Zoppoli P, Ceccarelli M, Botti G, Malanga D, Viglietto G. Signaling networks associated with AKT activation in non-small cell lung cancer (NSCLC): new insights on the role of phosphatidylinositol-3 kinase. *PloS one*. 2012;7(2):e30427. Epub 2012/03/01. doi: 10.1371/journal.pone.0030427. PubMed PMID: 22363436; PMCID: PMC3281846.

69. Fumarola C, Bonelli MA, Petronini PG, Alfieri RR. Targeting PI3K/AKT/mTOR pathway in non small cell lung cancer. *Biochemical pharmacology*. 2014;90(3):197-207. Epub 2014/05/28. doi: 10.1016/j.bcp.2014.05.011. PubMed PMID: 24863259.

70. Guertin DA, Sabatini DM. Defining the role of mTOR in cancer. *Cancer cell*. 2007;12(1):9-22. Epub 2007/07/07. doi: 10.1016/j.ccr.2007.05.008. PubMed PMID: 17613433.

71. Sarbassov DD, Ali SM, Sengupta S, Sheen JH, Hsu PP, Bagley AF, Markhard AL, Sabatini DM. Prolonged rapamycin treatment inhibits mTORC2 assembly and Akt/PKB. *Molecular cell*. 2006;22(2):159-68. Epub 2006/04/11. doi: 10.1016/j.molcel.2006.03.029. PubMed PMID: 16603397.

72. Hudes G, Carducci M, Tomczak P, Dutcher J, Figlin R, Kapoor A, Staroslawska E, Sosman J, McDermott D, Bodrogi I, Kovacevic Z, Lesovoy V, Schmidt-Wolf IG, Barbarash O, Gokmen E, O'Toole T, Lustgarten S, Moore L, Motzer RJ. Temsirolimus, interferon alfa, or both for advanced renal-cell carcinoma. *N Engl J Med*. 2007;356(22):2271-81. Epub 2007/06/01. doi: 10.1056/NEJMoa066838. PubMed PMID: 17538086.

73. Motzer RJ, Escudier B, Oudard S, Hutson TE, Porta C, Bracarda S, Grunwald V, Thompson JA, Figlin RA, Hollaender N, Urbanowitz G, Berg WJ, Kay A, Lebwohl D, Ravaud A. Efficacy of everolimus in advanced renal cell carcinoma: a double-blind, randomised, placebo-controlled phase III trial. *Lancet* (London, England). 2008;372(9637):449-56. Epub 2008/07/26. doi: 10.1016/s0140-6736(08)61039-9. PubMed PMID: 18653228.
74. Meng L, Zheng XS. Toward rapamycin analog (rapalog)-based precision cancer therapy. *Acta pharmacologica Sinica* 2015. p. 1163-9.
75. Rodrik-Outmezguine VS, Chandarlapaty S, Pagano NC, Poulikakos PI, Scaltriti M, Moskatel E, Baselga J, Guichard S, Rosen N. mTOR kinase inhibition causes feedback-dependent biphasic regulation of AKT signaling. *Cancer discovery*. 2011;1(3):248-59. doi: 10.1158/2159-8290.cd-11-0085. PubMed PMID: 22140653; PMCID: 3227125.
76. Garcia-Echeverria C. Allosteric and ATP-competitive kinase inhibitors of mTOR for cancer treatment. *Bioorganic & medicinal chemistry letters*. 2010;20(15):4308-12. Epub 2010/06/22. doi: 10.1016/j.bmcl.2010.05.099. PubMed PMID: 20561789.
77. Sun SY. mTOR kinase inhibitors as potential cancer therapeutic drugs. *Cancer Lett*. 2013;340(1):1-8. doi: 10.1016/j.canlet.2013.06.017. PubMed PMID: 23792225; PMCID: 3779533.
78. Bendell JC, Kelley RK, Shih KC, Grabowsky JA, Bergsland E, Jones S, Martin T, Infante JR, Mischel PS, Matsutani T, Xu S, Wong L, Liu Y, Wu X, Mortensen DS, Chopra R, Hege K, Munster PN. A phase I dose-escalation study to assess safety, tolerability, pharmacokinetics, and preliminary efficacy of the dual mTORC1/mTORC2 kinase inhibitor CC-223 in patients with advanced solid tumors or multiple myeloma.

Cancer. 2015;121(19):3481-90. Epub 2015/07/17. doi: 10.1002/cncr.29422. PubMed PMID: 26177599; PMCID: PMC4832308.

79. Basu B, Dean E, Puglisi M, Greystoke A, Ong M, Burke W, Cavallin M, Bigley G, Womack C, Harrington EA, Green S, Oelmann E, de Bono JS, Ranson M, Banerji U. First-in-Human Pharmacokinetic and Pharmacodynamic Study of the Dual m-TORC 1/2 Inhibitor AZD2014. *Clinical cancer research : an official journal of the American Association for Cancer Research*. 2015;21(15):3412-9. Epub 2015/03/26. doi: 10.1158/1078-0432.ccr-14-2422. PubMed PMID: 25805799; PMCID: PMC4512239.

80. Brachmann SM, Kleylein-Sohn J, Gaulis S, Kauffmann A, Blommers MJ, Kazic-Legueux M, Laborde L, Hattenberger M, Stauffer F, Vaxelaire J, Romanet V, Henry C, Murakami M, Guthy DA, Sterker D, Bergling S, Wilson C, Brummendorf T, Fritsch C, Garcia-Echeverria C, Sellers WR, Hofmann F, Maira SM. Characterization of the mechanism of action of the pan class I PI3K inhibitor NVP-BKM120 across a broad range of concentrations. *Mol Cancer Ther*. 2012;11(8):1747-57. Epub 2012/06/02. doi: 10.1158/1535-7163.mct-11-1021. PubMed PMID: 22653967.

81. Fruman DA, Rommel C. PI3K and cancer: lessons, challenges and opportunities. *Nature reviews Drug discovery*. 2014;13(2):140-56. Epub 2014/02/01. doi: 10.1038/nrd4204. PubMed PMID: 24481312; PMCID: PMC3994981.

82. Jansen VM, Mayer IA, Arteaga CL. Is There a Future for AKT Inhibitors in the Treatment of Cancer? *Clinical cancer research : an official journal of the American Association for Cancer Research*. 2016;22(11):2599-601. Epub 2016/03/17. doi: 10.1158/1078-0432.ccr-16-0100. PubMed PMID: 26979397; PMCID: PMC4891224.

83. Nitulescu GM, Margina D, Juzenas P, Peng Q, Olaru OT, Saloustros E, Fenga C, Spandidos DA, Libra M, Tsatsakis AM. Akt inhibitors in cancer treatment: The long journey from drug discovery to clinical use (Review). *Int J Oncol* 2016. p. 869-85.
84. Yap TA, Yan L, Patnaik A, Fearon I, Olmos D, Papadopoulos K, Baird RD, Delgado L, Taylor A, Lupinacci L, Riisnaes R, Pope LL, Heaton SP, Thomas G, Garrett MD, Sullivan DM, de Bono JS, Tolcher AW. First-in-man clinical trial of the oral pan-AKT inhibitor MK-2206 in patients with advanced solid tumors. *Journal of clinical oncology : official journal of the American Society of Clinical Oncology*. 2011;29(35):4688-95. Epub 2011/10/26. doi: 10.1200/jco.2011.35.5263. PubMed PMID: 22025163.
85. Chandarlapaty S, Sawai A, Scaltriti M, Rodrik-Outmezguine V, Grbovic-Huezo O, Serra V, Majumder PK, Baselga J, Rosen N. AKT inhibition relieves feedback suppression of receptor tyrosine kinase expression and activity. *Cancer cell*. 2011;19(1):58-71. doi: 10.1016/j.ccr.2010.10.031. PubMed PMID: 21215704; PMCID: 3025058.
86. Crouthamel MC, Kahana JA, Korenchuk S, Zhang SY, Sundaresan G, Eberwein DJ, Brown KK, Kumar R. Mechanism and management of AKT inhibitor-induced hyperglycemia. *Clinical cancer research : an official journal of the American Association for Cancer Research*. 2009;15(1):217-25. Epub 2009/01/02. doi: 10.1158/1078-0432.ccr-08-1253. PubMed PMID: 19118049.
87. Karnoub AE, Weinberg RA. Ras oncogenes: split personalities. *Nature reviews Molecular cell biology*. 2008;9(7):517-31. Epub 2008/06/24. doi: 10.1038/nrm2438. PubMed PMID: 18568040; PMCID: PMC3915522.

88. Bhattacharya S, Socinski MA, Burns TF. KRAS mutant lung cancer: progress thus far on an elusive therapeutic target. *Clin Transl Med* 2015.
89. Whyte DB, Kirschmeier P, Hockenberry TN, Nunez-Oliva I, James L, Catino JJ, Bishop WR, Pai JK. K- and N-Ras are geranylgeranylated in cells treated with farnesyl protein transferase inhibitors. *The Journal of biological chemistry*. 1997;272(22):14459-64. Epub 1997/05/30. PubMed PMID: 9162087.
90. Sánchez-Torres JM, Viteri S, Molina MA, Rosell R. BRAF mutant non-small cell lung cancer and treatment with BRAF inhibitors. *Transl Lung Cancer Res* 2013. p. 244-50.
91. Heidorn SJ, Milagre C, Whittaker S, Nourry A, Niculescu-Duvas I, Dhomen N, Hussain J, Reis-Filho JS, Springer CJ, Pritchard C, Marais R. Kinase-dead BRAF and oncogenic RAS cooperate to drive tumor progression through CRAF. *Cell*. 2010;140(2):209-21. Epub 2010/02/10. doi: 10.1016/j.cell.2009.12.040. PubMed PMID: 20141835; PMCID: PMC2872605.
92. Poulidakos PI, Zhang C, Bollag G, Shokat KM, Rosen N. RAF inhibitors transactivate RAF dimers and ERK signalling in cells with wild-type BRAF. *Nature*. 2010;464(7287):427-30. Epub 2010/02/25. doi: 10.1038/nature08902. PubMed PMID: 20179705; PMCID: PMC3178447.
93. Hatzivassiliou G, Song K, Yen I, Brandhuber BJ, Anderson DJ, Alvarado R, Ludlam MJ, Stokoe D, Gloor SL, Vigers G, Morales T, Aliagas I, Liu B, Sideris S, Hoefflich KP, Jaiswal BS, Seshagiri S, Koeppen H, Belvin M, Friedman LS, Malek S. RAF inhibitors prime wild-type RAF to activate the MAPK pathway and enhance growth. *Nature*. 2010;464(7287):431-5. Epub 2010/02/05. doi: 10.1038/nature08833. PubMed PMID: 20130576.

94. Holderfield M, Merritt H, Chan J, Wallroth M, Tandeske L, Zhai H, Tellew J, Hardy S, Hekmat-Nejad M, Stuart DD, McCormick F, Nagel TE. RAF inhibitors activate the MAPK pathway by relieving inhibitory autophosphorylation. *Cancer cell*. 2013;23(5):594-602. Epub 2013/05/18. doi: 10.1016/j.ccr.2013.03.033. PubMed PMID: 23680146.
95. Banerji U, Camidge DR, Verheul HM, Agarwal R, Sarker D, Kaye SB, Desar IM, Timmer-Bonte JN, Eckhardt SG, Lewis KD, Brown KH, Cantarini MV, Morris C, George SM, Smith PD, van Herpen CM. The first-in-human study of the hydrogen sulfate (Hyd-sulfate) capsule of the MEK1/2 inhibitor AZD6244 (ARRY-142886): a phase I open-label multicenter trial in patients with advanced cancer. *Clinical cancer research : an official journal of the American Association for Cancer Research*. 2010;16(5):1613-23. Epub 2010/02/25. doi: 10.1158/1078-0432.ccr-09-2483. PubMed PMID: 20179232.
96. Hainsworth JD, Cebotaru CL, Kanarev V, Ciuleanu TE, Damyanov D, Stella P, Ganchev H, Pover G, Morris C, Tzekova V. A phase II, open-label, randomized study to assess the efficacy and safety of AZD6244 (ARRY-142886) versus pemetrexed in patients with non-small cell lung cancer who have failed one or two prior chemotherapeutic regimens. *J Thorac Oncol*. 2010;5(10):1630-6. Epub 2010/08/31. doi: 10.1097/JTO.0b013e3181e8b3a3. PubMed PMID: 20802351.
97. Janne PA, Shaw AT, Pereira JR, Jeannin G, Vansteenkiste J, Barrios C, Franke FA, Grinsted L, Zazulina V, Smith P, Smith I, Crino L. Selumetinib plus docetaxel for KRAS-mutant advanced non-small-cell lung cancer: a randomised, multicentre, placebo-controlled, phase 2 study. *The Lancet Oncology*. 2013;14(1):38-

47. Epub 2012/12/04. doi: 10.1016/s1470-2045(12)70489-8. PubMed PMID: 23200175.
98. Blumenschein GR, Jr., Smit EF, Planchard D, Kim DW, Cadranel J, De Pas T, Dunphy F, Udud K, Ahn MJ, Hanna NH, Kim JH, Mazieres J, Kim SW, Baas P, Rappold E, Redhu S, Puski A, Wu FS, Janne PA. A randomized phase II study of the MEK1/MEK2 inhibitor trametinib (GSK1120212) compared with docetaxel in KRAS-mutant advanced non-small-cell lung cancer (NSCLC)dagger. *Annals of oncology : official journal of the European Society for Medical Oncology / ESMO*. 2015;26(5):894-901. Epub 2015/02/28. doi: 10.1093/annonc/mdv072. PubMed PMID: 25722381; PMCID: PMC4855243.
99. Pearce LR, Komander D, Alessi DR. The nuts and bolts of AGC protein kinases. *Nature reviews Molecular cell biology*. 2010;11(1):9-22. Epub 2009/12/23. doi: 10.1038/nrm2822. PubMed PMID: 20027184.
100. Aimbetov R, Chen CH, Bulgakova O, Abetov D, Bissenbaev AK, Bersimbaev RI, Sarbassov DD. Integrity of mTORC2 is dependent on the rictor Gly-934 site. *Oncogene*. 2012;31(16):2115-20. doi: 10.1038/onc.2011.404. PubMed PMID: 21909137; PMCID: 3305845.
101. Chen MY, Long Y, Devreotes PN. A novel cytosolic regulator, Pianissimo, is required for chemoattractant receptor and G protein-mediated activation of the 12 transmembrane domain adenylyl cyclase in Dictyostelium. *Genes & development*. 1997;11(23):3218-31. Epub 1998/02/12. PubMed PMID: 9389653; PMCID: PMC316743.
102. Jacinto E, Loewith R, Schmidt A, Lin S, Ruegg MA, Hall A, Hall MN. Mammalian TOR complex 2 controls the actin cytoskeleton and is rapamycin

insensitive. *Nature cell biology*. 2004;6(11):1122-8. Epub 2004/10/07. doi:

10.1038/ncb1183. PubMed PMID: 15467718.

103. Masri J, Bernath A, Martin J, Jo OD, Vartanian R, Funk A, Gera J. mTORC2 activity is elevated in gliomas and promotes growth and cell motility via overexpression of rictor. *Cancer research*. 2007;67(24):11712-20. doi: 10.1158/0008-5472.CAN-07-2223. PubMed PMID: 18089801.

104. Hagan GN, Lin Y, Magnuson MA, Avruch J, Czech MP. A Rictor-Myo1c complex participates in dynamic cortical actin events in 3T3-L1 adipocytes. *Mol Cell Biol*. 2008;28(13):4215-26. Epub 2008/04/23. doi: 10.1128/mcb.00867-07. PubMed PMID: 18426911; PMCID: PMC2447144.

105. Agarwal NK, Kazyken D, Sarbassov dos D. Rictor encounters RhoGDI2: the second pilot is taking a lead. *Small GTPases*. 2013;4(2):102-5. doi: 10.4161/sgtp.23346. PubMed PMID: 23354413; PMCID: 3747249.

106. Agarwal NK, Chen CH, Cho H, Boulbes DR, Spooner E, Sarbassov DD. Rictor regulates cell migration by suppressing RhoGDI2. *Oncogene*. 2013;32(20):2521-6. doi: 10.1038/onc.2012.287. PubMed PMID: 22777355; PMCID: 3470753.

107. Gildea JJ, Seraj MJ, Oxford G, Harding MA, Hampton GM, Moskaluk CA, Frierson HF, Conaway MR, Theodorescu D. RhoGDI2 is an invasion and metastasis suppressor gene in human cancer. *Cancer research*. 2002;62(22):6418-23. Epub 2002/11/20. PubMed PMID: 12438227.

108. McDonald PC, Oloumi A, Mills J, Dobreva I, Maidan M, Gray V, Wederell ED, Bally MB, Foster LJ, Dedhar S. Rictor and integrin-linked kinase interact and regulate Akt phosphorylation and cancer cell survival. *Cancer research*. 2008;68(6):1618-24. doi: 10.1158/0008-5472.CAN-07-5869. PubMed PMID: 18339839.

109. Serrano I, McDonald PC, Lock FE, Dedhar S. Role of the integrin-linked kinase (ILK)/Rictor complex in TGFbeta-1-induced epithelial-mesenchymal transition (EMT). *Oncogene*. 2013;32(1):50-60. doi: 10.1038/onc.2012.30. PubMed PMID: 22310280.
110. Gao D, Wan L, Wei W. Phosphorylation of Rictor at Thr1135 impairs the Rictor/Cullin-1 complex to ubiquitinate SGK1. *Protein & cell*. 2010;1(10):881-5. doi: 10.1007/s13238-010-0123-x. PubMed PMID: 21204013; PMCID: 3374330.
111. Gao D, Wan L, Inuzuka H, Berg AH, Tseng A, Zhai B, Shaik S, Bennett E, Tron AE, Gasser JA, Lau A, Gygi SP, Harper JW, DeCaprio JA, Toker A, Wei W. Rictor forms a complex with Cullin-1 to promote SGK1 ubiquitination and destruction. *Molecular cell*. 2010;39(5):797-808. doi: 10.1016/j.molcel.2010.08.016. PubMed PMID: 20832730; PMCID: 2939073.
112. Uesugi A, Kozaki K, Tsuruta T, Furuta M, Morita K, Imoto I, Omura K, Inazawa J. The tumor suppressive microRNA miR-218 targets the mTOR component Rictor and inhibits AKT phosphorylation in oral cancer. *Cancer research*. 2011;71(17):5765-78. doi: 10.1158/0008-5472.CAN-11-0368. PubMed PMID: 21795477.
113. Guertin DA, Stevens DM, Saitoh M, Kinkel S, Crosby K, Sheen JH, Mullholland DJ, Magnuson MA, Wu H, Sabatini DM. mTOR complex 2 is required for the development of prostate cancer induced by Pten loss in mice. *Cancer cell*. 2009;15(2):148-59. Epub 2009/02/03. doi: 10.1016/j.ccr.2008.12.017. PubMed PMID: 19185849; PMCID: PMC2701381.
114. Roulin D, Cerantola Y, Dormond-Meuwly A, Demartines N, Dormond O. Targeting mTORC2 inhibits colon cancer cell proliferation in vitro and tumor formation in vivo. *Molecular cancer*. 2010;9:57. doi: 10.1186/1476-4598-9-57. PubMed PMID: 20226010; PMCID: 2850884.

115. Hietakangas V, Cohen SM. TOR complex 2 is needed for cell cycle progression and anchorage-independent growth of MCF7 and PC3 tumor cells. *BMC cancer*. 2008;8:282. Epub 2008/10/04. doi: 10.1186/1471-2407-8-282. PubMed PMID: 18831768; PMCID: PMC2566983.
116. Papadimitrakopoulou V, Lee JJ, Wistuba, II, Tsao AS, Fossella FV, Kalhor N, Gupta S, Byers LA, Izzo JG, Gettinger SN, Goldberg SB, Tang X, Miller VA, Skoulidis F, Gibbons DL, Shen L, Wei C, Diao L, Peng SA, Wang J, Tam AL, Coombes KR, Koo JS, Mauro DJ, Rubin EH, Heymach JV, Hong WK, Herbst RS. The BATTLE-2 Study: A Biomarker-Integrated Targeted Therapy Study in Previously Treated Patients With Advanced Non-Small-Cell Lung Cancer. *Journal of clinical oncology : official journal of the American Society of Clinical Oncology*. 2016. Epub 2016/08/03. doi: 10.1200/jco.2015.66.0084. PubMed PMID: 27480147.
117. Cheng H, Zou Y, Ross JS, Wang K, Liu X, Halmos B, Ali SM, Liu H, Verma A, Montagna C, Chachoua A, Goel S, Schwartz EL, Zhu C, Shan J, Yu Y, Gritsman K, Yelensky R, Lipson D, Otto G, Hawryluk M, Stephens PJ, Miller VA, Piperdi B, Perez-Soler R. RICTOR amplification defines a novel subset of lung cancer patients who may benefit from treatment with mTOR1/2 inhibitors. *Cancer discovery*. 2015. doi: 10.1158/2159-8290.CD-14-0971. PubMed PMID: 26370156.
118. Yang F, Tang X, Riquelme E, Behrens C, Nilsson MB, Giri U, Varella-Garcia M, Byers LA, Lin HY, Wang J, Raso MG, Girard L, Coombes K, Lee JJ, Herbst RS, Minna JD, Heymach JV, Wistuba, II. Increased VEGFR-2 gene copy is associated with chemoresistance and shorter survival in patients with non-small-cell lung carcinoma who receive adjuvant chemotherapy. *Cancer research*. 2011;71(16):5512-

21. doi: 10.1158/0008-5472.CAN-10-2614. PubMed PMID: 21724587; PMCID: PMC3159530.

119. Cerami E, Gao J, Dogrusoz U, Gross BE, Sumer SO, Aksoy BA, Jacobsen A, Byrne CJ, Heuer ML, Larsson E, Antipin Y, Reva B, Goldberg AP, Sander C, Schultz N. The cBio cancer genomics portal: an open platform for exploring multidimensional cancer genomics data. *Cancer discovery*. 2012;2(5):401-4. Epub 2012/05/17. doi: 10.1158/2159-8290.cd-12-0095. PubMed PMID: 22588877; PMCID: PMC3956037.

120. Gao J, Aksoy BA, Dogrusoz U, Dresdner G, Gross B, Sumer SO, Sun Y, Jacobsen A, Sinha R, Larsson E, Cerami E, Sander C, Schultz N. Integrative analysis of complex cancer genomics and clinical profiles using the cBioPortal. *Science signaling*. 2013;6(269):p11. Epub 2013/04/04. doi: 10.1126/scisignal.2004088. PubMed PMID: 23550210; PMCID: PMC4160307.

121. Frampton GM, Fichtenholtz A, Otto GA, Wang K, Downing SR, He J, Schnall-Levin M, White J, Sanford EM, An P, Sun J, Juhn F, Brennan K, Iwanik K, Maillet A, Buell J, White E, Zhao M, Balasubramanian S, Terzic S, Richards T, Banning V, Garcia L, Mahoney K, Zwirko Z, Donahue A, Beltran H, Mosquera JM, Rubin MA, Dogan S, Hedvat CV, Berger MF, Puztai L, Lechner M, Boshoff C, Jarosz M, Vietz C, Parker A, Miller VA, Ross JS, Curran J, Cronin MT, Stephens PJ, Lipson D, Yelensky R. Development and validation of a clinical cancer genomic profiling test based on massively parallel DNA sequencing. *Nature Biotechnology*. 2013;31:1023-31. doi: doi:10.1038/nbt.2696.

122. Zhou P, Zhang N, Nussinov R, Ma B. Defining the Domain Arrangement of the Mammalian Target of Rapamycin Complex Component Rictor Protein. *J Comput Biol*.

2015;22(9):876-86. doi: 10.1089/cmb.2015.0103. PubMed PMID: 26176550; PMCID: PMC4575542.

123. Comprehensive molecular profiling of lung adenocarcinoma. *Nature*. 2014;511(7511):543-50. Epub 2014/08/01. doi: 10.1038/nature13385. PubMed PMID: 25079552; PMCID: PMC4231481.

124. Yang Q, Inoki K, Ikenoue T, Guan KL. Identification of Sin1 as an essential TORC2 component required for complex formation and kinase activity. *Genes & development*. 2006;20(20):2820-32. doi: 10.1101/gad.1461206. PubMed PMID: 17043309; PMCID: 1619946.

125. Feng J, Park J, Cron P, Hess D, Hemmings BA. Identification of a PKB/Akt hydrophobic motif Ser-473 kinase as DNA-dependent protein kinase. *The Journal of biological chemistry*. 2004;279(39):41189-96. doi: 10.1074/jbc.M406731200. PubMed PMID: 15262962.

126. Gao T, Furnari F, Newton AC. PHLPP: a phosphatase that directly dephosphorylates Akt, promotes apoptosis, and suppresses tumor growth. *Molecular cell*. 2005;18(1):13-24. Epub 2005/04/06. doi: 10.1016/j.molcel.2005.03.008. PubMed PMID: 15808505.

127. Laugier F, Finet-Benyair A, Andre J, Rachakonda PS, Kumar R, Bensussan A, Dumaz N. RICTOR involvement in the PI3K/AKT pathway regulation in melanocytes and melanoma. *Oncotarget*. 2015;6(29):28120-31. Epub 2015/09/12. doi: 10.18632/oncotarget.4866. PubMed PMID: 26356562; PMCID: PMC4695048.

128. Koo J, Yue P, Gal AA, Khuri FR, Sun SY. Maintaining glycogen synthase kinase-3 activity is critical for mTOR kinase inhibitors to inhibit cancer cell growth.

Cancer research. 2014;74(9):2555-68. Epub 2014/03/15. doi: 10.1158/0008-5472.can-13-2946. PubMed PMID: 24626091; PMCID: PMC4029841.

129. Chen BW, Chen W, Liang H, Liu H, Liang C, Zhi X, Hu LQ, Yu XZ, Wei T, Ma T, Xue F, Zheng L, Zhao B, Feng XH, Bai XL, Liang TB. Inhibition of mTORC2 Induces Cell-Cycle Arrest and Enhances the Cytotoxicity of Doxorubicin by Suppressing MDR1 Expression in HCC Cells. *Mol Cancer Ther.* 2015;14(8):1805-15. Epub 2015/05/31. doi: 10.1158/1535-7163.mct-15-0029. PubMed PMID: 26026051; PMCID: PMC4866512.

130. Breuleux M, Klopfenstein M, Stephan C, Doughty CA, Barys L, Maira SM, Kwiatkowski D, Lane HA. Increased AKT S473 phosphorylation after mTORC1 inhibition is rictor dependent and does not predict tumor cell response to PI3K/mTOR inhibition. *Mol Cancer Ther.* 2009;8(4):742-53. Epub 2009/04/18. doi: 10.1158/1535-7163.mct-08-0668. PubMed PMID: 19372546; PMCID: PMC3440776.

131. O'Reilly KE, Rojo F, She QB, Solit D, Mills GB, Smith D, Lane H, Hofmann F, Hicklin DJ, Ludwig DL, Baselga J, Rosen N. mTOR inhibition induces upstream receptor tyrosine kinase signaling and activates Akt. *Cancer research.* 2006;66(3):1500-8. Epub 2006/02/03. doi: 10.1158/0008-5472.can-05-2925. PubMed PMID: 16452206; PMCID: PMC3193604.

132. Lake D, Correa SA, Muller J. Negative feedback regulation of the ERK1/2 MAPK pathway. *Cellular and molecular life sciences : CMLS.* 2016. Epub 2016/06/28. doi: 10.1007/s00018-016-2297-8. PubMed PMID: 27342992.

133. Caunt CJ, Sale MJ, Smith PD, Cook SJ. MEK1 and MEK2 inhibitors and cancer therapy: the long and winding road. *Nature reviews Cancer.* 2015;15(10):577-92. doi: 10.1038/nrc4000. PubMed PMID: 26399658.

134. Shi GX, Cai W, Andres DA. Rit-mediated stress resistance involves a p38-mitogen- and stress-activated protein kinase 1 (MSK1)-dependent cAMP response element-binding protein (CREB) activation cascade. *The Journal of biological chemistry*. 2012;287(47):39859-68. Epub 2012/10/06. doi: 10.1074/jbc.M112.384248. PubMed PMID: 23038261; PMCID: PMC3501050.
135. Casanovas O, Miro F, Estanyol JM, Itarte E, Agell N, Bachs O. Osmotic stress regulates the stability of cyclin D1 in a p38SAPK2-dependent manner. *The Journal of biological chemistry*. 2000;275(45):35091-7. Epub 2000/08/23. doi: 10.1074/jbc.M006324200. PubMed PMID: 10952989.
136. Thornton TM, Rincon M. Non-classical p38 map kinase functions: cell cycle checkpoints and survival. *International journal of biological sciences*. 2009;5(1):44-51. Epub 2009/01/23. PubMed PMID: 19159010; PMCID: PMC2610339.
137. Sato M, Vaughan MB, Girard L, Peyton M, Lee W, Shames DS, Ramirez RD, Sunaga N, Gazdar AF, Shay JW, Minna JD. Multiple oncogenic changes (K-RAS(V12), p53 knockdown, mutant EGFRs, p16 bypass, telomerase) are not sufficient to confer a full malignant phenotype on human bronchial epithelial cells. *Cancer research*. 2006;66(4):2116-28. Epub 2006/02/21. doi: 10.1158/0008-5472.can-05-2521. PubMed PMID: 16489012.
138. Ramirez RD, Sheridan S, Girard L, Sato M, Kim Y, Pollack J, Peyton M, Zou Y, Kurie JM, Dimaio JM, Milchgrub S, Smith AL, Souza RF, Gilbey L, Zhang X, Gandia K, Vaughan MB, Wright WE, Gazdar AF, Shay JW, Minna JD. Immortalization of human bronchial epithelial cells in the absence of viral oncoproteins. *Cancer research*. 2004;64(24):9027-34. Epub 2004/12/18. doi: 10.1158/0008-5472.can-04-3703. PubMed PMID: 15604268.

139. Chou TC. Drug combination studies and their synergy quantification using the Chou-Talalay method. *Cancer research*. 2010;70(2):440-6. Epub 2010/01/14. doi: 10.1158/0008-5472.can-09-1947. PubMed PMID: 20068163.
140. Chen Z, Fillmore CM, Hammerman PS, Kim CF, Wong KK. Non-small-cell lung cancers: a heterogeneous set of diseases. *Nature reviews Cancer*. 2014;14(8):535-46. Epub 2014/07/25. doi: 10.1038/nrc3775. PubMed PMID: 25056707.
141. Cox AD, Fesik SW, Kimmelman AC, Luo J, Der CJ. Drugging the undruggable RAS: Mission possible? *Nature reviews Drug discovery*. 2014;13(11):828-51. Epub 2014/10/18. doi: 10.1038/nrd4389. PubMed PMID: 25323927; PMCID: PMC4355017.
142. Wang S, Song X, Li X, Zhao X, Chen H, Wang J, Wu J, Gao Z, Qian J, Han B, Bai C, Li Q, Lu D. RICTOR polymorphisms affect efficiency of platinum-based chemotherapy in Chinese non-small-cell lung cancer patients. *Pharmacogenomics*. 2016;17(15):1637-47. Epub 2016/09/28. doi: 10.2217/pgs-2016-0070. PubMed PMID: 27676404.
143. Hodi FS, Corless CL, Giobbie-Hurder A, Fletcher JA, Zhu M, Marino-Enriquez A, Friedlander P, Gonzalez R, Weber JS, Gajewski TF, O'Day SJ, Kim KB, Lawrence D, Flaherty KT, Luke JJ, Collichio FA, Ernstoff MS, Heinrich MC, Beadling C, Zukotynski KA, Yap JT, Van den Abbeele AD, Demetri GD, Fisher DE. Imatinib for melanomas harboring mutationally activated or amplified KIT arising on mucosal, acral, and chronically sun-damaged skin. *Journal of clinical oncology : official journal of the American Society of Clinical Oncology*. 2013;31(26):3182-90. Epub 2013/06/19. doi: 10.1200/jco.2012.47.7836. PubMed PMID: 23775962; PMCID: PMC4878082.

144. Cui Y, Zhao J, Yi L, Jiang Y. microRNA-153 Targets mTORC2 Component Rictor to Inhibit Glioma Cells. *PloS one*. 2016;11(6):e0156915. Epub 2016/06/15. doi: 10.1371/journal.pone.0156915. PubMed PMID: 27295037; PMCID: PMC4905671.
145. Wen SY, Li CH, Zhang YL, Bian YH, Ma L, Ge QL, Teng YC, Zhang ZG. Rictor is an independent prognostic factor for endometrial carcinoma. *Int J Clin Exp Pathol*. 2014;7(5):2068-78. Epub 2014/06/27. PubMed PMID: 24966915; PMCID: PMC4069916.
146. Kaibori M, Shikata N, Sakaguchi T, Ishizaki M, Matsui K, Iida H, Tanaka Y, Miki H, Nakatake R, Okumura T, Tokuhara K, Inoue K, Wada J, Oda M, Nishizawa M, Kon M. Influence of Rictor and Raptor Expression of mTOR Signaling on Long-Term Outcomes of Patients with Hepatocellular Carcinoma. *Digestive diseases and sciences*. 2015;60(4):919-28. Epub 2014/11/06. doi: 10.1007/s10620-014-3417-7. PubMed PMID: 25371154.
147. Wazir U, Newbold RF, Jiang WG, Sharma AK, Mokbel K. Prognostic and therapeutic implications of mTORC1 and Rictor expression in human breast cancer. *Oncology reports*. 2013;29(5):1969-74. Epub 2013/03/19. doi: 10.3892/or.2013.2346. PubMed PMID: 23503572.
148. Gupta S, Hau AM, Beach JR, Harwalker J, Mantuano E, Gonias SL, Egelhoff TT, Hansel DE. Mammalian target of rapamycin complex 2 (mTORC2) is a critical determinant of bladder cancer invasion. *PloS one*. 2013;8(11):e81081. doi: 10.1371/journal.pone.0081081. PubMed PMID: 24312263; PMCID: 3842329.
149. Morrison Joly M, Hicks DJ, Jones B, Sanchez V, Estrada MV, Young C, Williams M, Rexer BN, Sarbassov DD, Muller WJ, Brantley-Sieders D, Cook RS. Rictor/mTORC2 Drives Progression and Therapeutic Resistance of HER2-Amplified

Breast Cancers. *Cancer research*. 2016. Epub 2016/05/20. doi: 10.1158/0008-5472.can-15-3393. PubMed PMID: 27197158.

150. Lamouille S, Connolly E, Smyth JW, Akhurst RJ, Derynck R. TGF-beta-induced activation of mTOR complex 2 drives epithelial-mesenchymal transition and cell invasion. *Journal of cell science*. 2012;125(Pt 5):1259-73. Epub 2012/03/09. doi: 10.1242/jcs.095299. PubMed PMID: 22399812; PMCID: PMC3324583.

151. Zhang F, Zhang X, Li M, Chen P, Zhang B, Guo H, Cao W, Wei X, Cao X, Hao X, Zhang N. mTOR complex component Rictor interacts with PKCzeta and regulates cancer cell metastasis. *Cancer research*. 2010;70(22):9360-70. doi: 10.1158/0008-5472.CAN-10-0207. PubMed PMID: 20978191.

152. Das G, Shiras A, Shanmuganandam K, Shastry P. Rictor regulates MMP-9 activity and invasion through Raf-1-MEK-ERK signaling pathway in glioma cells. *Molecular carcinogenesis*. 2011;50(6):412-23. doi: 10.1002/mc.20723. PubMed PMID: 21557327.

153. Hall A. Rho GTPases and the actin cytoskeleton. *Science*. 1998;279(5350):509-14. Epub 1998/02/07. PubMed PMID: 9438836.

154. Padavano J, Henkhaus RS, Chen H, Skovan BA, Cui H, Ignatenko NA. Mutant K-RAS Promotes Invasion and Metastasis in Pancreatic Cancer Through GTPase Signaling Pathways. *Cancer growth and metastasis*. 2015;8(Suppl 1):95-113. Epub 2015/10/30. doi: 10.4137/cgm.s29407. PubMed PMID: 26512205; PMCID: PMC4612127.

155. Sunaga N, Imai H, Shimizu K, Shames DS, Kakegawa S, Girard L, Sato M, Kaira K, Ishizuka T, Gazdar AF, Minna JD, Mori M. Oncogenic KRAS-induced interleukin-8 overexpression promotes cell growth and migration and contributes to

aggressive phenotypes of non-small cell lung cancer. *Int J Cancer*. 2012;130(8):1733-44. Epub 2011/05/06. doi: 10.1002/ijc.26164. PubMed PMID: 21544811; PMCID: PMC3374723.

156. Diehl JA, Cheng M, Roussel MF, Sherr CJ. Glycogen synthase kinase-3beta regulates cyclin D1 proteolysis and subcellular localization. *Genes & development*. 1998;12(22):3499-511. Epub 1998/12/01. PubMed PMID: 9832503; PMCID: PMC317244.

157. Carayol N, Vakana E, Sassano A, Kaur S, Goussetis DJ, Glaser H, Druker BJ, Donato NJ, Altman JK, Barr S, Plataniias LC. Critical roles for mTORC2- and rapamycin-insensitive mTORC1-complexes in growth and survival of BCR-ABL-expressing leukemic cells. *Proceedings of the National Academy of Sciences of the United States of America*. 2010;107(28):12469-74. Epub 2010/07/10. doi: 10.1073/pnas.1005114107. PubMed PMID: 20616057; PMCID: PMC2906574.

158. Altman JK, Sassano A, Kaur S, Glaser H, Kroczyńska B, Redig AJ, Russo S, Barr S, Plataniias LC. Dual mTORC2/mTORC1 targeting results in potent suppressive effects on acute myeloid leukemia (AML) progenitors*. *Clinical cancer research : an official journal of the American Association for Cancer Research*. 2011;17(13):4378-88. doi: 10.1158/1078-0432.ccr-10-2285. PubMed PMID: 21415215; PMCID: 3131493.

159. Tamburini J, Green AS, Bardet V, Chapuis N, Park S, Willems L, Uzunov M, Ifrah N, Dreyfus F, Lacombe C, Mayeux P, Bouscary D. Protein synthesis is resistant to rapamycin and constitutes a promising therapeutic target in acute myeloid leukemia. *Blood*. 2009;114(8):1618-27. Epub 2009/05/22. doi: 10.1182/blood-2008-10-184515. PubMed PMID: 19458359.

160. Blasco RB, Francoz S, Santamaria D, Canamero M, Dubus P, Charron J, Baccarini M, Barbacid M. c-Raf, but not B-Raf, is essential for development of K-Ras oncogene-driven non-small cell lung carcinoma. *Cancer cell*. 2011;19(5):652-63. Epub 2011/04/26. doi: 10.1016/j.ccr.2011.04.002. PubMed PMID: 21514245; PMCID: PMC4854330.
161. Karreth FA, Frese KK, DeNicola GM, Baccarini M, Tuveson DA. C-Raf is required for the initiation of lung cancer by K-RasG12D. *Cancer discovery*. 2011;1(2):128-36. doi: 10.1158/2159-8290.cd-10-0044. PubMed PMID: 22043453; PMCID: 3203527.
162. Voice JK, Klemke RL, Le A, Jackson JH. Four human ras homologs differ in their abilities to activate Raf-1, induce transformation, and stimulate cell motility. *The Journal of biological chemistry*. 1999;274(24):17164-70. Epub 1999/06/08. PubMed PMID: 10358073.
163. Lito P, Saborowski A, Yue J, Solomon M, Joseph E, Gadad S, Saborowski M, Kasthuber E, Fellmann C, Ohara K, Morikami K, Miura T, Lukacs C, Ishii N, Lowe S, Rosen N. Disruption of CRAF-mediated MEK activation is required for effective MEK inhibition in KRAS mutant tumors. *Cancer cell*. 2014;25(5):697-710. Epub 2014/04/22. doi: 10.1016/j.ccr.2014.03.011. PubMed PMID: 24746704; PMCID: PMC4049532.
164. Lamming DW, Demirkan G, Boylan JM, Mihaylova MM, Peng T, Ferreira J, Neretti N, Salomon A, Sabatini DM, Gruppuso PA. Hepatic signaling by the mechanistic target of rapamycin complex 2 (mTORC2). *FASEB journal : official publication of the Federation of American Societies for Experimental Biology*.

2014;28(1):300-15. doi: 10.1096/fj.13-237743. PubMed PMID: 24072782; PMCID: PMC3868844.

165. Lavoie JN, L'Allemain G, Brunet A, Muller R, Pouyssegur J. Cyclin D1 expression is regulated positively by the p42/p44MAPK and negatively by the p38/HOGMAPK pathway. *The Journal of biological chemistry*. 1996;271(34):20608-16. Epub 1996/08/23. PubMed PMID: 8702807.

166. Yee AS, Paulson EK, McDevitt MA, Rieger-Christ K, Summerhayes I, Berasi SP, Kim J, Huang CY, Zhang X. The HBP1 transcriptional repressor and the p38 MAP kinase: unlikely partners in G1 regulation and tumor suppression. *Gene*. 2004;336(1):1-13. Epub 2004/07/01. doi: 10.1016/j.gene.2004.04.004. PubMed PMID: 15225871.

167. Khan MW, Biswas D, Ghosh M, Mandloi S, Chakrabarti S, Chakrabarti P. mTORC2 controls cancer cell survival by modulating gluconeogenesis. *Cell death discovery*. 2015;1:15016. Epub 2015/01/01. doi: 10.1038/cddiscovery.2015.16. PubMed PMID: 27551450; PMCID: PMC4979518.

168. Mascarenhas D, Routt S, Singh BK. Mammalian target of rapamycin complex 2 regulates inflammatory response to stress. *Inflammation research : official journal of the European Histamine Research Society [et al]*. 2012;61(12):1395-404. Epub 2012/08/18. doi: 10.1007/s00011-012-0542-7. PubMed PMID: 22899279; PMCID: PMC3496474.

169. Cota D. mTORC2, the "other" mTOR, is a new player in energy balance regulation. *Molecular metabolism* 2014. p. 349-50.

170. Kocalis HE, Hagan SL, George L, Turney MK, Siuta MA, Laryea GN, Morris LC, Muglia LJ, Printz RL, Stanwood GD, Niswender KD. Rictor/mTORC2 facilitates

central regulation of energy and glucose homeostasis. *Molecular metabolism*.

2014;3(4):394-407. Epub 2014/06/20. doi: 10.1016/j.molmet.2014.01.014. PubMed PMID: 24944899; PMCID: PMC4060224.

171. Wang J, Whiteman MW, Lian H, Wang G, Singh A, Huang D, Denmark T. A non-canonical MEK/ERK signaling pathway regulates autophagy via regulating Beclin 1. *The Journal of biological chemistry*. 2009;284(32):21412-24. Epub 2009/06/13. doi: 10.1074/jbc.M109.026013. PubMed PMID: 19520853; PMCID: PMC2755866.

172. Simone C. Signal-dependent control of autophagy and cell death in colorectal cancer cell: the role of the p38 pathway. *Autophagy*. 2007;3(5):468-71. Epub 2007/05/15. PubMed PMID: 17495519.

173. Dienstmann R, Rodon J, Serra V, Tabernero J. Picking the point of inhibition: a comparative review of PI3K/AKT/mTOR pathway inhibitors. *Mol Cancer Ther*. 2014;13(5):1021-31. Epub 2014/04/22. doi: 10.1158/1535-7163.mct-13-0639. PubMed PMID: 24748656.

174. Montagut C, Settleman J. Targeting the RAF-MEK-ERK pathway in cancer therapy. *Cancer Lett*. 2009;283(2):125-34. Epub 2009/02/17. doi: 10.1016/j.canlet.2009.01.022. PubMed PMID: 19217204.

175. Johnson L, Mercer K, Greenbaum D, Bronson RT, Crowley D, Tuveson DA, Jacks T. Somatic activation of the K-ras oncogene causes early onset lung cancer in mice. *Nature*. 2001;410(6832):1111-6. Epub 2001/04/27. doi: 10.1038/35074129. PubMed PMID: 11323676.

176. Wang Y, Kaiser CE, Frett B, Li HY. Targeting mutant KRAS for anticancer therapeutics: a review of novel small molecule modulators. *Journal of medicinal*

chemistry. 2013;56(13):5219-30. Epub 2013/04/10. doi: 10.1021/jm3017706. PubMed PMID: 23566315; PMCID: PMC4666308.

177. Meng J, Dai B, Fang B, Bekele BN, Bornmann WG, Sun D, Peng Z, Herbst RS, Papadimitrakopoulou V, Minna JD, Peyton M, Roth JA. Combination treatment with MEK and AKT inhibitors is more effective than each drug alone in human non-small cell lung cancer in vitro and in vivo. *PloS one*. 2010;5(11):e14124. Epub 2010/12/03. doi: 10.1371/journal.pone.0014124. PubMed PMID: 21124782; PMCID: PMC2993951.

178. Wee S, Jagani Z, Xiang KX, Loo A, Dorsch M, Yao YM, Sellers WR, Lengauer C, Stegmeier F. PI3K pathway activation mediates resistance to MEK inhibitors in KRAS mutant cancers. *Cancer research*. 2009;69(10):4286-93. Epub 2009/04/30. doi: 10.1158/0008-5472.can-08-4765. PubMed PMID: 19401449.

179. Broutin S, Stewart A, Thavasu P, Paci A, Bidart JM, Banerji U. Insights into significance of combined inhibition of MEK and m-TOR signalling output in KRAS mutant non-small-cell lung cancer. *British journal of cancer*. 2016;115(5):549-52. Epub 2016/07/22. doi: 10.1038/bjc.2016.220. PubMed PMID: 27441499.

180. Jokinen E, Koivunen J. MEK and PI3K inhibition in solid tumors: rationale and evidence to date. *Ther Adv Med Oncol*2015. p. 170-80.

181. Cheng H, Shcherba M, Pendurti G, Liang Y, Piperdi B, Perez-Soler R. Targeting the PI3K/AKT/mTOR pathway: potential for lung cancer treatment. *Lung cancer management*. 2014;3(1):67-75. Epub 2014/10/25. doi: 10.2217/lmt.13.72. PubMed PMID: 25342981; PMCID: PMC4203662.

Vitae

Dennis Ruder was born in Vitebsk, Belarus on December 19, 1988, the son of Inessa and Boris Ruder. After completing his work at Plano Senior High School, Plano, Texas in 2006, he entered Baylor University in Waco, Texas. He received the degree of Bachelor of Science with a major in Biology (Chemistry minor) from Baylor in December, 2009. For the next one year, he worked as a research technician in the Pathology Department at The University of Texas Southwestern Medical Center. In August of 2011 he entered The University of Texas Graduate School of Biomedical Sciences at Houston/MD Anderson Cancer Center.

Permanent address:

2002 Colby Lane
Wylie, Texas 75098